Molecular principles of enhanced complement activation by properdin

Ramon M. van den Bos

ISBN: 9789464191677

Doctoral Thesis
Molecular principles of enhanced complement activation by properdin
Ramon Marijs van den Bos
Crystal and Structural Chemistry
Bijvoet Centre for Biomolecular Research, Faculty of Science
Utrecht University, the Netherlands
Accomplished with financial support from the Dutch Kidney Foundation

Cover art: Mees van den Bos
Layout: Ramon M. van den Bos
Print: Gildeprint

Molecular principles of enhanced complement activation by properdin

Moleculaire principes van versterkte complement activatie door properdine
(met een samenvatting in het Nederlands)

Proefschrift

ter verkrijging van de graad van doctor aan de Universiteit Utrecht op gezag van de rector magnificus, prof.dr. H.R.B.M. Kummeling, ingevolge het besluit van het college voor promoties in het openbaar te verdedigen op maandag 26 april 2021 des middags te 2.30 uur

door

Ramon Marijs van den Bos

geboren op 9 maart 1990

te Elburg

Promotor: Prof. dr. P. Gros

"It's going to be legen -wait for it -

Barney Stinson

Table of contents

Chapter 1

General Introduction

Ramon M. van den Bos

Crystal and Structural Chemistry, Bijvoet Centre for Biomolecular Research, Department of Chemistry, Utrecht University, Utrecht, The Netherlands.

1

Our immune system is crucial for protection against invading microorganisms and for the clearance of foreign particles and altered host cells. The immune system consists of two branches, the innate and adaptive immunity. Whilst the adaptive immunity needs to be trained to target specific microorganisms, the innate immune system can immediately react against a wide variety of targets. A major component of the innate immune response is the complement system, which is a protein cascade that is vital for tagging microorganisms and foreign particles for clearance, for direct killing of microorganisms and for inducing an inflammatory response. Complement activation is highly regulated to prevent activation on and damage to healthy host cells and to promote complement activation on targeted surfaces. This thesis focusses on the positive regulation of the complement system by the protein properdin and on the interplay between positive and negative regulation.

1 The complement system

The complement system is part of human innate immunity, where it plays an important role in the defense against invading microorganism and in the clearance of apoptotic cells, foreign particles and immune complexes. Complement was discovered at the end of the 19th century as George Nuttal observed that serum has bactericidal properties (as reviewed by H. Chaplin Jr (1)). Subsequently, Jules Bordet found that serum can be divided in a heat sensitive and a heat resistant part that are both necessary for the bactericidal properties. Paul Erlich coined the name complement for the heat sensitive part as it complements antibodies in killing bacteria. Later it was discovered that the complement system is a protein cascade consisting of approximately 40 different proteins, which can be activated in an antibody dependent and independent manner.

1.1 Complement activation

Activation of the complement system can occur through three different initiation pathways: the lectin pathway (LP), the classical pathway (CP) and the alternative pathway (AP) (**Fig. 1**). Both the LP and CP depend on surface pattern recognition for activation; initiation of the LP is mediated by mannose binding lectin (MBL) and ficolins, which respectively recognize mannoses and acetylated glycans on the surfaces of microorganisms (2, 3). The CP is initiated when C1q is recruited to target surfaces by either direct binding to ligands on the surface (e.g. DNA or LPS (4)), or through interaction with various pattern recognition molecules (e.g. IgG, IgM, or C reactive protein) (5, 6). MBL, ficolin and C1q associate with pathway specific proteases (MASP in the LP, C1s and C1r in the CP) and these complexes can cleave C4 into C4a and C4b. After cleavage, C4b undergoes a conformational rearrangement, which exposes a reactive thioester that allows C4b to covalently attach to nucleophiles on surfaces (7–9). Subsequently, C2 binds to C4b and is then cleaved by MASP or C1s creating the heterodimeric enzyme complex, C4b2b, which is the C3 convertase of the LP and CP.

The AP does not rely on surface recognition for activation, instead it is continuously activated at a low level. This low-level activation is due to a spontaneous conformational change of C3 (0.3% per hour at 37 °C (10)) to a bioactive state C3*. Subsequently, factor B (FB) binds C3*, after which the bound FB is cleaved by factor D into Ba and Bb. Ba rapidly dissociates from the complex and Bb remains bound to C3b forming a heterodimeric complex C3*Bb, which is a C3 convertase. Both C4b2b and C3*Bb cleave C3 into anaphylatoxin C3a and opsonin C3b. Similar to C4b, C3b undergoes a conformational change (11, 12) and can, if generated in close proximity to a surface, react through its reactive thioester with nucleophiles on surfaces (7, 13). The conformation of C3b is similar to that of C3* (11, 14) and C3b can also interact with FB and form a C3 convertase, C3bBb (15, 16).

The generation of a surface bound C3bBb is the start of the amplification loop of the complement system. The C3bBb on the surface will cleave additional C3 resulting in the

deposition of C3b and, subsequently, the generation of additional C3 convertases on the surface. This positive feedback loop results in massive consumption of C3, generation of C3a and opsonization of the surface with C3b. An increasing C3b density on the surface results in a switch of substrate specificity of C3bBb and C4b2b from C3 to C5 (17–20). Cleavage of C5 into the anaphylatoxin C5a and C5b is the start of the terminal pathway and results in the recruitment of C6, C7, C8 and C9 to C5. Together these proteins form the membrane attack complex (MAC), which is a lytic pore that can directly kill targeted cells (21).

Besides lysis of targeted cells, there are several additional effector functions in which the complement system acts as a signaling pathway. The anaphylatoxins C3a and C5a can interact with the G-coupled receptors C3aR and C5aR, respectively, and this interaction induces a wide range of effects which vary from inducing an inflammatory response to promoting tissue regeneration (22). Both C3a and C5a are potent chemoattractants that recruit immune cells, like macrophages and neutrophiles, to sites of complement activation (22). These immune cells have receptors on their cell surface which allows them to recognize targeted cells through interaction with the deposited C3b and the C3b degradation fragments iC3b and C3d (23) that are generated through proteolytic inactivation of C3b by factor I (FI) in combination with a co-factor (24). Recognition of C3b coated surfaces by immune cells can lead to clearance through phagocytosis by macrophages. Furthermore, surfaces coated with C3b and C3b degradation products can activate the adaptive immune system by increasing the B-cell response and inducing proliferation of T-cells (25–27).

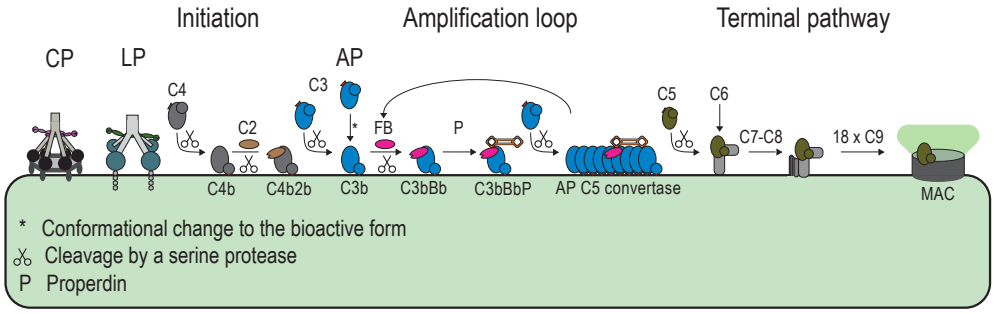

Figure 1 | Schematic representation of complement activation through the different pathways

2 Regulation of the complement system

The complement system is tightly regulated to prevent uncontrolled complement activation, which can lead to the depletion of complement components and can result in damage to healthy host cells.

2.1 Regulation at the level of the C3/C5 convertase

After complement initiation the C3 convertases C4b2b and especially C3bBb are the driving forces of complement activation. Both C3 convertases have a relative short half-life of approximately 1-3 minutes (18, 28) and decay of C3 convertases in their individual components is irreversible and leads to loss of activity. Alteration of the life-time of C3 convertases is an important mechanism for regulation of the complement system.

2.1.1 Decreased complement activation by negative regulators

There are several soluble and membrane proteins that reduce complement activation by decreasing the lifetime of C3 convertases or by preventing formation of new convertases. Negative regulators with decay-acceleration activity (DAA) dissociate the convertase, while regulators with co-factor activity (CA) act as a co-factor for FI-mediated inactivation of C4b and C3b. In plasma, C4b binding protein (C4BP), factor H (FH) and its splice form factor H like 1 (FHL-1) are responsible for preventing complement overactivation by exerting both DAA and CA. C4BP is specific for the CP/LP C3 convertase (C4b2b), whilst both FH and FHL-1 act on the AP C3 convertase (C3bBb). On the surface of cells, the proteins decay-acceleration factor (DAF), membrane-cofactor protein (MCP) and complement-receptor 1 (CR1) play a vital role in protecting healthy host cells against complement activation. CR1 has both DAA and CA whereas DAF and MCP only have DAA or CA, respectively. Additionally, the soluble negative regulators interact with various ligands on host cells, like sialic acid and glycosaminoglycans (29, 30), thereby providing additional protection against complement activation (31). The recruitment of soluble negative regulators to the surface is also a complement-evasion strategy used by various pathogens like *Neisseria meningitides* and *Neisseria gonorrhoeae* (32).

The negative regulators with DAA and/or CA have a common architecture (33). They consist of strings of several complement control protein (CCP) domains, which are elongated domains consisting of approximately sixty amino acids. The number of successive CCP domains varies form 4 CCP domains (MCP and DAF) to 30 CCP domains in CR1. However, for DAA only three successive CCP domains that interact with both components of the C3 convertase are required (33, 34). The interactions of negative regulators with C3b are well characterized and several structures of negative regulators in complex with C3b show that they all bind to a similar location on C3b (24, 33, 35). There are no published structures of a negative regulator with DAA in complex with either C2 or FB. However, based on distance restraints between FB and DAF obtained by electron paramagnetic resonance (36) and C2 and FB mutants that form C3 convertases, which are less susceptible to decay by negative regulators, it is likely that the interaction site lies in the Von Willebrand factor type A domain (VWA) of FB and C2 (34, 37, 38). Remarkably, in C3bBb the residues in FB important for DAA are located on the side of the VWA domain that is pointing away from the binding site of the negative

regulators on C3b (15, 39). How binding of negative regulators to both binding sites results in decay of the convertase is still unknown. Conversely, the molecular mechanism of the proteolytic inactivation of C4b of C3b by FI and a co-factor is more clearly defined. Unbound FI is catalytically inactive due to a partially disordered the serine protease (SP) domain (40), however when FI is bound to the complex of C3b or C4b with a regulator with CA, such as FH or C4BP, the SP domain becomes structurally ordered (24). This enables FI to cleave C3b and C4b up to three times into iC3b and iC4b (after two cleavages) and C3c/C4c plus C3d/C4d (after three cleavages) (24).

2.1.2 Enhanced complement activation by the positive regulator properdin

Properdin is a crucial positive regulator of the complement system. Its name is derived from the Latin word *properdere*, which means "prepare to destroy". The discovery of properdin coincided with the discovery of the alternative pathway of the complement system, when it was shown by Pillemer and colleagues that in the presence of properdin, complement could be activated in an antibody independent manner (41). Properdin enhances complement activation by increasing the lifetime of the AP C3 convertase by a factor of 5-10 (42). Additionally, properdin promotes formation of the C3 convertase and reduces proteolytic inactivation of C3b by FI (43–46).

Properdin is an oligomeric plasma protein that occurs as dimers, trimers and tetramers in the ratio 1:2:1 (47, 48). Properdin has a low systemic concentration (5-25 μg/ml (48)), however, release of properdin by immune cells could potentially result in a high local properdin concentration (49–51). Properdin oligomerization results in avidity towards C3b coated surfaces (44, 52), which is likely important for directing positive regulation by properdin to targeted surfaces. A properdin protomer has a molecular weight of

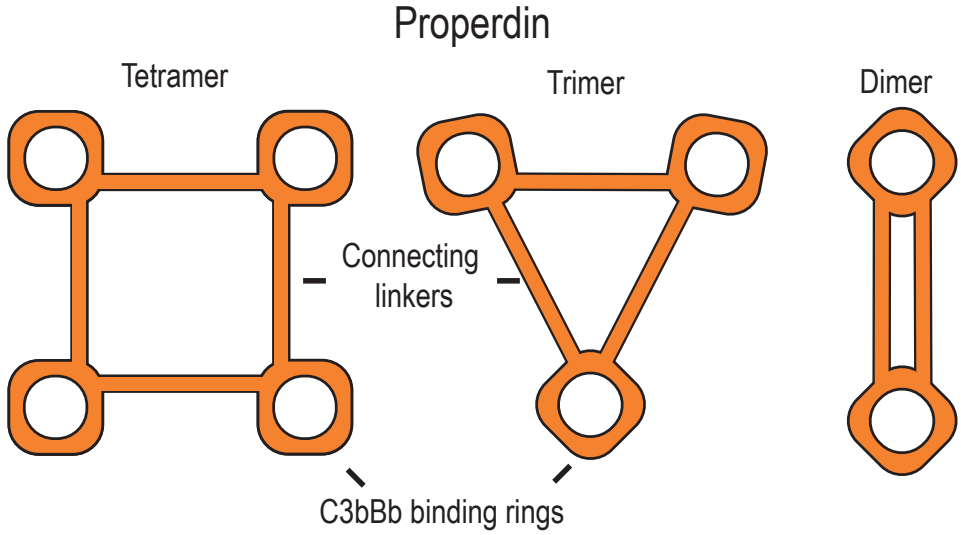

Figure 2 | Schematic representation of properdin oligomers.

~53 kDa and consists of a small N-terminal domain and six thrombospondin type-1 repeat (TSR) domains (53), which are thin elongated domains of approximately 60 residues (54). Properdin is highly glycosylated as it contains 1 N-linked glycan, 4 O-linked glycans and 14-17 mannosylated tryptophan residues (55, 56). Negative stain EM revealed that properdin consists of rings that are connected via thin linkers that have a length of approximately 3 TSR domains. It was suggested that these rings are formed by interactions between the N- and C-terminus of different properdin protomers (46, 47) (**Fig. 2**). With negative stain EM it was shown that each of these rings is capable of binding to C3bBb (46). The rings consist of the remaining domains and deletion studies of separate regions of properdin indicated that TSR4-5-6 are important for stabilizing the AP C3 convertase (53). Low-resolution EM and crystallography data revealed that properdin binds on the CTC domain of C3b in close proximity to Bb (46, 52), however the molecular mechanism of properdin induced stabilization remains elusive.

Although the AP does not require pattern recognition molecules for activation, it has been extensively reported that properdin can act as a pattern recognition molecule and promote AP activation on surfaces (57–61). Properdin is a positively charged protein and it is capable of binding to various negatively charged ligands (e.g. sulfated heparan, DNA) (53, 62–64). There have also been reports of direct properdin binding to various microorganisms (e.g. *Chlamydia pneumoniae* (65) and *Neisseria gonorrhoeae* (59)), although recently some of these results have been contributed to unnatural properdin aggregates that form by mistreating properdin (51, 66). For *Escherichia coli* and *Neisseria meningitidis* it has been shown that properdin binding to these bacteria depends on initial C3b deposition (67, 68).

2.2 Other forms of negative regulation

Apart from the lifetime of the C3 convertase, there are various other aspects of the complement cascade that are targeted by negative regulators. The C1 inhibitor is a serpin like molecule that reduces initiation of the CP and LP by irreversibly binding and inactivating C1s, C1q and MASP. Additionally, sMAP and MAP19 are decoy proteins that compete with MASP for binding to MBL and thereby reduce LP activation (69). Furthermore, there are several negative regulators that act on the level of the MAC pore. CD59 is a GPI-linked membrane protein that binds both C8 and C9 and prevents the further recruitment of C9 and thus the formation of the MAC pore (70). In addition to CD59, there are the soluble proteins clusterin and fibronectin that can prevent insertion of the MAC pore into the membrane by interacting with the exposed hydrophobic regions of MAC pore precursors and preventing the polymerization of C9 (71–74).

3 Complement related diseases

Loss of activation, overactivation or unwanted activation of the complement system can result in or exacerbate a wide variety of diseases, such as atypical hemolytic uremic syndrome (aHUS) (75) and systematic inflammatory response syndrome (SIRS) (76).

3.1 Reduced complement activation

Lack of complement activation generally leads to a higher prevalence of bacterial, viral and fungal infections (77). The main causes for reduced or abolished complement activation are genetic defects and inhibiting autoantibodies (77, 78). Besides an increased risk for infections, deficiencies in proteins involved in CP activation, like C1q and C2, and deficiencies in C3 have been linked to autoimmune and inflammatory diseases such as systemic lupus erythematosus (SLE) like diseases. SLE is a disease characterized by systemic inflammation that induces tissue damage (79). The percentages of complement deficient patients that have SLE like symptoms range from 10 % of the C2 deficient patients to 93 % of the C1q deficient patients (77). It has been hypothesized that SLE-like symptoms are due to the inability to clear immune complexes and apoptotic cells, which results in an inflammatory response against these particles (80).

Defects of the alternative and terminal pathway components are mainly associated with an increased risk of infections with *N. meningitides* (81). Patients deficient in properdin have a 250x higher occurrence of *N. meningitides* infection with associated higher mortality rates (82). Patients deficient in terminal pathway components have a ~5000x increased infection rate. However, these *N. meningitides* infections tend to be less severe with a reduced mortality compared to patients without any complement deficiencies (81, 83). This reduced mortality might be related to reduced endotoxin release due to the inability of forming MAC pores (81).

3.2 Overactivation and unwanted activation of the complement system

There are many different pathologies associated with complement overactivation (27), generally they are the result of uncontrolled complement activation on healthy host cells. Uncontrolled complement activation can be the result of: gain of function mutations in complement proteins important for activation (e.g. C3 and FB), mutations, autoantibodies or deficiencies that result in the loss of negative regulation by for example FH and FI or autoantibodies against complement components that increase C3 convertase stability or reduce negative regulation.

Overactivation of the AP is an important factor in complement mediated diseases (84). The loss of negative regulators on the surface leads to high susceptibility of the affected cells. For example, in paroxysmal nocturnal hemoglobinuria (PNH) there is a subset of erythrocytes that lack the GPI-linked negative regulators DAF and CD59. This is due

to an autosomal mutation in hematopoietic stem cells in the pigA gene, which is an enzyme essential for the synthesis of GPI-anchors (85–87). Without these regulators on the surface these erythrocytes are highly susceptible to complement attack resulting in lysis or phagocytosis. Similarly, mutations in or inhibiting autoantibodies against the domains responsible for host surface recognition in FH and FHL-1 potentially leads to overactivation of complement on host surfaces which can lead to diseases like aHUS and age-related macular degeneration (AMD) (88–90). Loss of DAA or CA of FH, or loss of function mutations in FI leads to complement overactivation in solution, which can result in dense deposit disease (DDD) and C3 glomerulopathy (C3G) (27). Furthermore, complement overactivation in solution depletes serum from complement components, resulting in higher susceptibility to microbial infection. Gain of function mutations in C3 and FB can also lead to overactivation of the complement pathway (91). These mutations can increase the stability of C3bBb, decrease the DAA of negative regulators or prevent the inactivation of C3b by FI and can result in similar diseases as with the loss of negative regulation (27). Finally, complement overactivation can be the result of so called C3 and C4 nephritic factors (C3/C4NEF), which are autoantibodies against the C3 convertase that increase complement activation by either prolonging the lifetime of the C3 convertase or by increasing its resistance against decay by negative regulators (92, 93)

Unwanted activation of the CP due to autoantibodies leads to complement activation on healthy host cells which may result in damage to specific tissues or cells such as to neuromuscular junctions in myasthenia gravis (94). In addition, CP activation plays an important role in antibody mediated rejection of transplanted organs (95, 96).

Excessive complement activation can also be the result of an overwhelming amount of complement activation triggers. These triggers can be due to excessive trauma, burns or bacterial and viral infections (97). Complement overactivation due to an overwhelming amount of activation triggers can result in SIRS, which results in tissue damage and is a life-threatening condition. The induced inflammatory response by the release of the anaphylatoxins C3a and C5a plays an important role in SIRS (98).

4.1 Complement therapeutics

Due to the many pathologies associated with complement overactivation, there is a great interest in novel therapeutic complement inhibitors. Currently, the only complement inhibitors that are approved for therapeutic use are eculizumab and ravulizumab (99–101). Both have been approved for treating PNH. In addition, eculizumab is approved for the treatment of aHUS, myasthenia gravis and neuromyelitis potica spectrum disorder (100). Both eculizumab and ravulizumab are antibodies against C5 and prevent the cleavage of C5 into C5a and C5b (101). Thus, they inhibit both the generation of the potent anaphylatoxin C5a and the activation of the terminal pathway.

Due to the (financial) success of Eculizumab, there is now a great interest in finding

novel complement inhibitors and the high complexity of the complement system makes it likely that multiple therapeutics are necessary to treat all complement related diseases. There is a wide variety of therapeutic compounds against different parts of the complement system in development. These compounds range from antibodies, proteins or peptides that function through competitive binding with various protein targets, such as C3 and FD, to small molecule protease inhibitors that are specific for FB or FD (100, 102–106).

Clinical trials are ongoing for a wide variety of complement related diseases, including diseases which are the result of mutations in or autoantibodies against complement components (e.g. PNH, aHUS, AMD and C3G) and diseases which are caused by external events like complement mediated complications in transplantation and SIRS due to viral infections (100, 103). Recent trials in treating patients that have acute respiratory distress syndrome as a result of COVID-19 with; AMY-101 (C3 specific complement inhibitor), eculizumab or an anti-C5a antibody showed that these are promising treatments in reducing the severity of the COVID-19 disease course (105, 107–109).

4.2 Properdin as a therapeutic target

The main limitation of inhibiting complement activation at the level of terminal pathway is that the targeted surface can still be opsonized with C3b. This can result in breakthrough events and clearance of opsonized cells by phagocytes (110–112). Inhibition of AP activation is an interesting alternative to inhibition of the TP. Properdin is an attractive therapeutic target for reducing AP activation as properdin is only involved in enhancing AP activation and it is not required for the CP and LP (113–115). Inhibition of properdin has been shown to be beneficial in mouse models for several diseases (e.g. aHUS and PNH) (116–119) and in contrast to inhibition with eculizumab the inhibition of properdin prevents extravascular hemolysis in a PNH mouse model.

Scope of this thesis

Properdin is a crucial positive regulator of AP activation, however the molecular mechanism behind positive regulation by properdin is still unknown. In **Chapter 2** we overcome the oligomeric nature of properdin by producing a monomerized properdin variant that is capable of stabilizing C3bBb. With this monomerized properdin variant we characterize the interaction between properdin and C3b, C3bB and C3bBb by surface plasmon resonance (SPR). Furthermore, monomerized properdin allowed us to solve crystal structures of free properdin and of properdin in complex with the CTC domain of C3b. The structural and biochemical characterization reveals that properdin likely stabilizes C3bBb by bridging C3b and Bb.

Chapter 3 explores the relation between positive and negative regulation and their effect on AP activation. We show that balance between positive and negative regulation by properdin and FH, respectively, is important for AP activation on C3b-coated liposomes and that properdin and FH exert their function independently of each other.

In **Chapter 4** we explore the therapeutic potential of the isolated CTC domain of C3b. We show that the CTC domain can act as a competitive binder and reduce complement activation on erythrocytes, albeit with a low efficacy. We succeeded in generating a CTC domain variant that has an increased affinity for properdin and an increased efficacy for inhibiting complement activation on erythrocytes.

Finally, in **Chapter 5** the implications of the main results obtained in chapters 2-4 for the complement field are discussed and a perspective on new developments in the field is given.

Acknowledgements

Thanks to Harma Brondijk and Wout Oosterheert for critically proofreading this chapter.

References

1. H Chaplin Jr. 2005. Review: the burgeoning history of the complement system 1888-2005. *Immunohematology* 21: 85-93.

2. Matsushita, M., Y. Endo, and T. Fujita. 2013. Structural and functional overview of the lectin complement pathway: Its molecular basis and physiological implication. *Arch. Immunol. Ther. Exp. (Warsz).* 61: 273–283.

3. Kjaer, T. R., S. Thiel, and G. R. Andersen. 2013. Toward a structure-based comprehension of the lectin pathway of complement. *Mol. Immunol.* 56: 222–231.

4. Merle, N. S., S. E. Church, V. Fremeaux-Bacchi, and L. T. Roumenina. 2015. Complement system part I - molecular mechanisms of activation and regulation. *Front. Immunol.* 6: 1–30.

5. Diebolder, C. A., F. J. Beurskens, R. N. De Jong, R. I. Koning, K. Strumane, M. A. Lindorfer, M. Voorhorst, D. Ugurlar, S. Rosati, A. J. R. Heck, et al. 2014. Complement is activated by IgG hexamers assembled at the cell surface. *Science (80-.).* 343: 1260–1263.

6. Ugurlar, D., S. C. Howes, B. J. De Kreuk, R. I. Koning, R. N. De Jong, F. J. Beurskens, J. Schuurman, A. J. Koster, T. H. Sharp, W. H. I. Parren, et al. 2018. Structures of C1-IgG1 provide insights into how danger pattern recognition activates complement. *Science (80-.).* 359: 794–797.

7. Law, S. K. A., and A. W. Dodds. 1996. The internal thioester and the covalent binding properties of the complement proteins C3 and C4. *Protein Sci.* 6: 263–274.

8. Mortensen, S., R. T. Kidmose, S. V. Petersen, Á. Szilágyi, Z. Prohászka, and G. R. Andersen. 2015. Structural Basis for the Function of Complement Component C4 within the Classical and Lectin Pathways of Complement. *J. Immunol.* 194: 5488–5496.

9. Kidmose, R. T., N. S. Laursen, J. Dobó, T. R. Kjaer, S. Sirotkina, L. Yatime, L. Sottrup-Jensen, S. Thiel, P. Gál, and G. R. Andersen. 2012. Structural basis for activation of the complement system by component C4 cleavage. *Proc. Natl. Acad. Sci. U. S. A.* 109: 15425–15430.

10. Pangburn, M. K., and H. J. Müller□Eberhard. 1983. Initiation of the Alternative Complement Pathway Due To Spontaneous Hydrolysis of the Thioester of C3. *Ann. N. Y. Acad. Sci.* 421: 291–298.

11. Janssen, B. J. C., A. Christodoulidou, A. McCarthy, J. D. Lambris, and P. Gros. 2006. Structure of C3b reveals conformational changes that underlie complement activity. *Nature* 444: 213–216.

12. Janssen, B. J. C., E. G. Huizinga, H. C. a Raaijmakers, A. Roos, M. R. Daha, K. Nilsson-Ekdahl, B. Nilsson, and P. Gros. 2005. Structures of complement component C3 provide insights into the function and evolution of immunity. *Nature* 437: 505–511.

13. Pangburn, M. K., and H. J. Muller-Eberhard. 1980. Relation of a putative thioester bond in C3 to activation of the alternative pathway and the binding of C3b to biological targets of complement. *J. Exp. Med.* 152: 1102–1114.

14. Chen, Z. A., R. Pellarin, L. Fischer, A. Sali, M. Nilges, P. N. Barlow, and J. Rappsilber. 2016. Structure of complement C3(H2O) revealed by quantitative cross-linking/mass spectrometry and modeling. *Mol. Cell. Proteomics* 15: 2730–2743.

15. Rooijakkers, S. H. M., J. Wu, M. Ruyken, R. van Domselaar, K. L. Planken, A. Tzekou, D. Ricklin, J. D. Lambris, B. J. C. Janssen, J. a G. van Strijp, et al. 2009. Structural and functional implications of the alternative complement pathway C3 convertase stabilized by a staphylococcal inhibitor. *Nat. Immunol.* 10: 721–727.

16. Forneris, F., D. Ricklin, J. Wu, A. Tzekou, R. S. Wallace, J. D. Lambris, and P. Gros. 2010. Structures of C3b in complex with factors B and D give insight into complement convertase formation. *Science (80-.).* 330: 1816–1820.

17. Rawal, N., and M. K. Pangburn. 1998. C5 convertase of the alternative pathway of complement: Kinetic analysis of the free and surface-bound forms of the enzyme. *J. Biol. Chem.* 273: 16828–16835.

18. Rawal, N., and M. K. Pangburn. 2003. Formation of high affinity C5 convertase of the classical pathway of complement. *J. Biol. Chem.* 278: 38476–38483.

19. Rawal, N., and M. K. Pangburn. 2001. Formation of High-Affinity C5 Convertases of the Alternative Pathway of Complement. *J. Immunol.* 166: 2635–2642.

20. Daha, M. R., D. T. Fearon, and K. F. Austen. 1976. C3 requirements for formation of alternative pathway C5 convertase. *J. Immunol.* 117: 630–634.

21. Menny, A., M. Serna, C. M. Boyd, S. Gardner, A. P. Joseph, B. P. Morgan, M. Topf, N. J. Brooks, and D. Bubeck. 2018. CryoEM reveals how the complement membrane attack complex ruptures lipid bilayers. *Nat. Commun.* 9: 1–11.

22. Klos, A., A. J. Tenner, K. O. Johswich, R. R. Ager, E. S. Reis, and J. Köhl. 2009. The role of the anaphylatoxins in health and disease. *Mol. Immunol.* 46: 2753–2766.

23. van Lookeren Campagne, M., C. Wiesmann, and E. J. Brown. 2007. Macrophage complement receptors and pathogen clearance. *Cell. Microbiol.* 9: 2095–2102.

24. Xue, X., J. Wu, D. Ricklin, F. Forneris, P. Di Crescenzio, C. Q. Schmidt, J. Granneman, T. H. Sharp, J. D. Lambris, and P. Gros. 2017. Regulator-dependent mechanisms of C3b processing by factor i allow differentiation of immune responses. *Nat. Struct. Mol. Biol.* 24: 643–651.

25. Carroll, M. C., and D. E. Isenman. 2012. Regulation of Humoral Immunity by Complement. *Immunity* 37: 199–207.

26. Dempsey, P. W., M. E. D. Allison, S. Akkaraju, C. C. Goodnow, and D. T. Fearon. 1996. C3d of complement as a molecular adjuvant: Bridging innate and acquired immunity. *Science (80-.).* 271: 348–350.

27. Ricklin, D., E. S. Reis, and J. D. Lambris. 2016. Complement in disease: a defence system turning offensive. *Nat. Rev. Nephrol.* 12: 383–401.

28. Pangburn, M. K., and H. J. Muller-Eberhard. 1986. The C3 convertase of the alternative pathway of human complement. Enzymic properties of the bimolecular proteinase. *Biochem. J.* 235: 723–730.

29. Morgan, H. P., C. Q. Schmidt, M. Guariento, B. S. Blaum, D. Gillespie, A. P. Herbert, D. Kavanagh, H. D. T. Mertens, D. I. Svergun, C. M. Johansson, et al. 2011. Structural basis for engagement by complement factor H of C3b on a self surface. *Nat. Struct. Mol. Biol.* 18: 463–70.

30. Blaum, B. S., J. P. Hannan, A. P. Herbert, D. Kavanagh, D. Uhrín, and T. Stehle. 2014. Structural basis for sialic acid-mediated self-recognition by complement factor H. *Nat. Chem. Biol.* 11: 77–83.

31. Ermert, D., and A. M. Blom. 2016. C4b-binding protein: The good, the bad and the deadly. Novel functions of an old friend. *Immunol. Lett.* 169: 82–92.

32. Lambris, J. D., D. Ricklin, and B. V. Geisbrecht. 2008. Complement evasion by human pathogens. *Nat. Rev. Microbiol.* 6: 132–142.

33. Forneris, F., J. Wu, X. Xue, D. Ricklin, Z. Lin, G. Sfyroera, A. Tzekou, E. Volokhina, J. C. Granneman, R. Hauhart, et al. 2016. Regulators of complement activity mediate inhibitory mechanisms through a common C3b-binding mode. *EMBO J.* 35: 1133–1149.

34. Harris, C. L., D. M. Pettigrew, S. M. Lea, and B. P. Morgan. 2007. Decay-Accelerating Factor Must Bind Both Components of the Complement Alternative Pathway C3 Convertase to Mediate Efficient Decay. *J. Immunol.* 178: 352–359.

35. Wu, J., Y. Q. Wu, D. Ricklin, B. J. C. Janssen, J. D. Lambris, and P. Gros. 2009. Structure of complement fragment C3b-factor H and implications for host protection by complement regulators. *Nat. Immunol.* 10: 728–733.

36. Lovett, J. E., R. J. M. Abbott, P. Roversi, S. Johnson, J. J. E. Caesar, M. Doria, G. Jeschke, C. R. Timmel, and S. M. Lea. 2013. Investigating the structure of the factor B vWF-A domain/CD55 protein-protein complex using DEER spectroscopy: Successes and pitfalls. *Mol. Phys.* 111: 2865–2872.

37. Kuttner-Kondo, L. A., M. P. Dybvig, L. M. Mitchell, N. Muqim, J. P. Atkinson, M. E. Medof, and D. E. Hourcade. 2003. A Corresponding Tyrosine Residue in the C2/Factor B Type A Domain Is a Hot Spot in the Decay Acceleration of the Complement C3 Convertases. *J. Biol. Chem.* 278: 52386–52391.

38. Hourcade, D. E., L. Mitchell, L. A. Kuttner-Kondo, J. P. Atkinson, and M. Edward Medof. 2002. Decay-accelerating factor (DAF), complement receptor 1 (CR1), and factor H dissociate the complement AP C3 convertase (C3bBb) via sites on the type A domain of Bb. *J. Biol. Chem.* 277: 1107–1112.

39. Wu, J., Y. Q. Wu, D. Ricklin, B. J. C. Janssen, J. D. Lambris, and P. Gros. 2009. Structure of complement fragment C3b-factor H and implications for host protection by complement regulators. *Nat. Immunol.* 10: 728–733.

40. Roversi, P., S. Johnson, J. J. E. Caesar, F. McLean, K. J. Leath, S. A. Tsiftsoglou, B. P. Morgan, C. L. Harris, R. B. Sim, and S. M. Lea. 2011. Structural basis for complement factor I control and its disease-associated sequence polymorphisms. *Proc. Natl. Acad. Sci. U. S. A.* 108: 12839–12844.

41. Pillemer, L., L. Blum, I. H. Lepow, O. A. Ross, E. W. Todd, and A. C. Wardlaw. 1954. The properdin system and immunity: I. Demonstration and isolation of a new serum protein, properdin, and its role in immune phenomena. *Science (80-.).* 120: 279–285.

42. Fearon, D. T., and K. F. Austen. 1975. Properdin: binding to C3b and stabilization of the C3b-dependent C3 convertase. *J. Exp. Med.* 142: 856–63.

43. Hourcade, D. E. 2006. The role of properdin in the assembly of the alternative pathway C3 convertases of complement. *J. Biol. Chem.* 281: 2128–2132.

44. Farries, T. C., P. J. Lachmann, and R. A. Harrison. 1988. Analysis of the interactions between properdin, the third component of complement (C3), and its physiological activation products. *Biochem. J.* 252: 47–54.

45. Medicus, R. G., O. Götze, and H. J. Müller-Eberhard. 1976. Alternative pathway of complement: Recruitment of precursor properdin by the labile C3/C5 convertase and the potentiation of the pathway. *J. Exp. Med.* 144: 1076–1093.

46. Alcorlo, M., A. Tortajada, S. Rodríguez de Córdoba, and O. Llorca. 2013. Structural basis for the stabilization of the complement alternative pathway C3 convertase by properdin. *Proc. Natl. Acad. Sci. U. S. A.* 110: 13504–9.

47. Smith CA, Pangburn MK, Vogel CW, Müller-Eberhard HJ. 1984. Molecular architecture of human properdin, a positive regulator of the alternative pathway of complement. *J. Biol. Chem.* 259: 4582–4588.

48. Pangburn, M. K. 1989. Analysis of the natural polymeric forms of human properdin and their functions in complement activation. *J. Immunol.* 142: 202–7.

49. Wirthmueller, U., B. Dewald, M. Thelen, M. K. Schäfer, C. Stover, K. Whaley, J. North, P. Eggleton, K. B. Reid, and W. J. Schwaeble. 1997. Properdin, a positive regulator of complement activation, is released from secondary granules of stimulated peripheral blood neutrophils. *J. Immunol.* 158.

50. Lubbers, R., M. F. van Essen, C. van Kooten, and L. A. Trouw. 2017. Production of complement components by cells of the immune system. *Clin. Exp. Immunol.* 188: 183–194.

51. Cortes, C., J. A. Ohtola, G. Saggu, and V. P. Ferreira. 2012. Local release of properdin in the cellular microenvironment: Role in pattern recognition and amplification of the alternative pathway of complement. *Front. Immunol.* 3: 412.

52. Pedersen, D. V, L. Roumenina, R. K. Jensen, T. A. Gadeberg, C. Marinozzi, C. Picard, T. Rybkine, S. Thiel, U. B. Sørensen, C. Stover, et al. 2017. Functional and structural insight into properdin control of complement alternative pathway amplification. *EMBO J.* 36: 1084–1099.

53. Higgins, J. M., H. Wiedemann, R. Timpl, and K. B. Reid. 1995. Characterization of mutant forms of recombinant human properdin lacking single thrombospondin type I repeats. Identification of modules important for function. *J. Immunol.* 155: 5777–85.

54. Tan, K., M. Duquette, J. H. Liu, Y. Dong, R. Zhang, A. Joachimiak, J. Lawler, and J. H. Wang. 2002. Crystal structure of the TSP-1 type 1 repeats: A novel layered fold and its biological implication. *J. Cell Biol.* 159: 373–382.

55. Hartmann, S., and J. Hofsteenge. 2000. Properdin, the positive regulator of complement, is highly C-mannosylated. *J. Biol. Chem.* 275: 28569–28574.

56. Yang, Y., F. Liu, V. Franc, L. A. Halim, H. Schellekens, and A. J. R. Heck. 2016. Hybrid mass spectrometry approaches in glycoprotein analysis and their usage in scoring biosimilarity. *Nat. Commun.* 7: 13397.

57. Vuagnat, B. B., J. P. Mach, and J. M. Le Doussal. 2000. Activation of the alternative pathway of human complement by autologous cells expressing transmembrane recombinant properdin. *Mol. Immunol.* 37: 467–478.

58. Pedersen, D. V., T. Rösner, A. G. Hansen, K. R. Andersen, S. Thiel, G. R. Andersen, T. Valerius, and N. S. Laursen. 2020. Recruitment of properdin by bi-specific nanobodies activates the alternative pathway of complement. *Mol. Immunol.* 124: 200–210.

59. Spitzer, D., L. M. Mitchell, J. P. Atkinson, and D. E. Hourcade. 2007. Properdin Can Initiate Complement Activation by Binding Specific Target Surfaces and Providing a Platform for De Novo Convertase Assembly. *J. Immunol.* 179: 2600–2608.

60. Kemper, C., J. P. Atkinson, and D. E. Hourcade. 2010. Properdin: Emerging Roles of a Pattern-Recognition Molecule. *Annu. Rev. Immunol* 28: 131–55.

61. Ferreira, V. P., C. Cortes, and M. K. Pangburn. 2010. Native polymeric forms of properdin selectively bind to targets and promote activation of the alternative pathway of complement. *Immunobiology* 215: 932–940.

62. Zaferani, A., R. R. Vivès, P. Van Der Pol, G. J. Navis, M. R. Daha, C. Van Kooten, H. Lortat-Jacob, M. A. Seelen, and J. Van Den Born. 2012. Factor H and properdin recognize different epitopes on renal tubular epithelial heparan sulfate. *J. Biol. Chem.* 287: 31471–31481.

63. Xu, W., S. P. Berger, L. A. Trouw, H. C. de Boer, N. Schlagwein, C. Mutsaers, M. R. Daha, and C. van Kooten. 2008. Properdin Binds to Late Apoptotic and Necrotic Cells Independently of C3b and Regulates Alternative Pathway Complement Activation. *J. Immunol.* 180: 7613–7621.

64. Lammerts, R. G. M., D. T. Talsma, W. A. Dam, M. Daha, M. Seelen, S. P. Berger, and J. Van Den Born. 2020. Properdin pattern recognition on proximal tubular cells is heparan sulfate/Syndecan-1 but not C3b dependent and can be blocked by tick protein Salp20. *Front. Immunol.* 11: 1643.

65. Cortes, C., V. P. Ferreira, and M. K. Pangburn. 2011. Native properdin binds to Chlamydia pneumoniae and promotes complement activation. *Infect. Immun.* 79: 724–731.

66. Farries, T. C., J. T. Finch, P. J. Lachmann, and R. A. Harrison. 1987. Resolution and analysis of "native" and "activated" properdin. *Biochem. J.* 243: 507–517.

67. Harboe, M., C. Johnson, S. Nymo, K. Ekholt, C. Schjalm, J. K. Lindstad, A. Pharo, B. C. Hellerud, K. Nilsson Ekdahl, T. E. Mollnes, et al. 2017. Properdin binding to complement activating surfaces depends on initial C3b deposition. *Proc. Natl. Acad. Sci.* 114: E534–E539.

68. Harboe, M., P. Garred, J. K. Lindstad, A. Pharo, F. Müller, G. L. Stahl, J. D. Lambris, and T. E. Mollnes. 2012. The Role of Properdin in Zymosan- and Escherichia coli -Induced Complement Activation . *J. Immunol.* 189: 2606–2613.

69. Iwaki, D., K. Kanno, M. Takahashi, Y. Endo, N. J. Lynch, W. J. Schwaeble, M. Matsushita, M. Okabe, and T. Fujita. 2006. Small Mannose-Binding Lectin-Associated Protein Plays a Regulatory Role in the Lectin Complement Pathway. *J. Immunol.* 177: 8626–8632.

70. Ninomiya, H., and P. J. Sims. 1992. The human complement regulatory protein CD59 binds to the α-chain of C8 and to the "b" domain of C9. *J. Biol. Chem.* 267: 13675–13680.

71. Schmidt, C. Q., J. D. Lambris, and D. Ricklin. 2016. Protection of host cells by complement regulators. *Immunol. Rev.* 274: 152–171.

72. Podack, E. R., and H. J. Muller-Eberhard. 1979. Isolation of human S-protein, an inhibitor of the membrane attack complex of complement. *J. Biol. Chem.* 254: 9908–9914.

73. Hadders, M. A., D. Bubeck, P. Roversi, S. Hakobyan, F. Forneris, B. P. Morgan, M. K. Pangburn, O. Llorca, S. M. Lea, and P. Gros. 2012. Assembly and Regulation of the Membrane Attack Complex Based on Structures of C5b6 and sC5b9. *Cell Rep.* 1: 200–207.

74. Jenne, D. E., and J. Tschopp. 1989. Molecular structure and functional characterization of a human complement cytolysis inhibitor found in blood and seminal plasma: Identity to sulfated glycoprotein 2, a constituent of rat testis fluid. *Proc. Natl. Acad. Sci. U. S. A.* 86: 7123–7127.

75. Goicoechea De Jorge, E., C. L. Harris, J. Esparza-Gordillo, L. Carreras, E. Aller Arranz, C. Abarrategui Garrido, M. López-Trascasa, P. Sánchez-Corral, B. P. Morgan, and S. Rodríguez De Córdoba. 2007. Gain-of-function mutations in complement factor B are associated with atypical hemolytic uremic syndrome. *Proc. Natl. Acad. Sci. U. S. A.* 104: 240–245.

76. Neher, M. D., S. Weckbach, M. A. Flierl, M. S. Huber-Lang, and P. F. Stahel. 2011. Molecular mechanisms of inflammation and tissue injury after major trauma-is complement the "bad guy"? *J. Biomed. Sci.* 18: 90.

77. Pettigrew, H. D., S. S. Teuber, and M. E. Gershwin. 2009. Clinical significance of complement deficiencies. *Ann. N. Y. Acad. Sci.* 1173: 108–123.

78. Dragon-Durey, M. A., C. Blanc, M. C. Marinozzi, R. A. Van Schaarenburg, and L. A. Trouw. 2013. Autoantibodies against complement components and functional consequences. *Mol. Immunol.* 56: 213–221.

79. Macedo, A. C. L., and L. Isaac. 2016. Systemic lupus erythematosus and deficiencies of early components of the complement classical pathway. *Front. Immunol.* 7: 55.

80. Leffler, J., A. A. Bengtsson, and A. M. Blom. 2014. The complement system in systemic lupus erythematosus: An update. *Ann. Rheum. Dis.* 73: 1601–1606.

81. Lewis, L. A., and S. Ram. 2014. Meningococcal disease and the complement system. *Virulence* 5: 98–126.

82. Fijen, C. A. P., E. J. Kuijper, M. T. Te Bulte, M. R. Daha, and J. Dankert. 1999. Assessment of complement deficiency in patients with meningococcal disease in the Netherlands. *Clin. Infect. Dis.* 28.

83. Schröder-Braunstein, J., and M. Kirschfink. 2019. Complement deficiencies and dysregulation: Pathophysiological consequences, modern analysis, and clinical management. *Mol. Immunol.* 114: 299–311.

84. Thurman, J. M., and V. M. Holers. 2006. The Central Role of the Alternative Complement Pathway in Human Disease. *J. Immunol.* 176: 1305–1310.

85. Risitano, A. M. 2012. Paroxysmal nocturnal hemoglobinuria and other complement-mediated hematological disorders. *Immunobiology* 217: 1080–1087.

86. Takahashi, M., J. Takeda, S. Hirose, R. Hyman, N. Inoue, T. Miyata, E. Ueda, T. Kitani, M. Edward Medof, and T. Kinoshita. 1993. Deficient biosynthesis of N-acetylglucosaminyl-phosphatidylinositol, the first intermediate of glycosyl phosphatidylinositol anchor biosynthesis, in cell lines established from patients with paroxysmal nocturnal hemoglobinuria. *J. Exp. Med.* 177: 517–521.

87. Takeda, J., T. Miyata, K. Kawagoe, Y. Iida, Y. Endo, T. Fujita, M. Takahashi, T. Kitani, and T. Kinoshita. 1993. Deficiency of the GPI anchor caused by a somatic mutation of the PIG-A gene in paroxysmal nocturnal hemoglobinuria. *Cell* 73: 703–711.

88. Józsi, M., S. Strobel, H. M. Dahse, W. S. Liu, P. F. Hoyer, M. Oppermann, C. Skerka, and P. F. Zipfel. 2007. Anti-factor H autoantibodies block C-terminal recognition function of factor H in hemolytic uremic syndrome. *Blood* 110: 1516–1518.

89. Parente, R., S. J. Clark, A. Inforzato, and A. J. Day. 2017. Complement factor H in host defense and immune evasion. *Cell. Mol. Life Sci.* 74: 1605–1624.

90. McHarg, S., S. J. Clark, A. J. Day, and P. N. Bishop. 2015. Age-related macular degeneration and the role of the complement system. *Mol. Immunol.* 67: 43–50.

91. Hourcade, D. E., L. M. Mitchell, and T. J. Oglesby. 1999. Mutations of the type A domain of complement factor B that promote high- affinity C3b-binding. *J. Immunol.* 162: 2906–2911.

92. Daha, M. R., D. T. Fearon, and K. F. Austen. 1976. C3 nephritic factor (C3NeF): stabilization of fluid phase and cell-bound alternative pathway convertase. *J. Immunol.* 116: 1–7.

93. Daha, M. R., D. J. Kok, and L. A. Van Es. 1982. Regulation of the C3 nephritic factor stabilized C3/C5 convertase of complement by purified human erythrocyte C3b receptor. *Clin. Exp. Immunol.* 50: 209–214.

94. Howard, J. F. 2018. Myasthenia gravis: the role of complement at the neuromuscular junction. *Ann. N. Y. Acad. Sci.* 1412: 113–128.

95. Stites, E., M. Le Quintrec, and J. M. Thurman. 2015. The Complement System and Antibody-Mediated Transplant Rejection. *J. Immunol.* 195: 5525–5531.

96. Bhalla, A., N. Alachkar, and S. Alasfar. 2020. Complement-Based Therapy in the Management of Antibody-Mediated Rejection. *Adv. Chronic Kidney Dis.* 27: 138–148.

97. Risitano, A. M., D. C. Mastellos, M. Huber-Lang, D. Yancopoulou, C. Garlanda, F. Ciceri, and J. D. Lambris. 2020. Complement as a target in COVID-19? *Nat. Rev. Immunol.* 20: 343–344.

98. Ricklin, D., and J. D. Lambris. 2013. Complement in Immune and Inflammatory Disorders: Pathophysiological Mechanisms. *J. Immunol.* 190: 3831–3838.

99. Kulasekararaj, A. G., A. Hill, S. T. Rottinghaus, S. Langemeijer, R. Wells, F. A. Gonzalez-Fernandez, A. Gaya, J. W. Lee, E. O. Gutierrez, C. I. Piatek, et al. 2019. Ravulizumab (ALXN1210) vs eculizumab in C5-inhibitor–experienced adult patients with PNH: The 302 study. *Blood* 133: 540–549.

100. Harris, C. L., R. B. Pouw, D. Kavanagh, R. Sun, and D. Ricklin. 2018. Developments in anti-complement therapy;

from disease to clinical trial. *Mol. Immunol.* 102: 89–119.

101. Rother, R. P., S. A. Rollins, C. F. Mojcik, R. A. Brodsky, and L. Bell. 2007. Discovery and development of the complement inhibitor eculizumab for the treatment of paroxysmal nocturnal hemoglobinuria. *Nat. Biotechnol.* 25: 1256–1264.

102. Karki, R. G., J. Powers, N. Mainolfi, K. Anderson, D. B. Belanger, D. Liu, N. Ji, K. Jendza, C. F. Gelin, A. Mac Sweeney, et al. 2019. Design, Synthesis, and Preclinical Characterization of Selective Factor D Inhibitors Targeting the Alternative Complement Pathway. *J. Med. Chem.* 62: 4656–4668.

103. Ricklin, D., D. C. Mastellos, E. S. Reis, and J. D. Lambris. 2017. The renaissance of complement therapeutics. *Nat. Rev. Nephrol.* 14: 26–47.

104. Mainolfi, N., T. Ehara, R. G. Karki, K. Anderson, A. Mac Sweeney, S. M. Liao, U. A. Argikar, K. Jendza, C. Zhang, J. Powers, et al. 2020. Discovery of 4-((2 S,4 S)-4-Ethoxy-1-((5-methoxy-7-methyl-1 H-indol-4-yl)methyl)piperidin-2-yl) benzoic Acid (LNP023), a Factor B Inhibitor Specifically Designed to Be Applicable to Treating a Diverse Array of Complement Mediated Diseases. *J. Med. Chem.* 63: 5697–5722.

105. Mastaglio, S., A. Ruggeri, A. M. Risitano, P. Angelillo, D. Yancopoulou, D. C. Mastellos, M. Huber-Lang, S. Piemontese, A. Assanelli, C. Garlanda, et al. 2020. The first case of COVID-19 treated with the complement C3 inhibitor AMY-101. *Clin. Immunol.* 215: 108450.

106. Maibaum, J., S. M. Liao, A. Vulpetti, N. Ostermann, S. Randl, S. Rüdisser, E. Lorthiois, P. Erbel, B. Kinzel, F. A. Kolb, et al. 2016. Small-molecule factor D inhibitors targeting the alternative complement pathway. *Nat. Chem. Biol.* 12: 1105–1110.

107. Diurno, F., F. G. Numis, G. Porta, F. Cirillo, S. Maddaluno, A. Ragozzino, P. D. E. Negri, C. D. I. Gennaro, A. Pagano, E. Allegorico, et al. 2020. Eculizumab treatment in patients with COVID-19: Preliminary results from real life ASL Napoli 2 Nord experience. *Eur. Rev. Med. Pharmacol. Sci.* 24: 4040–4047.

108. Mastellos, D. C., B. G. P. Pires da Silva, B. A. L. Fonseca, N. P. Fonseca, M. Auxiliadora-Martins, S. Mastaglio, A. Ruggeri, M. Sironi, P. Radermacher, A. Chrysanthopoulou, et al. 2020. Complement C3 vs C5 inhibition in severe COVID-19: Early clinical findings reveal differential biological efficacy. *Clin. Immunol.* 220: 108598.

109. Vlaar, A. P. J., S. de Bruin, M. Busch, S. A. M. E. G. Timmermans, I. E. van Zeggeren, R. Koning, L. ter Horst, E. B. Bulle, F. E. H. P. van Baarle, M. C. G. van de Poll, et al. 2020. Anti-C5a antibody IFX-1 (vilobelimab) treatment versus best supportive care for patients with severe COVID-19 (PANAMO): an exploratory, open-label, phase 2 randomised controlled trial. *Lancet Rheumatol.* .

110. Lin, Z., C. Q. Schmidt, S. Koutsogiannaki, P. Ricci, A. M. Risitano, J. D. Lambris, and D. Ricklin. 2015. Complement C3dg-mediated erythrophagocytosis: Implications for paroxysmal nocturnal hemoglobinuria. *Blood* 126: 891–894.

111. Harder, M. J., N. Kuhn, H. Schrezenmeier, B. Höchsmann, I. Von Zabern, C. Weinstock, T. Simmet, D. Ricklin, J. D. Lambris, A. Skerra, et al. 2017. Incomplete inhibition by eculizumab: Mechanistic evidence for residual C5 activity during strong complement activation. *Blood* 129: 970–980.

112. De Latour, R. P., V. Fremeaux-Bacchi, R. Porcher, A. Xhaard, J. Rosain, D. C. Castaneda, P. Vieira-Martins, S. Roncelin, P. Rodriguez-Otero, A. Plessier, et al. 2015. Assessing complement blockade in patients with paroxysmal nocturnal hemoglobinuria receiving eculizumab. *Blood* 125: 775–783.

113. Kimura, Y., T. Miwa, L. Zhou, and W. C. Song. 2008. Activator-specific requirement of properdin in the initiation and amplification of the alternative pathway complement. *Blood* 111: 732–740.

114. Smith-Jackson, K., and K. J. Marchbank. 2018. Targeting properdin in the treatment of atypical haemolytic uraemic syndrome: better than eculizumab? *Ann. Transl. Med.* 6: S62–S62.

115. Pauly, D., B. M. Nagel, J. Reinders, T. Killian, M. Wulf, S. Ackermann, B. Ehrenstein, P. F. Zipfel, C. Skerka, and B. H. F. Weber. 2014. A novel antibody against human properdin inhibits the alternative complement system and specifically detects properdin from blood samples. *PLoS One* 9.

116. Ueda, Y., T. Miwa, D. Gullipalli, S. Sato, D. Ito, H. Kim, M. Palmer, and W. C. Song. 2018. Blocking Properdin Prevents Complement-Mediated Hemolytic Uremic Syndrome and Systemic Thrombophilia. *J. Am. Soc. Nephrol.* 29: 1928–1937.

117. Gullipalli, D., F. Zhang, S. Sato, Y. Ueda, Y. Kimura, M. Golla, T. Miwa, J. Wang, and W.-C. Song. 2018. Antibody

Inhibition of Properdin Prevents Complement-Mediated Intravascular and Extravascular Hemolysis. *J. Immunol.* 201: 1021–1029.

118. Kimura, Y., L. Zhou, T. Miwa, and W. C. Song. 2010. Genetic and therapeutic targeting of properdin in mice prevents complement-mediated tissue injury. *J. Clin. Invest.* 120: 3545–3554.

119. Sisa, C., Q. Agha-Shah, B. Sanghera, A. Carno, C. Stover, and M. Hristova. 2019. Properdin: A Novel Target for Neuroprotection in Neonatal Hypoxic-Ischemic Brain Injury. *Front. Immunol.* 10: 2610.

Chapter 2

Insights into enhanced complement activation by structures of properdin and its complex with the C-terminal domain of C3b

Ramon M. van den Bos, Nicholas M. Pearce, Joke Granneman, T. Harma C. Brondijk and Piet Gros on behalf of the COMBAT consortium

Crystal and Structural Chemistry, Bijvoet Centre for Biomolecular Research, Department of Chemistry, Utrecht University, Utrecht, The Netherlands.

Corresponding author; PG (p.gros@uu.nl)

This chapter has been published in *Frontiers in Immunology* (2019) **10**: 2097

Abstract

Properdin enhances complement-mediated opsonization of targeted cells and particles for immune clearance. Properdin occurs as dimers, trimers and tetramers in human plasma, which recognize C3b-deposited surfaces, promote formation and prolong the lifetime of C3bBb-enzyme complexes that convert C3 into C3b, thereby enhancing the complement-amplification loop. Here, we report crystal structures of monomerized properdin, which was produced by co-expression of separate N- and C-terminal constructs that yielded monomer-sized properdin complexes that stabilized C3bBb. Consistent with previous low-resolution X-ray and EM data, the crystal structures revealed ring-shaped arrangements that are formed by interactions between thrombospondin type-I repeat (TSR) domains 4 and 6 of one protomer interacting with the N-terminal domain (which adopts a short transforming-growth factor B binding protein-like fold) and domain TSR1 of a second protomer, respectively. Next, a structure of monomerized properdin in complex with the C-terminal domain of C3b showed that properdin-domain TSR5 binds along the C-terminal α-helix of C3b, while two loops, one from domain TSR5 and one from TSR6, extend and fold around the C3b C-terminus like stirrups. This suggest a mechanistic model in which these TSR5 and TSR6 'stirrups' bridge interactions between C3b and factor B or its fragment Bb, and thereby enhance formation of C3bB pro-convertases and stabilize C3bBb convertases. In addition, properdin TSR6 would sterically block binding of the protease factor I to C3b, thus limiting C3b proteolytic degradation. The presence of a valine instead of a third tryptophan in the canonical Trp-ladder of TSR domains in TSR4 allows a remarkable ca. 60°-domain bending motion of TSR4. Together with variable positioning of TSR2 and, putatively, TSR3, this explains the conformational flexibility required for properdin to form dimers, trimers and tetramers. In conclusion, the results indicate that binding avidity of oligomeric properdin is needed to distinguish surface-deposited C3b molecules from soluble C3b or C3 and suggests that properdin-mediated interactions bridging C3b-B and C3b-Bb enhance affinity, thus promoting convertase formation and stabilization. These mechanisms explain the enhancement of complement-mediated opsonization of targeted cells and particle for immune clearance.

Introduction

Complement plays an important role in humoral immune responses against invading microbes, clearance of apoptotic cells and debris, and modulation of adaptive immune responses (1, 2). Initiation of the complement cascades through either the classical, lectin or alternative pathway converges in the formation of C3 convertase complexes, consisting of C3b and protease fragment Bb forming C3bBb, which generates a positive-feedback loop that amplifies the complement cascade yielding massive deposition of C3b onto the targeted surface. At this critical step, the complement system is heavily regulated. Intrinsically, the non-covalent C3bBb enzyme dissociates irreversibly into its components C3b and Bb with a half-life time of 1-2 minutes (3, 4). Host regulators, such as factor H (FH), decay-accelerating factor (DAF) and membrane-cofactor protein (MCP), provide protection of host cells against complement attack (5). FH and DAF inactivate the C3 convertase by promoting dissociation of C3bBb into C3b and Bb (5). FH and MCP have cofactor activity that enables factor I (FI) to bind and cleave C3b into iC3b, rendering it inactive and unable to form new convertases (5, 6).

Properdin is the only known intrinsic positive regulator of the complement system (7–9). Properdin stabilizes C3bBb, increasing the half-life of the enzyme complex five- to ten-fold (10). In addition, it has been indicated that properdin accelerates formation of pro-convertases C3bB (11) and reduces C3b inactivation by FI (12, 13). Furthermore, it has been suggested that, for some bacterial surfaces, apoptotic/necrotic cells or renal epithelial cells, properdin can function as a pattern recognition molecule, forming an initiating platform for the alternative pathway (14–19), although others claim that properdin binding to surfaces depends on initial C3b deposition (20, 21). Properdin deficiency results in increased susceptibility to infection by *Neisseria meningitidis* (22), with high mortality rates compared to deficiency of protein components (C5-C9) of the terminal pathway (23). In addition, properdin deficiency has been associated with other diseases, such as otitis media and pneumonia, as reviewed in Chen *et al.* (23)

Human properdin is an oligomeric plasma protein that is present in serum at relatively low concentrations (4-25 μg/ml) (8), compared to other complement components (~1.2 mg/ml for C3 and ~0.6 mg/ml for factor B (FB)) (24). In contrast to most other complement proteins, properdin is not produced by the liver, but expressed locally by various immune cells including neutrophils, monocytes and dendritic cells (23, 25, 26). Therefore, at sites of inflammation properdin concentrations might be considerably higher than serum concentration. In serum, properdin is predominantly found as dimers, trimers and tetramers in the percentage ratios of 26:54:20% (8), although a small amount of pentamers and hexamers are also found (13, 27). At physiological conditions, no exchange between the oligomeric states of properdin is observed (8), but higher order aggregates form upon freeze-thaw cycles (28). A properdin protomer consists of 442 amino-acid residues with a fully-glycosylated molecular weight of 53 kDa (29). Properdin forms seven domains, an N-terminal domain of unknown fold, followed by six thrombospondin type I repeats (TSR) domains (29). TSR domains consist of approximately 60 amino-acid residues and have a thin and elongated shape (30),

formed by only three anti-parallel peptide chains. The TSR-fold is structurally stabilized by regions forming β-sheets, three conserved disulphide bonds and by a structural WRWRWR motif (also referred to as Trp-ladder (31)) that forms a stack of alternating tryptophans and arginines through π-cation interactions (30). The N-terminal domain has often been referred to as TSR0 (9, 13, 32, 33), despite missing the WRWRWR motif. Properdin is highly post-translationally modified, resulting in 14-17 C-mannosylated tryptophans, four O-linked glycans and one N-linked glycan (34, 35). Negative-stain electron microscopy (EM) has shown that oligomeric properdin forms ring-shaped vertices connected by extended and flexible edges (13, 27). Based on EM images and TSR domain deletions, it has been proposed that the vertices consist of interlocking C- and N-terminal domains of properdin protomers and the edges consist of three bridging TSR domains from a single protomer (13, 27, 29). EM images indicate that each properdin vertex binds a single C3bBb complex (13). Higgens *et al.* (29) showed that domain deletions of properdin TSR domains 4 through 6 results in altered oligomerization and loss of function, whereas deletion of TSR3 has no significant effect on either oligomerization or properdin function. Pedersen *et al.* (32) introduced a proteolytic cleavage site between properdin-domains TSR3 and TSR4 and thereby generated single properdin vertices for crystallographic studies. A 6.0-Å resolution crystal structure of a single properdin vertex in complex with C3bBb (32) (that was stabilized by *S. aureus* inhibitor SCIN (36)) showed that properdin binds to the α-chain region of C3b, revealing density adjacent to the C-terminal C345c (CTC) domain of C3b. However, the resolution of the crystallographic data (PDB ID: 5M6W) did not allow atomic modelling of the cleaved properdin (Pc) fragment.

In this study, we present the production of monomerized properdin variants that stabilize C3bBb using co-expression of properdin N- and C-terminal fragments. We determined crystal structures of monomerized properdin and its complex with the CTC domain of C3/C3b with diffraction data up to 2.0- and 2.3-Å resolution, respectively. These structures reveal the fold of the properdin N-terminal domain, the properdin domain arrangement that yields the properdin ring-shaped vertex structure, stabilization of Trp-Arg interactions in the Trp-ladder provided by tryptophan C-mannosylation, structural flexibility of the TSR4 domain and functionally important extensions of the TSR5 and TSR6 domains. The structure of monomerized properdin in complex with the C3/C3b-CTC domain identifies the specific regions of properdin involved in binding FB and Bb that enhance pro-convertase formation and convertase stabilization, respectively. Finally, we propose a model for properdin oligomers stabilizing convertases on surfaces based on re-analysis of the 5M6W-diffraction data set.

Results

Production of monomerized properdin by co-expression of N- and C-terminal fragments

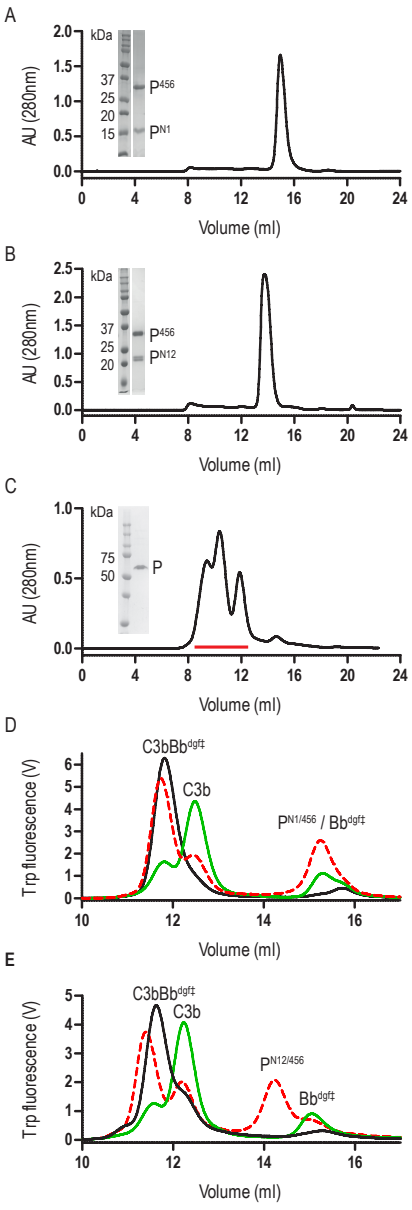

Figure 1 | Purification of properdin and stabilization of C3 convertase.

(A-C) SEC elution profile and SDS-page of **(A)** $P^{N1/456}$, **(B)** $P^{N12/456}$ and **(C)** properdin. Pooled properdin fractions are indicated by the red line. **(D)** SEC elution profiles of C3 convertase ($C3bBb^{dgf‡}$) incubated in the presence (red dashed line) or absence (green line) of $P^{N1/456}$ for one hour at 37°C compared to the sample at t=0 (black line). **(E)** As panel D but with $P^{N12/456}$ instead of $P^{N1/456}$.

We generated N-terminal constructs of properdin, comprising the N-terminal domain of unknown fold and TSR1, TSR2 and TSR3, denoted P^{N1} (res. 28-132), P^{N12} (res. 28-191) and P^{N123} (res. 28-255), and a C-terminal construct comprising TSR4, TSR5 and TSR6, P^{456} (res. 256-469). Small scale expression of isolated His_6-tagged terminal fragments followed by IMAC-affinity purification resulted in no significant expression of P^{456}, whereas co-expression of N- and C-terminal fragments yielded both fragments in approximately 1:1 ratio in all cases. We therefore decided to continue with large-scale co-expression of the two shorter N-terminal fragments, P^{N1} and P^{N12}, with P^{456} with the latter carrying a C-terminal His_6-tag (see **Methods**). IMAC-affinity purification yielded stable protein complexes consistent with one-to-one non-covalent complexes of P^{N1} with P^{456} and P^{N12} with P^{456}, denoted $P^{N1/456}$ and $P^{N12/456}$, respectively. Both $P^{N1/456}$ and $P^{N12/456}$ yielded monodisperse peaks during size-exclusion chromatography (SEC) consistent with a single monomerized species (**Fig. 1A-B**), whereas recombinant full-length properdin produced a SEC spectrum with multiple peaks consistent with a mixture of dimeric, trimeric and tetrameric properdin (**Fig. 1C**). Large-scale expression and purification of $P^{N1/456}$ and $P^{N12/456}$ yielded ca. 5-8 mg per liter culture.

Monomerized properdin binds and stabilizes C3 convertases

Stabilization of C3 convertases was analyzed by monitoring the decay of pre-formed C3bBb in the presence and absence of properdin (**Fig. 1D-E**). In the absence of properdin, ~75% of the $C3bBb^{dgf‡}$ was dissociated into C3b and $Bb^{dgf‡}$ after one hour at 37 °C, whereas in the presence of $P^{N1/456}$ or $P^{N12/456}$ dissociation of $C3bBb^{dgf‡}$ was reduced to ~20-25%, indicating that $P^{N1/456}$ and $P^{N12/456}$ stabilized C3 convertase to a similar extent.

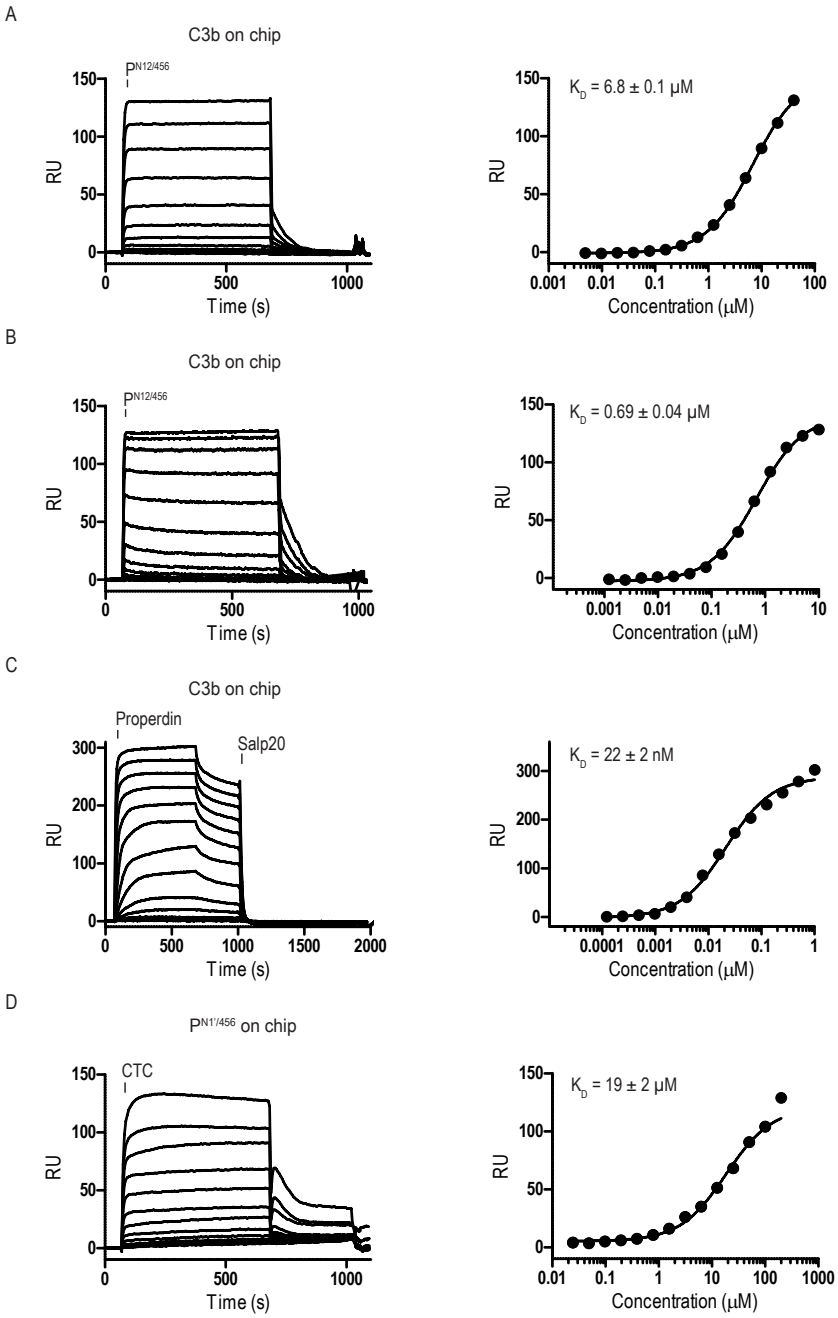

Figure 2 | Surface Plasmon Resonance (SPR) analysis showing interaction of properdin with C3b and the C3b/C3 CTC domain.

SPR sensorgrams (left) and equilibrium binding plots (right). **(A)** Interaction of $P^{N12/456}$ (concentration range: $4.9x10^{-3}$ µM to 40 µM) with a C3b coated chip at physiological ionic strength (150 mM NaCl). **(B)** interaction of $P^{N12/456}$ (concentration range: $1.2x10^{-3}$ µM to 10 µM) with a C3b coated chip at low ionic strength (50 mM NaCl). **(C)** Interaction of properdin (concentration range: $1.2x10^{-4}$ µM to 1 µM) with a C3b coated chip. **(D)** Binding of the C3/C3b CTC domain (concentration range: $2.4x10^{-2}$ µM to 200 µM) to a $P^{N1'/456}$ coated chip. The data point at 200 µM C3/C3b CTC was considered as an outlier and was not used to determine the K_D. Where indicated Salp20 was used to regenerate the surface.

Binding affinities of $P^{N12/456}$ for C3b, pro-convertase C3bB and convertase C3bBb were determined using surface plasmon resonance (SPR) equilibrium binding experiments. C3b was biotinylated at its reactive thioester, which allows coupling to streptavidin-coated SPR sensor chips in an orientation reflecting that of surface bound C3b. Under physiological salt conditions, $P^{N12/456}$ bound C3b with a K_D of 6.8 ± 0.2 μM, which is similar to the K_D of 7.8 μM reported by Pedersen *et al.* for single properdin vertices generated by proteolytic cleavage (32), but much lower than the apparent K_D of 22 ± 2 nM for oligomeric properdin (**Fig. 2**). At low ionic strength (50 mM NaCl), interaction between $P^{N12/456}$ and C3b appeared much stronger with a K_D of 0.69 ± 0.04 μM. Next, we generated pro-convertases C3bB and convertases C3bBb on the chip (see **Methods**). $P^{N12/456}$ bound C3bB and C3bBb with a K_D of 98 ± 2 nM and 34 ± 1 nM, respectively (**Fig. 3**), whereas properdin oligomers bound with an apparent K_D of 4.6 ± 1 nM and 4.4 ± 1 nM, respectively. Thus, $P^{N12/456}$ binds to C3b, C3bB and C3bBb (in order of increasing affinity).

Previous data (13, 32) suggested that the main interaction site of properdin with C3b is localized on the C3b-CTC domain. Therefore, we analyzed binding of the isolated C3/C3b-CTC domain to a $P^{N1'/456}$ coated SPR chip. The C3/C3b-CTC domain binds $P^{N1'/456}$ with a K_D of 18.6 ± 1.6 μM, which is comparable to the K_D of 6.8 ± 0.2 μM we observed for C3b and $P^{N12/456}$, suggesting that the primary binding interface of C3b is indeed provided by the CTC domain (**Fig. 2**). Overall, these data indicated that the non-covalent complexes $P^{N1/456}$ and $P^{N12/456}$ bound C3b and stabilized C3bBb similar to an excised monomeric version of full-length oligomeric properdin.

Structure determination of monomerized properdin and its complex with C3/C3b-CTC

$P^{N1/456}$ and $P^{N12/456}$ crystallized as thin plates, and resulted in highly anisotropic data, with anisotropic resolution limits of 2.0-2.9 Å and 2.5-3.9 Å, respectively. $P^{N1/456}$ in complex with C3/C3b-CTC crystallized as long rods and pyramids. While the pyramid-shaped crystals showed poor diffraction, $P^{N1/456}$-CTC rod-shaped crystals diffracted anisotropically with resolution limits of 2.3-2.7 Å. Data collection statistics are shown in **Table 1.**

We first determined the crystal structure of $P^{N1/456}$ in complex with C3/C3b-CTC using the C3b-CTC domain (PDB ID: 5FO7 (37)) as a search model for molecular replacement with Phaser (38). A minimal TSR model was generated with Sculptor (39) using a sequence alignment (40) of TSR1, TSR4, TSR5 and TSR6 in combination with TSR2 from thrombospondin-1 (PDB ID: 1LSL (30)). This model was then used in subsequent rounds of molecular replacement, which resulted in the positioning of TSR1, 4, 5 and half of TSR6 accounting for approximately 80% of the total structure. The N-terminal domain and the remaining part of TSR6 were built using Coot (41). Structure determination continued with further rounds of model building (41) and structure refinement (42), until convergence. The refined model of $P^{N1/456}$ taken from $P^{N1/456}$-

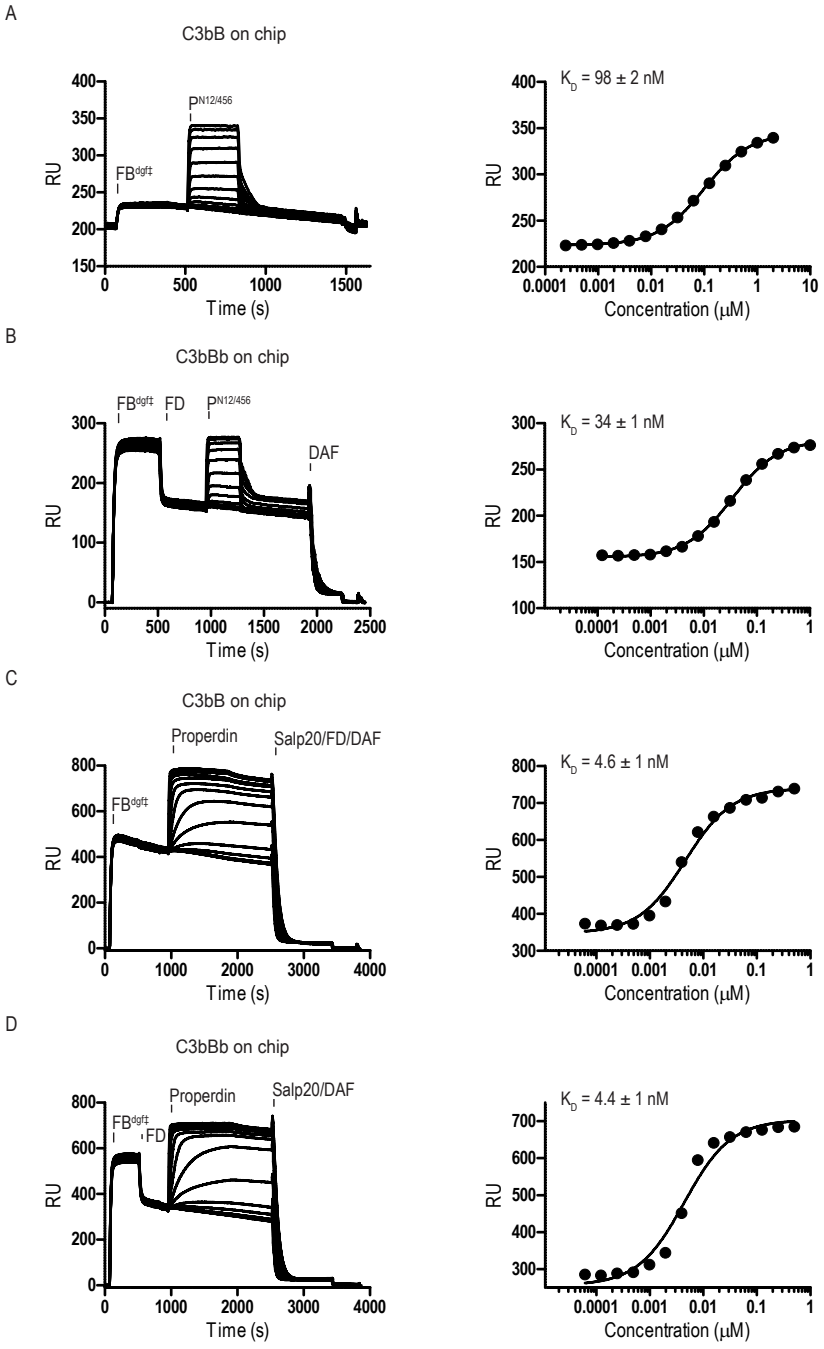

Figure 3 | SPR analysis showing interaction of properdin with C3 (pro)-convertase.

SPR sensorgrams (left) and equilibrium binding plots (right). $C3bB^{dgf‡}$ and $C3bBb^{dgf‡}$ were generated on the chip by injecting $FB^{dgf‡}$ or $FB^{dgf‡}$ and subsequently FD on a C3b coated chip. **(A)** Interaction of $P^{N12/456}$ (concentration range: $2.4x10^{-4}$ μM to 2 μM) with $C3bB^{dgf‡}$. **(B)** Interaction of $P^{N12/456}$ (concentration range: $1.2x10^{-4}$ μM to 1 μM) with $C3bBb^{dgf‡}$. **(C)** Interaction of properdin (concentration range: $6.1x10^{-5}$ μM to 0.5 μM) with $C3bB^{dgf‡}$. **(D)** Interaction of properdin (concentration range: $6.1x10^{-5}$ μM to 0.5 μM) with $C3bBb^{dgf‡}$. Where indicated Salp20, FD and DAF were used to regenerate the surface.

CTC was used in molecular replacement to solve the structures of $P^{N1/456}$ and $P^{N12/456}$. After initial placement, $P^{N12/456}$ was completed by molecular replacement using the TSR model. Model refinement statistics for all structures are listed in **Table 1**, final models are shown in **Figure 4**.

Fold of the properdin N-terminal domain

The crystal structure of properdin revealed that the N-terminal domain (res. 28-76) adopts a compact globular fold, containing two β-sheets and a single α-helix stabilized by three disulphide bonds (**Fig. 4B**). A homology search using the Dali server (43) indicated that the properdin N-terminal domain is most closely related to transforming growth factor β binding protein-like (TB) domains; the closest structural homologues for the properdin N-terminal domain are the TB domains of human follistatin (PDB ID 5JHW, chain C/D, Dali z-score 5.9) and follistatin-like 3 (PDB ID 3B4V chain H, Dali z-score 5.6) and the hyb2 and TB4 domains of human Fibrillin-1 (respectively: PDB ID 2W86, Dali z-score 5.4; PDB ID: 1UZQ, Dali z-score 5.2) (44). TB domains are characterized by 8 cysteines resulting in a 1-3, 2-6, 4-7 and, though not always present, 5-8 disulphide pattern, where the 5-8 disulphide links the domain core to the C-terminal tail and Cys3, 4 and 5 form a characteristic triple cysteine motif (45, 46). The properdin N-terminal domain contains three disulphides that match the 1-3, 2-6, 4-7 disulphides of the TB core and misses the 5-8 disulphide and connecting C-terminal tail. We refer to this as the short TB (STB) fold.

Properdin-TSR domains

Five of the six TSR domains of properdin are present in the structures of $P^{N1/456}$, $P^{N12/456}$ and $P^{N1/456}$-CTC (**Fig. 4**). The TSR domains of properdin display minor to major variations from the TSR domain fold as described for the structures of TSR2 and 3 from thrombospondin-1 (30); these are shown schematically in **Figure 4B**.

Compared to TSR2 and 3 from thrombospondin-1, properdin domain TSR1 (res. 77-133) lacks a five-residue β-bulge preceding β-strand C, referred to as 'jar-handle' motif, that provides H-bonding interactions with the indole ring of the first tryptophan of the Trp-ladder. Instead of this β-bulge, the C-strand in TSR1 is extended by two residues and the typical H-bonding interactions of the β-bulge are substituted by Ser112 in the B-C loop, which is observed within H-bond distance of the Trp80 indole ring. In the TSR1-Trp ladder, a glutamine residue resides at the position of the third arginine, resulting in a lost π-cation interaction with the last Trp. Preceding the prototypical C-terminal Cys (Cys133), TSR1 contains an additional cysteine (Cys132) that connects to Cys170 of TSR2, as observed in the structure of $P^{N12/456}$ (**Fig. 5A**). However, our construct P^{N1} is terminated at Cys132. As a consequence, we observed a non-native disulphide bond between Cys93-Cys132 and increased disorder at the C-terminal end

2

Table 1, Diffraction-data collection and refinement statistics

	$P^{N1/456}$-CTC	$P^{N1/456}$	$P^{N12/456}$
Wavelength (Å)	0.9789	0.9789	0.9763
Resolution range	63.08 - 2.31 (2.60-2.31)	79.61 - 2.03 (2.31 - 2.03)	102.88 - 2.52 (2.71 - 2.52)
Space group	P 21 21 21	C 1 2 1	I 4 2 2
Cell dimensions			
a, b, c (Å)	71.47, 71.50, 134.18	112.00, 114.86, 39.82	114.75, 114.75, 232.26
α, β, γ (°)	90, 90, 90	90, 99.56, 90	90, 90, 90
Total reflections	113,523 (7,011)	60,691 (2,967)	142,792 (8,720)
Unique reflections	21,145 (1,538)	17,424 (871)	16,212 (810)
Multiplicity	5.4 (4.6)	3.5 (3.4)	8.8 (10.8)
Completeness (Spherical)	68.6 (17.1)	54.5 (8.7)	60.5 (15.5)
Completeness (ellipsoidal)	90.3 (71.1)	89.5 (61.1)	93.6 (71.3)
Diffraction limits & eigenvectors of ellipsoid fitted to diffraction cut-off surface: (Å)	a*: 2.705 b*: 2.647 c*: 2.287	0.952 a* - 0.307 c*: 2.027 b*: 2.289 0.926 a* + 0.377 c*: 2.979	a*: 2.515 b*: 2.515 c*: 3.914
Mean I/sigma(I)	11.1 (1.5)	3.4 (1.5)	7.5 (1.5)
Wilson B-factor (Å²)	47.02	23.66	53.29
R-merge	0.100 (1.267)	0.161 (1.249)	0.185 (1.639)
R-pim	0.047 (0.637)	0.100 (0.784)	0.089 (0.726)
CC1/2	0.996 (0.560)	0.982 (0.469)	0.996 (0.629)
Reflections used in refinement	21,137	17,421	16,209
R-work/R-free	0.230/0.277	0.212/0.248	0.248/0.267
Number of non-hydrogen atoms	3,645	2,589	2,906
Macromolecules	3,452	2,343	2,705
Ligands	123	130	190
Solvent	70	116	11
RMS (bonds) (Å)/ (angles) (°)	0.014 / 1.82	0.014 / 1.87	0.014 / 1.97
Ramachandran outliers (%)	0.67	0	0.55
Rotamer outliers (%)	3.65	2.38	7.42
Clashscore	2.80	5.92	8.24
Average ADP (Å²)	52.83	29.76	64.02
macromolecules	52.88	29.62	63.25
ligands	58.33	34.92	76.76
Solvent	40.23	26.87	32.57

Values in parentheses are for reflections in the highest resolution shell. The * denotes reciprocal space.

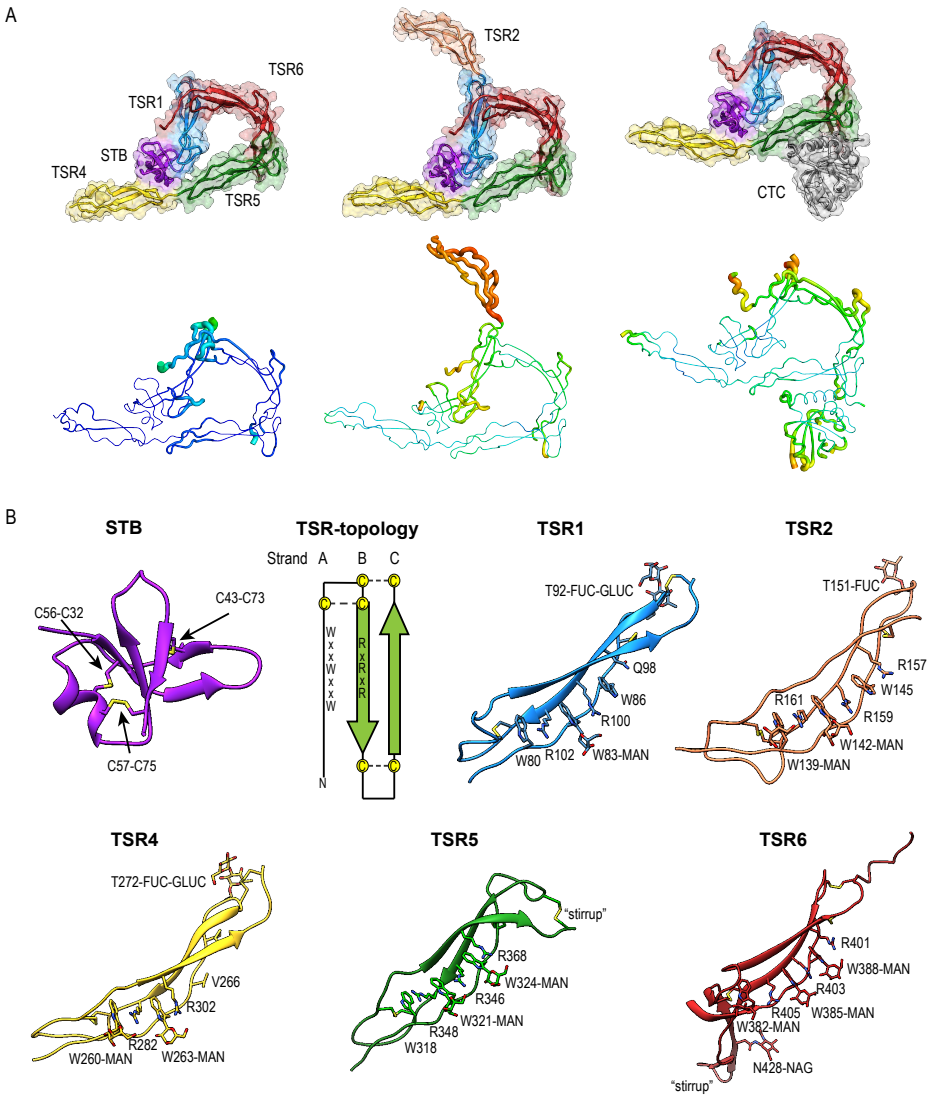

Figure 4 | Overview of properdin structures.

(A) From left to right: $P^{N1/456}$, $P^{N12/456}$ and $P^{N1/456}$-CTC. Structures are depicted in cartoon representation with a semi-transparent molecular surface (top row) and as ADP cartoon putty (bottom row)). ADP colors for all three structures are on the same scale of 10-140 Å^2. **(B)** Cartoon representation of individual properdin domains; the TSR Trp-ladder residues, disulphides and glycans are depicted as sticks. A schematic representation of the general TSR domain topology is included, showing the three strands and the position of the WxxWxxW and RxRxR motifs; the three disulphides are represented by dashed lines. TSR domains are shown with the Trp-ladder in approximately the same orientation. TSR1 and TSR2 were taken from $FP^{N12/456}$, TSR6 from $FP^{N1/456}$-CTC and STB, TSR4 & TSR5 from $FP^{N1/456}$. Unless stated otherwise, domains are colored as follows: STB (purple), TSR1 (blue), TSR2 (coral), TSR4 (yellow), TSR5 (green), TSR6 (red) from properdin and the C3/C3b CTC domain (grey).

of TSR1 in the structure of $P^{N1/456}$ and $P^{N1/456}$-CTC (**Fig. 5B**); however, the overall fold of TSR1 was not affected.

TSR2 (res. 134-191) displayed the consensus TSR fold, with only minor deviations besides the additional cysteine (Cys170).However, this domain was not well defined by

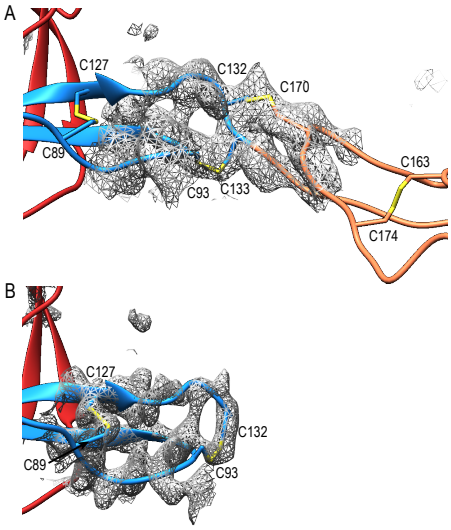

Figure 5 | Disulphides at the properdin TSR1-TSR2 interface.

(A) Cartoon representation of the TSR1-TSR2 interface in $P^{N12/456}$ with disulphides represented as sticks. The terminal Cys133 of TSR1 forms the canonical disulphide with Cys93 in the TSR1 A-B loop, whereas Cys132 forms a disulphide with Cys170 in the B-C loop of TSR2. **(B)** The TSR1 distal end in $P^{N1/456}$ showing the "incorrect" disulphide between Cys132 and Cys93. Electron density is shown at 1-rmsd contour level. Colors are as follows: TSR1 (blue), TSR2 (coral), TSR6 (red) and disulphides are shown in yellow.

the density as reflected by its high atomic displacement parameters (ADP) (**Fig. 4A**).

TSR4 (res. 256-312) showed striking variations in the structures of $P^{N1/456}$, $P^{N12/456}$ and $P^{N1/456}$-CTC (**Fig. 6A-B**). In the Trp-ladder of TSR4 the canonical third tryptophan is replaced by a valine (Val266). A comparison of TSR4 from all three structures shows that TSR4 displays a bending-like motion at this position (**Fig. 6A-B**). The distal part of TSR4 is held in place by interaction with the STB domain, but the proximal part, where the short Trp-ladder, comprising Trp260 and Trp263 in strand A, Arg282 in strand B and Arg302 in strand C, is located is at a different position in each of the three structures resulting in a distance of 28.3 Å between the Cα atoms of TSR4 Ser255 in $P^{N1/456}$ and $P^{N12/456}$.

TSR5 (res. 313-376) displayed well-defined electron density in all three structures and closely resembled the TSR-consensus fold. However, the canonical third arginine in strand B of TSR5 is replaced by Gln344. Gln344 forms a H-bond with Arg368 from strand C and Arg364 is in π-cation stacking conformation with Trp324. Thus, the stacking of Trp-ladder residues is effectively conserved. The most striking feature of TSR5 is a six-residue insertion (res. 328-333) (29), in the A-B loop between Cys327 and Cys337 that forms a loop that protrudes from the TSR domain.

TSR6 (res. 377-469) showed a larger deviation from the typical TSR-fold and has a boomerang-like appearance, due to a 22 residue-long insertion (res. 412-434) (29) in the B-C loop. This insertion forms a β-hairpin loop that protrudes from the TSR6-core (**Fig. 4B**). The core part of TSR6 makes an angle of 147° with TSR5, pointing towards TSR1, and the TSR6 β-hairpin protrudes at a 70° angle from the domain core towards and beyond TSR5. Residues 430-438 from the TSR6 β-hairpin are part of a β-sheet with the end of strand C from TSR5 (**Fig. 7**). A hydrophobic core consisting of Pro435, Tyr371 and Ile373 from TSR5 and Leu378, Leu411, Pro412, Tyr414, Val418, Val429 and Phe431 from TSR6 stabilizes the base of the β-hairpin. Similar to TSR1, TSR6 lacks a 'jar-handle' motif. In this case, the jar-handle H-bonding interactions are substituted by the backbone carbonyl from Glu440 in the B-C loop, which forms a H-bond with NH1 of the first Trp, Trp382, of the Trp-ladder. In TSR6 Arg405 is not stabilized by a residue from strand C and both Arg405 and Trp382 are not in a π-cation stacking conformation and thus do not contribute to the stability of the Trp-ladder.

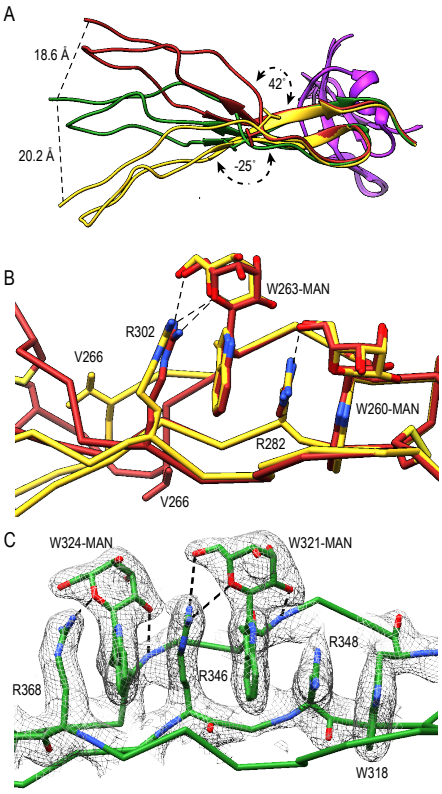

Figure 6 | A shorter Trp-ladder allows structural flexibility of TSR4.

(A) Cartoon representation of TSR4 from $P^{N1/456}$ (yellow), $P^{N12/456}$ (red) and $P^{N1/456}$-CTC (green). Structures were superposed using the STB domain, shown in purple, as reference. The TSR4 domain is bent at the position of V266 (shown in sticks) resulting in distances of 18.6 Å, 20.2 Å and 28.3 Å between the Cα-atoms of the N-terminal residues (S255) in each of the three models. The angle between the proximal (residues 256-266 and 279-303) and distal (residues 267-278 and 304-312) parts of TSR4 are indicated. **(B)** Trp-ladder residues in TSR4 from $P^{N1/456}$ (yellow) and $P^{N12/456}$ (red) showing the distortion of the TSR domain at the position of the missing third tryptophan, which is replaced by Val266. **(C)** Trp-ladder residues in TSR5 (green) shown as representative for a prototypical TSR Trp-ladder, The TSR-fold is stabilised by mannosyl-Trp/Arg H-bonds. Trp-ladder residues are shown in sticks and electron density is shown at 1-rmsd contour level. H-bonds are indicated as dashed lines.

Properdin glycosylation

The tryptophans of TSR Trp-ladders are typically C-type mannosylated, where the C1 of an α-mannose is attached to the C2 in the indole ring of the Trp (34, 35, 47). We could clearly identify C-mannosylation for 11 out of 14 Trp-ladder tryptophans (**Fig. 4B**). For the majority of these, we observe that the O2 oxygen of the mannosyl-Trp moiety interacts with its backbone nitrogen, whereas the O5 and O6 oxygens form H-bonds with the side chain of the adjacent Arg, which further stabilizes the TSR domain fold (**Fig. 6B-C**). In addition to C-mannosylation, TSR domains usually display O-linked glycosylation of a Thr or Ser residue that precedes the cysteine in loop A-B (35, 48, 49). This glycosylation constitutes the attachment of a β-glucose-1,3-α-fucose glycan through a linkage between the C1 atom of the fucose and the Thr or Ser side chain oxygen (49). In $P^{N12/456}$, we observe O-fucosylation of TSR1 (Thr92), TSR2 (Thr151) and TSR4 (Thr272) (**Fig. 4B**), although the TSR2 glycan is poorly defined. In all structures, the O-fucosylation of TSR4 is especially well defined and is involved in properdin oligomerization, as described below. Finally, we observe N-glycosylation of Asn428, which is located in the B-C loop insertion in TSR6 and has been shown not to be important in properdin function (29).

Properdin oligomerization

A previously reported model for properdin oligomerization described the properdin vertex as a ring formed by four TSR domains each comprising a quarter of the ring (13) and formed by two inter protomer contacts (13, 27). The structures of $P^{N1/456}$ and $P^{N12/456}$ showed that the properdin vertex consists of the STB domain, TSR1, part of TSR4, TSR5 and TSR6 domains. These domains form a ring-like structure through interfaces formed by the STB and TSR1 domains with TSR4 and TSR6, respectively. TSR2 and approximately 66% of TSR4 are protruding from the

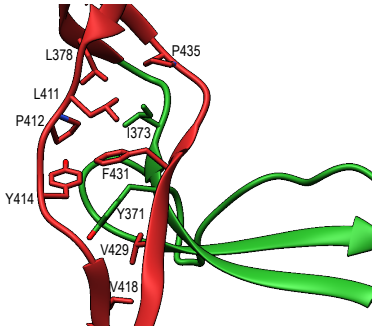

Figure 7 | Interactions between TSR5 and TSR6 stabilise the TSR6 β-hairpin.

Cartoon representation of the TSR5/TSR6 (green/red) interface with residues that form the hydrophobic core that stabilises the TSR6 β-hairpin shown in sticks.

vertex and form the properdin edges along with TSR3, which is absent in $P^{N1/456}$ and $P^{N12/456}$. The boomerang-shaped TSR6 forms approximately half of the ring, with an extensive interface between the distal end of TSR6 and TSR1, and the long insertion in the B-C loop of TSR6 locked firmly in place by interactions with TSR5 (**Fig. 7**).

The interface between TSR6 and TSR1 is formed by the distal end of TSR6, which includes the A-B loop and the C-terminal region of strand C, and the β-sheet of TSR1 (**Fig. 8 AB**). This interface is predominantly mediated by hydrophobic interactions, involving residues Leu99, Tyr101, Trp122 and Leu124 from TSR1 and Pro399, Pro459, Pro464, Cys391-Cys455 and Cys395-Cys461 from TSR6. In addition, hydrogen bonds are formed between the backbone atoms of Leu124 from TSR1 and Cys391 in TSR6, respectively, and between sidechains of Ser90 and Ser97 and the backbone carbonyl of His457 and Leu456 respectively. Additionally, salt bridges are formed between Glu95 and Arg103 in TSR1 and Arg401 and Asp463 in TSR6. The interaction between Glu95 and Arg401 is not visible in $P^{N1/456}$-CTC since the region containing Glu95 is not well defined in this structure.

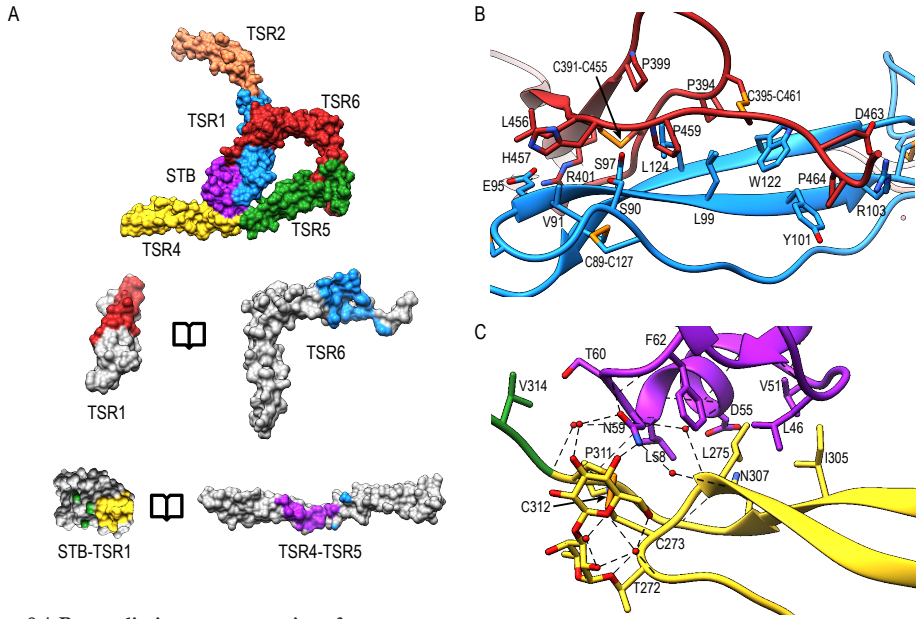

Figure 8 | Properdin inter-protomer interfaces.

(A) (top) Surface representation of $P^{N12/456}$ colored by individual domains: STB (purple), TSR1 (blue), TSR2 (coral), TSR4 (yellow), TSR5 (green), and TSR6 (red). (bottom) Individual TSR domains with atoms colored by interaction with the opposing protomer (contacts defined as atoms within 5 Å). **(B)** Interactions between TSR1 and TSR6 with key residues involved in the interaction shown in stick representations. **(C)** As panel B for interactions between STB and TSR4/5. For clarity disulphides are colored orange.

The second interface between properdin protomers is formed by the STB domain and TSR4 (**Fig. 8A-B**). This interface is characterized by a hydrophobic core involving Leu47, Val51, Leu58, Phe62 from the STB domain and Leu275, Ile305 and Pro311 in TSR4. In addition, there are hydrophilic interactions between Asp55 and the backbone carbonyl moiety of Leu58 from the STB domain and Asn307 and the backbone nitrogen of Cys312 of TSR4, respectively. The O-linked glycan on Thr272 from TSR4 contributes directly to the interaction via a hydrogen bond with Asn59 on the STB domain as well as multiple water-mediated interactions.

Interaction of properdin with C3b

In $P^{N1/456}$-CTC, properdin-TSR5 sits on top of the C3/C3b-CTC domain with an approximate angle of 20° between the main body of TSR5 and the C3/C3b-CTC C-terminal α-helix (**Fig. 9A**). This interface is characterized by mainly hydrophilic interactions, involving TSR5 residues Gln343, Gln363, Gln364, His369, and C3/C3b-CTC residues Gln1638, Gln1643 and Glu1654, and a salt bridge between TSR5 Arg359 and C3/C3b-CTC Asp1639 (**Fig. 9B**). The C-terminal end of the C3/C3b-CTC α-helix is embraced by two loops, which resemble stirrups, formed by the insertions in the core structure of properdin TSR5 and TSR6, respectively (TSR5 res. 328-333 and TSR 6 res. 419-426) (**Fig. 9C**). The TSR6 stirrup is partially disordered in the absence of C3/C3b-CTC, but well defined in the $P^{N1/456}$-CTC complex. The two 'stirrups' provide additional properdin-C3b interactions; the TSR5 stirrup interacts with C3/C3b-CTC through cation-π stacking of Arg329 with C3/C3b Phe1659 and a hydrogen bond between Arg330 and the main-chain oxygen of C3/C3b Gly1660. In the TSR6 stirrup, Lys427 forms a salt bridge with C3/C3b Glu1654. This interaction is further stabilized by hydrogen bonds between the TSR6 Glu422 side chain with backbone atoms from Ser1571 and Thr1568 from the C3/C3b-CTC domain and backbone mediated interactions between Val421 and Glu422 from the TSR6 stirrup with C3/C3b Val1657 and Val1658, respectively (**Fig. 9C**).

To gain insights into the properdin interactions with the C3bBb complex, we modeled and refined the structure of the proteolytic fragment Pc in complex with the SCIN-stabilized C3bBb convertase (PDB ID: 5M6W) (32). Modeling properdin in the density of 5M6W (**see Methods**) resulted in a significant improvement of the refinement statistics (Rfree/Rwork = 0.264/0.219, compared to Rfree/Rwork = 0.315/0.262, when not including properdin). The structure comprises two copies of the SCIN stabilized C3bBbPc complex with density for TSR3 only detectable in one copy (**Fig. 9D**). In both copies of the C3bBb-SCIN-Pc complex, the ring-like structure of properdin and the interface with C3b are similar as observed for $P^{N1/456}$ in complex with C3/C3b CTC domain. Although the stirrup loops of TSR5 and TSR6 are in the vicinity of the VWA domain of Bb, we observe only two contacts between properdin and Bb within 3.2 Å in the model. The side chains of Lys350 (325 in 5M6W) of Bb and Val421 of properdin are within 2.8 Å and the side chains Met394 (369 in 5M6W) of Bb and Glu422 of

properdin are within 3.1 Å distance, thus no direct interactions are apparent between properdin and Bb in the structural model (**Fig. 9E**).

The two C3bBbPc complexes in the asymmetric unit show variation in both TSR4 and TSR2-TSR3; In one of the complexes the conformation of TSR4 is similar to that of TSR4 from $P^{N1/456}$, in the second C3bBbPc complex TSR4 is once again bent at the position of V266, but at an angle that does not correspond to TSR4 in $P^{N1/456}$, $P^{N112/456}$ or $P^{N1/456}$-CTC, showing that TSR4 has an even greater range of motion. This structural

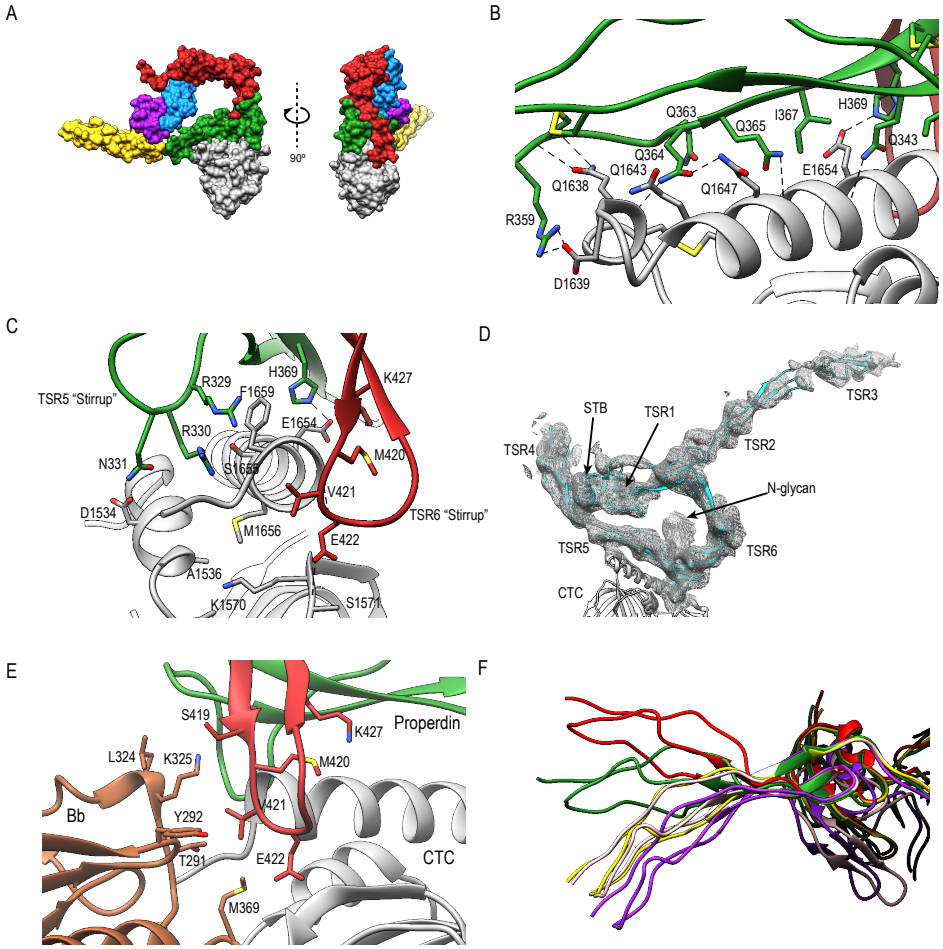

Figure 9 | Properdin-convertase interactions.

(A) Surface representation of $P^{N1/456}$-CTC. Domains colored as follows: STB (purple), TSR1 (blue), TSR4 (yellow), TSR5 (green), TSR6 (red) from properdin, the C3/C3b CTC domain (grey) and Bb (brown). **(B)** Detailed view of the interaction between TSR5 and the C3/C3b CTC C-terminal α-helix. **(C)** Side view of $P^{N1/456}$-CTC, 90° rotated compared to panel B showing details of the interaction between the TSR5 and TSR6 stirrup loops and C3/C3b-CTC. In panels B and C proteins are shown in cartoon representation with side chains of key residues that are involved in the interaction shown in sticks. H-bonds are indicated as dashed lines. **(D)** Detail of the properdin-C3bBb-SCIN complex showing electron density at 1-rmsd contour level. **(E)** Close-up of the properdin-C3b-Bb interface showing the two properdin stirrup-loops that are sandwiched between C3b and Bb. Putative interaction in the properdin-C3bBb interface are shown as sticks. **(F)** TSR4 from all five properdin structures that are described in this paper: $P^{N1/456}$ (yellow), $P^{N12/456}$ (red), $P^{N1/456}$-CTC (green) and two copies of properdin in the properdin-C3bBb-SCIN complex (purple and pink) with models superposed using the distal part of TSR4 (residues 267-278 and 304-312).

variability of the TSR4 conformation results in a ~60° angle that is covered by TSR4 in all properdin models **(Fig. 9F).** Similarly, TSR2 also shows structural flexibility; the orientation of TSR2 in one C3bBbPc complex matches the orientation observed in $P^{N12/456}$, whereas in the other copy TSR2 is at a 58° angle compared to TSR2 from $P^{N12/456}$ (**Fig. 10A**). Using the different conformations observed for TSR2 and TSR4 we were able to build models for properdin dimers, trimers and tetramers bound to a C3bBb coated surface **(Fig. 10B)**. In these models, the properdin ring-like vertices (comprising STB, TSR1 and (the distal end of) TSR4', TSR5' and TSR6' (with domains from a second protomer indicated by an apostrophe), are orientated perpendicular to the plane of the surface, with the edges comprising TSR2, TSR3 and the proximal part of TSR4 roughly parallel to the surface.

Discussion

Previous biochemical data (11, 12, 21) has indicated that properdin enhances complement activity by binding and stabilizing surface-bound C3 pro-convertases (C3bB) and convertases (C3bBb) of the alternative-pathway. Low-resolution structural data suggested that properdin binds C3 convertases at the α'-chain of C3b (13, 32), consistent with stabilization through putative bridging interactions between C3b and FB or fragment Bb of the pro-convertase and convertase, respectively. The crystallographic data presented here has provided atomic models of the ring-shaped structures previously observed in low-resolution EM images of full-length oligomeric properdin (13, 27) and in a crystal of C3bBb-SCIN in complex with the proteolytic Pc fragment at 6-Å resolution (32). Our high-resolution data reveals the STB-domain fold adopted by the N-terminal domain, the structural variations and post-translational modifications present in the TSR domains and the non-covalent binding interfaces between N-terminal domains STB and TSR1 and C-terminal domains TSR4 and TSR6, respectively, of two different protomers needed to form the ring-shaped structures of properdin. Next, our data of properdin in complex with the CTC domain of C3b shows the interaction details that position properdin on top of a C3b molecule, when C3b is covalently bound to a target surface, and identified two 'stirrup-like' loops, formed by inserts into TSR-folds of TSR5 and TSR6, as interaction sites for binding the VWA domain of FB and Bb for stabilizing the C3 pro-convertase and convertase, respectively.

Mass spectrometry of plasma-derived full-length properdin indicated complete C-mannosylation of 14 out of the 17 tryptophans present in the WRWRWR motifs and no or partial C-mannosylation of the remaining three (Trp80, 202 and 318), in addition to three fully (Thr151, Ser208 and Thr272) and one partially occupied (Thr92) O-fucosylation sites and a single N-linked glycosylation site (Asn428) (34, 35) (**Fig. 4B**). We observed that the C-mannosyl moieties on tryptophan are part of common H-bonding networks that also include the backbone nitrogen of the mannosylated Trp (positioned on strand A), the guanidium head group of the arginine distal to the Trp (in strand B) and a polar or negatively charged side chain of the residue opposing the Arg (in strand C),

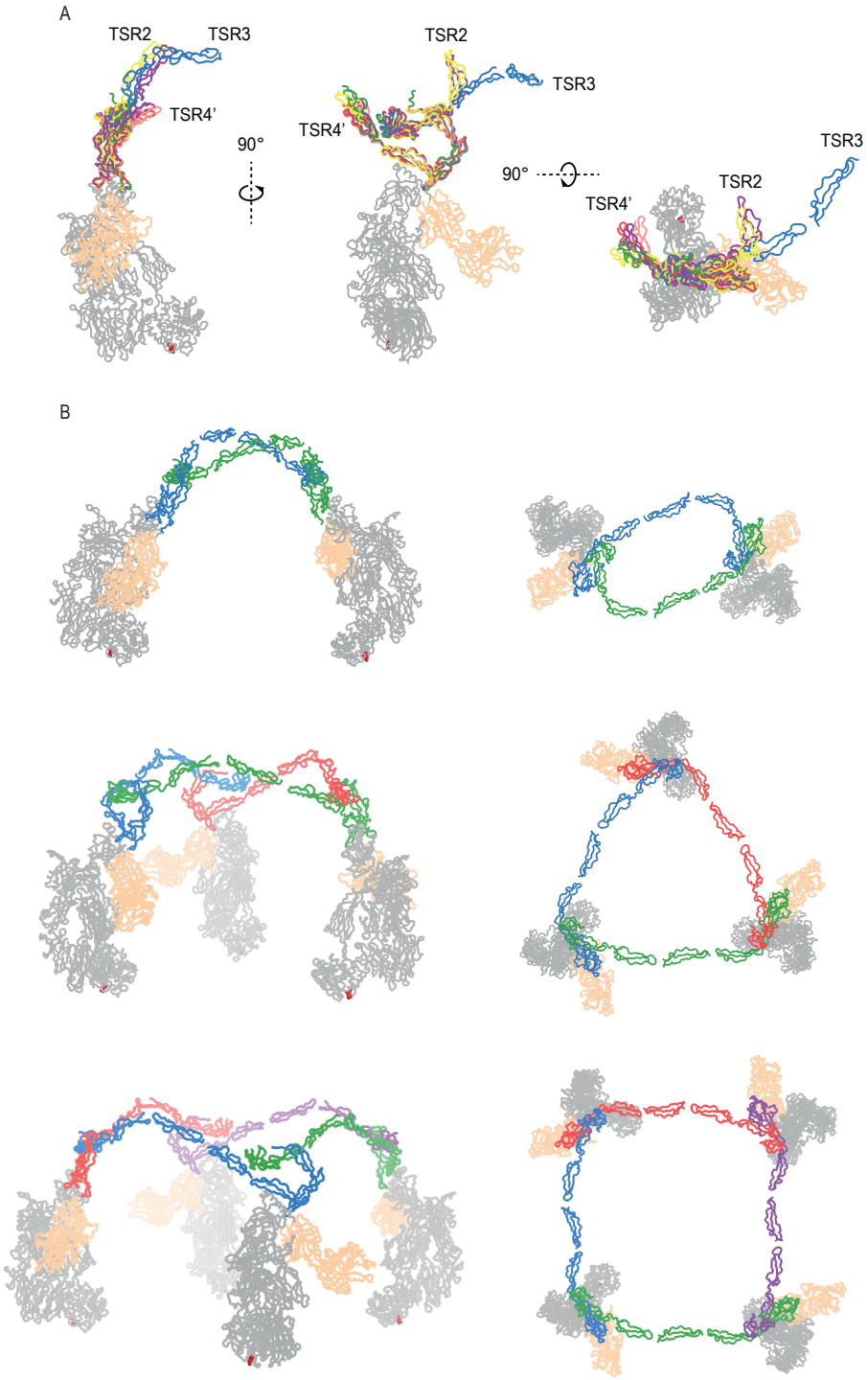
A
TSR2
TSR3
TSR4'
90°
TSR2
TSR3
TSR4'
90°
TSR3
TSR2
TSR4'
B

Figure 10 | Models of properdin oligomers binding to surface bound C3 convertases.

(A) Structures of $P^{N1/456}$ (red), $P^{N12/456}$ (yellow), $P^{N1/456}$-CTC (green) and the copy from Pc-C3bBb-SCIN lacking density for TSR3 (pink) superimposed on TSR5 of the other copy of Pc-C3bBb-SCIN (purple). **(B)** Ribbon representation of properdin oligomers binding to C3 convertases viewed from the front (left panel) and top (right panel). C3b and Bb are colored grey and wheat, respectively, Gln1013 from the C3b thioester is shown as red spheres. Each protomer in a properdin oligomers is colored differently. Top panel: Properdin dimer binding to two C3 convertases (for this model we used $P^{N12/456}$ with TSR3 positioned relative to TSR2 as it is in the copy of Pc-C3bBb-SCIN that contains TSR3) Middle panel: Properdin trimer binding to 3 C3 convertases (for this model the properdin copy from Pc-C3bBb-SCIN that contains TSR3 was used). Bottom panel: Properdin tetramer binding to four C3 convertases (this model was generated with TSR2 as in the middle panel but using TSR4 from $P^{N1/456}$).

thus bridging all three strands providing stabilization to the TSR fold (**Fig. 6C**). Similar arrangements are found in the structure of TSR domains of C8 (PDB ID: 3OJY), C9 (PDB ID 6CXO), ADAMTS13 (PDB ID:3VN4) and Unc5a (PDBID: 4V2A). In the case of Unc5a (determined at 2.4-Å resolution), the two mannosyl moieties have not been included in the model, but are clearly visible in the density in a conformation similar to that observed in properdin. In C6 structures (3T5O, 4E0S, 4A5W), the mannoses in TSR1 and TSR3 domains are absent or modeled in various alternative conformations, possibly due to the relatively low resolution of these structures, ranging from 2.9-4.2 Å. In our structures, we observed clear density for all mannosyl moieties, except two (Trp86 and Trp145), of the reported fully C-mannosylated tryptophans (35). Trp145 is located on TSR2, which exhibits overall poor density in the crystal structure of $P^{N12/456}$. Very weak densities for a mannosyl moiety at Trp86 of TSR1 were observed in all three structures. The WRWRWR motif in TSR1 lacks the final arginine residue, instead a glutamine residue is observed at this position. Most likely, the absence of H-bonding potential with a guanidinium moiety at the final position causes local flexibility, explaining the weak density observed for the mannosyl on Trp86. Properdin is N-glycosylated at Asn428 of TSR6, which is located at the base of the β-hairpin insertion. In our structures this glycan is only partially present, however, there is clear density for this glycan in 5M6W. This glycan would not interact with C3bBb upon binding, which is in agreement with previous findings that removal of N-linked glycans had no effect on properdin activity in a hemolytic assay (29). Properdin O-fucosylation is observed in the density at Thr92, Thr151 and Thr272, which are positioned at structural homologous positions in the A-B-loop of TSR1, TSR2 and TSR4. The A-B loop in 63 out of 88 TSR sequences contains the sequence C-X-X-S/T-C, where the serine or threonine is O-fucosylated (48). Similar to TSR1 from C6 and the TSR domain from ADAMTS13, the O-glucosyl-β1,3-fucose is packed against the disulphide bridge that connects loop A-B to the terminal residue of the TSR domain.

Oligomeric full-length properdin consists of ring-shaped vertices, formed by N- and C-terminal domains of separate protomers (13, 27). The crystal structures of $P^{N1/456}$ and $P^{N12/456}$, obtained by co-expression of N- and C-terminal parts, clearly revealed that the ring-shaped vertices are formed by two contact interfaces between N-terminal domains of one protomer and the C-terminal domains of another protomer (**Fig. 4A**). The N-terminal domain adopts a STB fold and binds the TSR4' domain of another protomer. This interface, which is dominated by hydrophobic interactions, is further stabilized by additional H-bonds between STB Asn59 and the O-glucosyl-β1,3-fucose on Thr272 of TSR4'. A second protomer-protomer interface is observed between TSR1

and TSR6'. This interface is formed between the distal end of TSR6' and the β-sheet at the core of TSR1 and involves hydrophobic interactions as well as several H-bonds and two salt bridges. Overall, the ring-shaped vertex of properdin is formed by STB-TSR1 of one protomer and (approximately ~1/3 of) TSR4', TSR5' and, an extended and curved, TSR6' of a second protomer (**Fig. 8**). TSR2, TSR3 and the remaining part of TSR4 consequently form the edges in properdin oligomers.

Consistent with low-resolution EM and X-ray data (13, 32), we have shown that the TSR5 domain of properdin provides the main interaction interface with C3b by binding along the length of the C-terminal α-helix of the C3b α'-chain (**Fig. 9A**). Protonation of properdin His369, at this main interface, would yield formation of a salt-bridge with C3b Glu1654 (**Fig. 9C**), explaining increased binding of properdin to C3b at low pH (32, 50). Comparison with other structures of C3b (37) indicates that binding of properdin to the CTC domain does not require nor likely induces large conformational changes in C3b. We identified two 'stirrup'-like loops, residues 328-336 of TSR5 and 419-426 of TSR6, which embrace the end of the C-terminal α-helix of CTC (**Fig. 9C)**. Cleavage of properdin in the TSR5-stirrup loop (between res. 333-334) leads to loss of C3b binding (and, hence, loss of convertase stabilization) (29), which indicates the importance of an intact TSR5 stirrup in C3b binding. The only known properdin type III (loss-of-function) mutation, Y414D (51), is located at the base of the TSR6 β-hairpin that constitutes the TSR6 stirrup. Tyr414 is part of a hydrophobic core between TSR5 and TSR6 (**Fig. 7**) and Y414D likely disturbs this hydrophobic core and destabilizes the TSR6 stirrup and hence affects C3b binding or convertase stabilization (51).

Monomerized properdin binds the C3 convertase (C3bBb) and pro-convertase (C3bB) strongly, and C3b weakly (K_D's of 34 nM, 98 nM and 6.8 μM, respectively, in agreement with previous data (12, 32); **Fig. 2 and 3**). Superposition of $P^{N1/456}$-CTC onto C3bB and C3bBD (PDB ID: 2XWJ and 2XWB) (52) suggests that the two stirrups are ideally positioned to bridge interactions between C3b and the VWA domain of FB

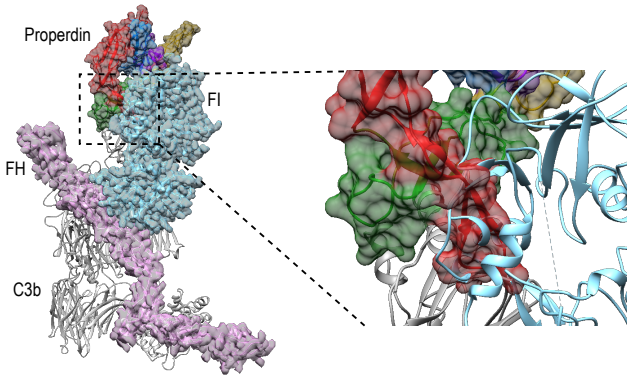

Figure 11 | Properdin binding to C3b is incompatible with FI binding.

Superposition of $P^{N1/456}$-CTC and C3b-FH-FI (PDB ID:5O32). Models were superposed on the C3b-CTC domains (rmsd 0.7 Å). Left: overview of the structures with FH (Pink), FI (light blue) and properdin (multicolored model, with TSR5 in green and TSR6 in red) in ribbon presentation with semi-transparent molecular surface and C3b (grey) shown in ribbon. Right: close up showing FI occupies the same space as the properdin TSR6 (red) stirrup loop.

and Bb. The TSR5 stirrup is in close proximity to the N-terminal region of CCP1 in the Ba region of FB, with only one potential H-bond between properdin Asn331 and FB Ser78. The proximity of properdin to FB-CCP1 explains the cross-links observed between Ba and properdin by Farries *et al.* (53). Re-analysis of C3bBb-SCIN with Pc (at 6-Å resolution) is consistent with the interactions that we observed at high resolution between $P^{N1/456}$ and an isolated C3/C3b-CTC domain (**Fig. 9D-E**). The low-resolution data of Pc-C3bBb-SCIN suggests small rearrangements in the TSR6 stirrup loop. Nevertheless, the expected additional interactions between Bb and properdin are not observed in Pc-C3bBb-SCIN. Potentially, the inhibitor SCIN enforces a C3bBb conformation that is not compatible with stabilization by properdin (32). Therefore, the interaction details between properdin and FB and Bb that explain higher binding affinities for the pro-convertase and convertase remain unfortunately unresolved.

Besides promoting the formation of, and stabilizing the alternative-pathway C3 convertase, properdin is also known to inhibit FI activity (12, 13, 54); based on kinetic data, this is likely due to competition for the same binding site on C3b (12). Superposition of $P^{N1/456}$-CTC with C3b in complex with FH and FI (55) (PDB ID: 5O32) shows that, in a putative properdin-C3b-FH-FI complex, TSR6 of properdin severely clashes with the FI membrane-attack complex domain in FI **(Fig. 11)**. Therefore, the structural data supports competitive binding of properdin and FI for the same binding site. No overlaps are observed between properdin and regulators FH, DAF and MCP, when superposing $P^{N1/456}$-CTC with other C3b-regulator complexes (37). Thus reduced decay-acceleration activity of FH and DAF (32) is most likely due to the increased stability of C3bBb upon properdin binding.

Native properdin occurs predominantly as a mixture of dimers, trimers and tetramers (8), observed as flexible lines, triangles and quadrilaterals in negative-stain EM (13, 27). The oligomers bind with high avidity (with an apparent K_D of 22 nM) to surface-bound C3b compared to monomerized properdin binding a single C3b (K_D of 6.8 μM). Consistently, properdin tetramers are more active than trimers, which are more active than dimers (8, 9). In the structures presented here, overlaid in **Figure 10A,** we observed structural variability predominantly in TSR2 and TSR4. These variations occur mostly in the plane of the membrane of a properdin oligomer bound to an opsonized surface, which allowed us to create composite models representing symmetric properdin dimers, trimers and tetramers binding to surface-bound C3b, C3bB or C3bBb in a straightforward manner (**Fig. 10B**). The ability of properdin to form flexible oligomers is crucial to enhance complement activation only on surfaces by binding deposited C3b molecules with high avidity, while promoting convertase formation (11) and stabilizing formed convertases by binding C3bB and C3bBb complexes with high affinity (12, 32). Local production of properdin by immune cells would result in further enhancement near affected sites (23, 25, 26).

Materials and Methods

Molecular cloning and construct design

Human properdin (UniProtKB-P27918) cDNA was obtained from Open Biosystems (Dharmacon Inc.). Domain boundaries were chosen based on both UniProt assignment and crystal structures of thrombospondin I domains TSR2 and TSR3 (PDB ID: 1LSL) (30). In addition to full-length properdin (res. 28-469), four N-terminal constructs were created, P^{N1} (res. 28-132), $P^{N1'}$ (res. 28-134), P^{N12} (res. 28-191) and P^{N123} (res. 28-255), comprising the first two, three and four N-terminal domains of properdin; and P^{456} (res. 256-469) comprising the three C-terminal domains. The N-terminal domain boundary of the C3/C3b-CTC domain (res. 1517-1663) was chosen based on the structure of C3b (PDB ID: 5FO7 (37)). All inserts were generated by PCR using clone specific primers that include a 5' BamHI restriction site that results in an N-terminal Gly-Ser cloning scar in all constructs and a NotI restriction site at the 3' end of the insert. The NotI site results in a C-terminal extension of three alanine's in all constructs, except for P^{N12} and C3/C3b-CTC, where a stop codon was introduced prior to the NotI site. All inserts were cloned into pUPE expression vectors (U-Protein Express BV, Utrecht, the Netherlands). For small-scale (4 ml) expression tests, one of the constructs (either the N- or C-terminal fragment) included a 6x-His purification tag. In large-scale co-expressions P^{456} included a C-terminal 6xHis-tag, with no tag on the N-terminal constructs. Similarly, constructs for full-length properdin included a C-terminal 6xHis-tag and the C3/C3b-CTC construct contained an N-terminal 6xHis-tag.

Recombinant proteins were transiently expressed in Epstein-Barr virus nuclear antigen I (EBNA1)- expressing, HEK293 cells (HEK293-EBNA) (U-Protein Express BV, Utrecht, the Netherlands). For crystallization purposes, proteins were expressed in GnTI$^-$ HEK293-EBNA cells. N-terminal and C-terminal properdin fragments were co-expressed using a 1:1 DNA ratio. Cells were grown in suspension culture at 37 °C for 6 days post-transfection. For each culture, supernatant was collected by a low-speed spin (1,000 x g for 10 min), followed by a high-speed spin (4,000 x g for 10 min) to remove any remaining cell debris. Subsequently, 3 ml/L Ni-Sepharose Excel beads (GE Healthcare) was added to the supernatant and the mixture was incubated for 2 to 16 hours with constant agitation at 4 °C. The beads were washed with 10-column volumes of buffer A (20 mM HEPES pH 7.8, 500 mM NaCl) and 10 column volumes of buffer A supplemented with 10 mM imidazole. Bound protein was subsequently eluted with buffer A supplemented with 250 mM imidazole. For small-scale (4 ml) expression tests of properdin fragments no further purification steps were performed, whilst for large-scale (1 L) expressions, pooled fractions were concentrated and further purified by size-exclusion chromatography (SEC). $P^{N12/456}$ for SPR was purified with a Superdex 200 16/600 (GE Healthcare) using 25 mM HEPES pH 7.8, 150 mM NaCl as the running buffer. All other properdin complexes were purified on a Superdex 200 10/300 Increase (GE Healthcare) column using either 20mM HEPES pH 7.4, 150 mM NaCl (properdin, $P^{N1/456}$, $P^{N1'/456}$) or 25mM HEPES pH 7.8 with 100 mM NaCl ($P^{N12/456}$ for crystallizations) as the running buffer. The C3/C3b-CTC domain was purified on a Superdex 200

16/600 (GE Healthcare) in 20 mM HEPES pH 7.4, 150 mM NaCl. Human wild type FB, catalytically inactive (S699A) double-gain-of-function (D279G, N285D) FB mutant ($FB^{dgf‡}$) (56), factor D (FD), DAF1-4 and Salp20 were purified as described previously (52, 57, 58). C3 and C3b were purified from human plasma as described in Wu *et al.* (57). Full-length properdin was stored at 4 °C and all other proteins were flash frozen by plunging into liquid N_2 and stored at -80 °C.

C3 convertase stability assay

To generate C3 convertase, purified C3b (obtained after cleavage of human serum-derived C3) was mixed with catalytically inactive $FB^{dgf‡}$ at a ratio of 1:1.1 in the presence of 5 mM $MgCl_2$. After incubation for 5 min at 37 °C, FD was added to a ratio of C3bB:FD of 1:0.1 and the mixture was incubated for another 5 min at 37 °C, after which the C3 convertase was stored on ice till further use. C3 convertase was diluted to 1.5 μM with ice-cold buffer (20 mM HEPES pH 7.4, 150 mM NaCl and 5 mM $MgCl_2$). Either 6 μM $P^{N1/456}$ or $P^{N12/456}$ or an equal volume of buffer (control) was added to the C3 convertase in a ratio of 1:2 resulting in a final concentration of 2 μM $P^{N1/456}$ or $P^{N12/456}$ and 1 μM C3 convertase. The mixture was incubated at 37°C for one hour and subsequently put on ice. The amount of C3 convertase was analyzed by analytical SEC using a Superdex 200 10/300 Increase pre-equilibrated with 20 mM HEPES pH 7.4, 150 mM NaCl and 5 mM $MgCl_2$ at 18 °C on a Shimadzu FPLC.

Surface-plasmon resonance

C3b was generated from C3 through the addition of FB and FD to a C3:FB:FD molar ratio of 1:0.5:0.03 in the presence of 5 mM $MgCl_2$ and incubation at 37 °C. At 10 minute intervals fresh FB was added to ensure complete conversion of C3 to C3b. Subsequently, C3b was biotinylated on the free cysteine that is generated after hydrolysis of the reactive thioester (59); EZ-Link Maleimide-PEG2-Biotin (Thermofisher) was added to a final concentration of 1 mM to the freshly produced C3b (13 μM) and the mixture was incubated for 3 hours at room temperature. C3b was separated from unreacted Biotin-Peg2-Maleimide by SEC using a S200 10/300 increase column pre-equilibrated in 20 mM HEPES pH 7.4, 150 mM NaCl. Purity and conversion of C3 to C3b were analyzed by SDS-PAGE. To analyze equilibrium binding to monomerized properdin, we used $P^{N1'/456}$ that includes an additional Cys-Pro (res. 133-134) at the C-terminus of TSR1. $P^{N1'/456}$ (45 μM) was biotinylated as described for C3b and separated from excess biotin with a 5 mL HiTrap Desalting column (GE Healthcare) pre-equilibrated in 20 mM HEPES pH 7.4, 150 mM NaCl. Biotinylated proteins were spotted on a SensEye P-Strep chip (SensEye) at 50 nM for 60 min with a continuous flow microspotter (CFM, Wasatch). Equilibrium binding kinetics were analyzed using an IBIS-MX96 (IBIS Technologies). All experiments were performed in 20 mM HEPES pH 7.4, 0.005% (v/v) Tween-20, 150 mM NaCl at 4 μl/sec. For experiments involving C3bB and C3bBb the

buffer was supplemented with 5 mM $MgCl_2$. Analyses at low ionic strength were performed at a NaCl concentration of 50 mM. Analytes were injected from low to high concentration in 14 twofold incremental steps. In equilibrium binding analyses involving C3bB or C3bBb, C3bB was generated on a C3b coated SPR surface by injecting 100 nM FB^{dgf} for 5 min prior to each analyte injection. C3bBb was generated from C3bB by injections of 100 nM FD for 5 min after each FB injection. Where indicated, DAF1-4 (1 μM), FD (100 nM) and/or Salp20 (1 μM for experiments with C3b alone and 5 μM in experiments with C3 (pro) convertase) were injected, to regenerate the C3b surface. Salp20, a properdin inhibitor from deer tick (60), was required to dissociate full length properdin from C3b. In all experiments, the SPR surface was washed with buffer supplemented with 1 M NaCl at 8 μl/sec for 30 sec at the end of each cycle. Temperature was kept constant at 25 °C. Prism (GraphPad) was used for data analysis. K_D's were determined by fitting the end point data to $Y = \frac{Bmax * x}{KD + x} + Background$.

Crystallization, data collection and structure determination

$P^{N1/456}$ and the C3/C3b-CTC domain were dialyzed overnight at 4 °C using a 3.5 kDa cutoff Slide-A-Lyzer Mini Dialysis Unit (Thermo Scientific) against 10 mM HEPES, 50 mM NaCl, pH 7.4. The N-linked glycan on Asn428 of $P^{N1/456}$ was removed by including 1% v/v EndoHF (New England BioLabs) during the dialysis. $P^{N1/456}$, $P^{N12/456}$ and the C3/C3b-CTC domain were concentrated to 8.7 mg/ml, 10 mg/ml and 10.3 mg/ml, respectively.

Crystals were obtained using the sitting drop vapor diffusion method at 18 °C. Crystals of $P^{N12/456}$ were grown in 100 mM sodium citrate pH 5.5 and 20% (w/v) PEG 3000 and cryoprotected by soaking in mother liquor supplemented with 25% (v/v) glycerol. Crystals of $P^{N1/456}$ were grown in 0.2 M potassium sulfate and 20% (w/v) PEG 3350 and cryoprotected by soaking in mother liquor supplemented with 25% (v/v) ethylene glycol. $P^{N1/456}$ and C3/C3b-CTC were mixed in a 1:1 molar ratio at 8 mg/ml and crystals were grown in 8% v/v Tacsimate pH 5.0 and 20% (w/v) PEG 3350 and cryoprotected by soaking in mother liquor supplemented with 25% glycerol. After harvesting, crystals were cryo-cooled by plunge freezing in liquid N_2. All diffraction data were collected at the European Synchrotron Radiation Facility (ESRF) on beamlines ID29 ($P^{N12/456}$) and ID23-1 ($P^{N1/456}$-CTC, $P^{N1/456}$). The diffraction images were processed with DIALS (61) and the integrated reflection data were then anisotropically truncated with the STARANISO web server (62).

Structures were solved by molecular replacement using Phaser (38). Atomic models were optimized by alternating between refinement using REFMAC (42) and manual building in Coot (41). C- and O-linked glycosylation restraints were generated within Coot, using ACEDRG (63). The structure of $P^{N12/456}$ was refined with restraints generated from $P^{N1/456}$ using ProSMART (64). Data was deposited at the RSCB Protein Data Bank (65) with PDB IDs 6S08, 6S0A and 6S0B. We also re-analyzed data deposited

for Pc in complex with C3bBb-SCIN (32) (PDB ID: 5M6W). An initial position for the properdin molecule was obtained by superposing our $P^{N1/456}$-CTC model onto the CTC domain of the two C3b molecules in the model deposited by Pedersen et al. (32). Subsequently, TSR2 from $P^{N12/456}$ was added and manually adjusted to fit the density. In addition, for one of the two copies in the asymmetric unit, density corresponding to TSR3 was apparent. A TSR model derived from TSR2 from thrombospondin-1 (PDB ID: 1LSL (30)), containing the canonical cysteines and Trp-ladder residues, but otherwise consisting of poly-alanines, was placed into this density. The resulting model was further refined using the LORESTR refinement pipeline (66). Coordinates of the re-refined properdin-C3bBb-SCIN complex (PDB ID: 5M6W) are available from the authors upon request.

Abbreviations:

ADP, atomic displacement parameters; Bb, cleavage product b of factor B; C3, complement component 3; C3b, cleavage product b of complement component 3; CTC, C-terminal C345c; DAF, decay-accelerating factor; EM, negative-stain electron microscopy; FB, factor B; FH, factor H; FI, factor I; IMAC, immobilized metal affinity chromatography; MCP, membrane-cofactor protein; Pc, cleaved properdin; PDB, protein data bank; rmsd, root-mean square deviation; SCIN, *Staphylococcus aureus* inhibitor; SEC, size exclusion chromatography; SPR, surface-plasmon resonance; STB, short transforming-growth factor B binding protein-like; TSR, thrombospondin type-I repeat.

Acknowledgements

We gratefully thank Xiaoguang Xue for initial help with C3 and C3b purification. We thank the members of the Crystal and Structural Chemistry lab for helpful discussions. We thank the members of Utrecht Protein Express BV for the HEK-cell cultures. We gratefully thank the beamline scientists of the ESRF for the excellent assistance. We thank the European Synchrotron Radiation Facility (ESRF) for the provision of synchrotron radiation facilities.

This study was performed on behalf of the COMBAT Consortium. This is an interuniversity collaboration in the Netherlands that is formed to study basic mechanisms, assay development, and therapeutic translation of complement-mediated renal diseases. Principal investigators are (in alphabetical order): S. Berger (Department of Internal Medicine-Nephrology, University Medical Center Groningen, Groningen, Netherlands), J. van den Born (Department of Internal Medicine-Nephrology, University Medical Center Groningen, Groningen, Netherlands), P. Gros (Department of Chemistry, Utrecht University, Utrecht, Netherlands), L. van den Heuvel (Department of Pediatric Nephrology, Radboud University Medical Center, Nijmegen, Netherlands), N. van de Kar (Department of Pediatric Nephrology, Radboud University Medical Center, Nijmegen,

Netherlands), C. van Kooten (Department of Internal Medicine-Nephrology, Leiden University Medical Center, Leiden, Netherlands), M. Seelen (Department of Internal Medicine-Nephrology, University Medical Center Groningen, Groningen, Netherlands), A. de Vries (Department of Internal Medicine-Nephrology, Leiden University Medical Center, Leiden, Netherlands).

2

Funding disclosures

This work was supported by the Dutch Kidney Foundation (13OCA27 COMBAT Consortium). and the European Community's Seventh Framework Programmes (FP7/2007-2013) under BioStruct-X (grant no. 283570).

Author contributions

RvdB and PG designed the project. RvdB and JG cloned the constructs. RvdB carried out protein purification, crystallization and biochemical assays. RvdB and NP collected and processed diffraction data, determined and refined structures. RvdB, HB and PG analyzed the data. RvdB, HB and PG wrote the manuscript.

Conflict of Interest

The authors declare no competing financial interest.

References

1. Ricklin, D., G. Hajishengallis, K. Yang, and J. D. Lambris. 2010. Complement: A key system for immune surveillance and homeostasis. *Nat. Immunol.* 11: 785–797.

2. Merle, N. S., R. Noe, L. Halbwachs-Mecarelli, V. Fremeaux-Bacchi, and L. T. Roumenina. 2015. Complement system part II: Role in immunity. *Front. Immunol.* 6: 1–26.

3. Pangburn, M. K., and H. J. Muller-Eberhard. 1986. The C3 convertase of the alternative pathway of human complement. Enzymic properties of the bimolecular proteinase. *Biochem. J.* 235: 723–730.

4. Ricklin, D., E. S. Reis, D. C. Mastellos, P. Gros, and J. D. Lambris. 2016. Complement component C3 – The "Swiss Army Knife" of innate immunity and host defense. *Immunol. Rev.* 274: 33–58.

5. Schmidt, C. Q., J. D. Lambris, and D. Ricklin. 2016. Protection of host cells by complement regulators. *Immunol. Rev.* 274: 152–171.

6. Merle, N. S., S. E. Church, V. Fremeaux-Bacchi, and L. T. Roumenina. 2015. Complement system part I - molecular mechanisms of activation and regulation. *Front. Immunol.* 6: 1–30.

7. Pillemer, L., L. Blum, I. H. Lepow, O. A. Ross, E. W. Todd, and A. C. Wardlaw. 1954. The properdin system and immunity: I. Demonstration and isolation of a new serum protein, properdin, and its role in immune phenomena. *Science (80-.).* 120: 279–285.

8. Pangburn, M. K. 1989. Analysis of the natural polymeric forms of human properdin and their functions in comple-

ment activation. *J. Immunol.* 142: 202–7.

9. Blatt, A. Z., S. Pathan, and V. P. Ferreira. 2016. Properdin: a tightly regulated critical inflammatory modulator. *Immunol. Rev.* 274: 172–190.

10. Fearon, D. T., and K. F. Austen. 1975. Properdin: binding to C3b and stabilization of the C3b-dependent C3 convertase. *J. Exp. Med.* 142: 856–63.

11. Hourcade, D. E. 2006. The role of properdin in the assembly of the alternative pathway C3 convertases of complement. *J. Biol. Chem.* 281: 2128–2132.

12. Farries, T. C., P. J. Lachmann, and R. A. Harrison. 1988. Analysis of the interactions between properdin, the third component of complement (C3), and its physiological activation products. *Biochem. J.* 252: 47–54.

13. Alcorlo, M., A. Tortajada, S. Rodríguez de Córdoba, and O. Llorca. 2013. Structural basis for the stabilization of the complement alternative pathway C3 convertase by properdin. *Proc. Natl. Acad. Sci. U. S. A.* 110: 13504–9.

14. Spitzer, D., L. M. Mitchell, J. P. Atkinson, and D. E. Hourcade. 2007. Properdin Can Initiate Complement Activation by Binding Specific Target Surfaces and Providing a Platform for De Novo Convertase Assembly. *J. Immunol.* 179: 2600–2608.

15. Kemper, C., J. P. Atkinson, and D. E. Hourcade. 2010. Properdin: Emerging Roles of a Pattern-Recognition Molecule. *Annu. Rev. Immunol* 28: 131–55.

16. Ferreira, V. P., C. Cortes, and M. K. Pangburn. 2010. Native polymeric forms of properdin selectively bind to targets and promote activation of the alternative pathway of complement. *Immunobiology* 215: 932–940.

17. Xu, W., S. P. Berger, L. A. Trouw, H. C. de Boer, N. Schlagwein, C. Mutsaers, M. R. Daha, and C. van Kooten. 2008. Properdin Binds to Late Apoptotic and Necrotic Cells Independently of C3b and Regulates Alternative Pathway Complement Activation. *J. Immunol.* 180: 7613–7621.

18. Zaferani, A., R. R. Vivès, P. Van Der Pol, G. J. Navis, M. R. Daha, C. Van Kooten, H. Lortat-Jacob, M. A. Seelen, and J. Van Den Born. 2012. Factor H and properdin recognize different epitopes on renal tubular epithelial heparan sulfate. *J. Biol. Chem.* 287: 31471–31481.

19. O'Flynn, J., J. Kotimaa, R. Faber-Krol, K. Koekkoek, N. Klar-Mohamad, A. Koudijs, W. J. Schwaeble, C. Stover, M. R. Daha, and C. van Kooten. 2018. Properdin binds independent of complement activation in an in vivo model of anti–glomerular basement membrane disease. *Kidney Int.* 94: 1141–1150.

20. Harboe, M., P. Garred, J. K. Lindstad, A. Pharo, F. Müller, G. L. Stahl, J. D. Lambris, and T. E. Mollnes. 2012. The Role of Properdin in Zymosan- and Escherichia coli -Induced Complement Activation . *J. Immunol.* 189: 2606–2613.

21. Harboe, M., C. Johnson, S. Nymo, K. Ekholt, C. Schjalm, J. K. Lindstad, A. Pharo, B. C. Hellerud, K. Nilsson Ekdahl, T. E. Mollnes, et al. 2017. Properdin binding to complement activating surfaces depends on initial C3b deposition. *Proc. Natl. Acad. Sci.* 114: E534–E539.

22. Fijen, C. A. P., R. van den Bogaard, M. Schipper, M. Mannens, M. Schlesinger, F. G. Nordin, J. Dankert, M. R. Daha, A. G. Sjöholm, L. Truedsson, et al. 1999. Properdin deficiency: molecular basis and disease association. *Mol. Immunol.* 36: 863–867.

23. Chen, J. Y., C. Cortes, and V. P. Ferreira. 2018. Properdin: A multifaceted molecule involved in inflammation and diseases. *Mol. Immunol.* 102: 58–72.

24. Scholl, H. P. N., P. C. Issa, M. Walier, S. Janzer, B. Pollok-Kopp, F. Börncke, L. G. Fritsche, N. V. Chong, R. Fimmers, T. Wienker, et al. 2008. Systemic complement activation in age-related macular degeneration. *PLoS One* 3: e2593.

25. Cortes, C., J. A. Ohtola, G. Saggu, and V. P. Ferreira. 2012. Local release of properdin in the cellular microenvironment: Role in pattern recognition and amplification of the alternative pathway of complement. *Front. Immunol.* 3: 412.

26. Lubbers, R., M. F. van Essen, C. van Kooten, and L. A. Trouw. 2017. Production of complement components by cells of the immune system. *Clin. Exp. Immunol.* 188: 183–194.

27. Smith CA, Pangburn MK, Vogel CW, Müller-Eberhard HJ. 1984. Molecular architecture of human properdin, a positive regulator of the alternative pathway of complement. *J. Biol. Chem.* 259: 4582–4588.

28. Farries, T. C., J. T. Finch, P. J. Lachmann, and R. A. Harrison. 1987. Resolution and analysis of 'native' and 'activated' properdin. *Biochem. J.* 243: 507–517.

29. Higgins, J. M., H. Wiedemann, R. Timpl, and K. B. Reid. 1995. Characterization of mutant forms of recombinant human properdin lacking single thrombospondin type I repeats. Identification of modules important for function. *J. Immunol.* 155: 5777–85.

30. Tan, K., M. Duquette, J. H. Liu, Y. Dong, R. Zhang, A. Joachimiak, J. Lawler, and J. H. Wang. 2002. Crystal structure of the TSP-1 type 1 repeats: A novel layered fold and its biological implication. *J. Cell Biol.* 159: 373–382.

31. Olsen, J. G., and B. B. Kragelund. 2014. Who climbs the tryptophan ladder? On the structure and function of the WSXWS motif in cytokine receptors and thrombospondin repeats. *Cytokine Growth Factor Rev.* 25: 337–341.

32. Pedersen, D. V, L. Roumenina, R. K. Jensen, T. A. Gadeberg, C. Marinozzi, C. Picard, T. Rybkine, S. Thiel, U. B. Sørensen, C. Stover, et al. 2017. Functional and structural insight into properdin control of complement alternative pathway amplification. *EMBO J.* 36: 1084–1099.

33. Sun, Z., K. B. M. M. Reid, and S. J. Perkins. 2004. The dimeric and trimeric solution structures of the multidomain complement protein properdin by X-ray scattering, analytical ultracentrifugation and constrained modelling. *J. Mol. Biol.* 343: 1327–1343.

34. Hartmann, S., and J. Hofsteenge. 2000. Properdin, the positive regulator of complement, is highly C-mannosylated. *J. Biol. Chem.* 275: 28569–28574.

35. Yang, Y., F. Liu, V. Franc, L. A. Halim, H. Schellekens, and A. J. R. Heck. 2016. Hybrid mass spectrometry approaches in glycoprotein analysis and their usage in scoring biosimilarity. *Nat. Commun.* 7: 13397.

36. Rooijakkers, S. H. M., J. Wu, M. Ruyken, R. van Domselaar, K. L. Planken, A. Tzekou, D. Ricklin, J. D. Lambris, B. J. C. Janssen, J. a G. van Strijp, et al. 2009. Structural and functional implications of the alternative complement pathway C3 convertase stabilized by a staphylococcal inhibitor. *Nat. Immunol.* 10: 721–727.

37. Forneris, F., J. Wu, X. Xue, D. Ricklin, Z. Lin, G. Sfyroera, A. Tzekou, E. Volokhina, J. C. Granneman, R. Hauhart, et al. 2016. Regulators of complement activity mediate inhibitory mechanisms through a common C3b-binding mode. *EMBO J.* 35: 1133–1149.

38. McCoy, A. J., R. W. Grosse-Kunstleve, P. D. Adams, M. D. Winn, L. C. Storoni, and R. J. Read. 2007. Phaser crystallographic software. *J. Appl. Crystallogr.* 40: 658–674.

39. Bunkóczi, G., and R. J. Read. 2011. Improvement of molecular-replacement models with Sculptor. *Acta Crystallogr. Sect. D Biol. Crystallogr.* 67: 303–312.

40. Thompson, J. D., D. G. Higgins, and T. J. Gibson. 1994. CLUSTAL W: Improving the sensitivity of progressive multiple sequence alignment through sequence weighting, position-specific gap penalties and weight matrix choice. *Nucleic Acids Res.* 22: 4673–4680.

41. Emsley, P., B. Lohkamp, W. G. Scott, and K. Cowtan. 2010. Features and development of Coot. *Acta Crystallogr. Sect. D Biol. Crystallogr.* 66: 486–501.

42. Murshudov, G. N., A. A. Vagin, and E. J. Dodson. 1997. Refinement of macromolecular structures by the maximum-likelihood method. *Acta Crystallogr. Sect. D Biol. Crystallogr.* 53: 240–255.

43. Holm, L., and L. M. Laakso. 2016. Dali server update. *Nucleic Acids Res.* 44: 351–355.

44. Lee, S. S. J., V. Knott, J. Jovanović, K. Harlos, J. M. Grimes, L. Choulier, H. J. Mardon, D. I. Stuart, and P. A. Handford. 2004. Structure of the integrin binding fragment from fibrillin-1 gives new insights into microfibril organization. *Structure* 12: 717–729.

45. Piha-Gossack, A., W. Sossin, and D. P. Reinhardt. 2012. The Evolution of Extracellular Fibrillins and Their Functional Domains. *PLoS One* 7: 33560.

46. Yuan, X. 1997. Solution structure of the transforming growth factor beta -binding protein-like module, a domain associated with matrix fibrils. *EMBO J.* 16: 6659–6666.

47. Hofsteenge, J., D. R. Müller, T. de Beer, A. Löffler, W. J. Richter, and J. F. G. Vliegenthart. 1994. New Type of Linkage between a Carbohydrate and a Protein: C-Glycosylation of a Specific Tryptophan Residue in Human RNase Us.

Biochemistry 33: 13524–13530.

48. Gonzalez de Peredo, A., D. Klein, B. Macek, D. Hess, J. Peter-Katalinic, and J. Hofsteenge. 2002. C- Mannosylation and O- Fucosylation of Thrombospondin Type 1 Repeats . *Mol. Cell. Proteomics* 1: 11–18.

49. Hofsteenge, J., K. G. Huwiler, B. Macek, D. Hess, J. Lawler, D. F. Mosher, and J. Peter-Katalinic. 2001. C-Mannosylation and O-Fucosylation of the Thrombospondin Type 1 Module. *J. Biol. Chem.* 276: 6485–6498.

50. Fishelson, Z., R. D. Horstmann, and H. J. Müller-Eberhard. 1987. Regulation of the alternative pathway of complement by pH. *J. Immunol.* 138: 3392–5.

51. Fredrikson, G. N., J. Westberg, E. J. Kuijper, C. C. Tijssen, A. G. Sjöholm, M. Uhlén, and L. Truedsson. 1996. Molecular characterization of properdin deficiency type III: dysfunction produced by a single point mutation in exon 9 of the structural gene causing a tyrosine to aspartic acid interchange. *J. Immunol.* 157: 3666–71.

52. Forneris, F., D. Ricklin, J. Wu, A. Tzekou, R. S. Wallace, J. D. Lambris, and P. Gros. 2010. Structures of C3b in complex with factors B and D give insight into complement convertase formation. *Science (80-.).* 330: 1816–1820.

53. Farries, T. C., P. J. Lachmann, and R. A. Harrison. 1988. Analysis of the interaction between properdin and Factor B, components of the alternative-pathway C3 convertase of complement. *Biochem. J.* 253: 667–675.

54. Medicus, R. G., O. Götze, and H. J. Müller-Eberhard. 1976. Alternative pathway of complement: Recruitment of precursor properdin by the labile C3/C5 convertase and the potentiation of the pathway. *J. Exp. Med.* 144: 1076–1093.

55. Xue, X., J. Wu, D. Ricklin, F. Forneris, P. Di Crescenzio, C. Q. Schmidt, J. Granneman, T. H. Sharp, J. D. Lambris, and P. Gros. 2017. Regulator-dependent mechanisms of C3b processing by factor i allow differentiation of immune responses. *Nat. Struct. Mol. Biol.* 24: 643–651.

56. Hourcade, D. E., L. M. Mitchell, and T. J. Oglesby. 1999. Mutations of the type A domain of complement factor B that promote high- affinity C3b-binding. *J. Immunol.* 162: 2906–2911.

57. Wu, J., Y. Q. Wu, D. Ricklin, B. J. C. Janssen, J. D. Lambris, and P. Gros. 2009. Structure of complement fragment C3b-factor H and implications for host protection by complement regulators. *Nat. Immunol.* 10: 728–733.

58. Michels, M. A. H. M., N. C. A. J. Van De Kar, R. M. Van Den Bos, T. J. A. M. Van Der Velden, S. A. W. Van Kraaij, S. A. Sarlea, V. Gracchi, M. J. S. Oosterveld, E. B. Volokhina, L. P. W. J. Van Den Heuvel, et al. 2019. Novel assays to distinguish between properdin-dependent and properdin-independent C3 nephritic factors provide insight into properdin-inhibiting therapy. *Front. Immunol.* 10.

59. Law, S. K. A., and A. W. Dodds. 1996. The internal thioester and the covalent binding properties of the complement proteins C3 and C4. *Protein Sci.* 6: 263–274.

60. Tyson, K. R., C. Elkins, and A. M. de Silva. 2008. A Novel Mechanism of Complement Inhibition Unmasked by a Tick Salivary Protein That Binds to Properdin. *J. Immunol.* 180: 3964–3968.

61. Winter, G., D. G. Waterman, J. M. Parkhurst, A. S. Brewster, R. J. Gildea, M. Gerstel, L. Fuentes-Montero, M. Vollmar, T. Michels-Clark, I. D. Young, et al. 2018. DIALS: Implementation and evaluation of a new integration package. *Acta Crystallogr. Sect. D Struct. Biol.* 74: 85–97.

62. Tickle, I. J., C. Flensburg, P. Keller, W. Paciorek, A. Sharff, C. Vonrhein, and G. Bricogne. 2018. STARANISO. *Cambridge, UK Glob. Phasing Ltd.* .

63. Long, F., R. A. Nicholls, P. Emsley, S. Gražulis, A. Merkys, A. Vaitkus, and G. N. Murshudov. 2017. AceDRG: A stereochemical description generator for ligands. *Acta Crystallogr. Sect. D Struct. Biol.* 73: 112–122.

64. Nicholls, R. A., F. Long, and G. N. Murshudov. 2012. Low-resolution refinement tools in REFMAC5. *Acta Crystallogr. Sect. D Biol. Crystallogr.* 68: 404–417.

65. Berman HM, Westbrook J, Feng Z, Gilliland G, Bhat TN, Weissig H, Shindyalov IN, B. P. 2000. The protein data bank. *Nucleic Acids Res.* 28: 235–242.

66. Kovalevskiy, O., R. A. Nicholls, and G. N. Murshudov. 2016. Automated refinement of macromolecular structures at low resolution using prior information. *Acta Crystallogr. Sect. D Struct. Biol.* 72: 1149–1161.

Chapter 3

Properdin and factor H act independently and their balance is critical for activation of complement

Ramon M. van den Bos*, Itziar Serna Martin*, Jeroen van Amstel and Piet Gros

**These authors contributed equally*

Crystal and Structural Chemistry, Bijvoet Centre for Biomolecular Research, Department of Chemistry, Faculty of Science, Utrecht University, Utrecht, Netherlands.

Abstract

Properdin is crucial for activation of the complement system through the alternative pathway in serum. It stimulates complement activation by promoting C3-convertase formation, stabilizing C3 convertases and reducing factor I-mediated proteolytic C3b inactivation. However, the relative importance of each these properdin functions on alternative-pathway activation remains unclear. We developed a liposome-based leakage assay that allows evaluation of alternative-pathway complement activation in the presence and absence of properdin. This assay circumvents the initiation through uncontrolled slow auto-activation of C3 (also referred to as 'tick-over') by chemically pre-labelling liposomes with C3b. Using this set-up, we showed that properdin is critical for alternative-pathway activation induced by serum, but not for activation when adding purified complement components, factor B, factor D and C5 through to C9. Only in the presence of negative regulators, which decay C3 convertases, properdin became critical for complement activation. Furthermore, surface-plasmon resonance experiments showed that properdin and factor H exert their effects on C3 convertases independently from each other. Properdin acts primarily through increasing the lifetime of C3 convertases, whereas enhanced formation of C3 convertases and reduced factor I-mediated inactivation of C3b in the presence of properdin only played a minor role in activation. Our work shows that balance between stabilization and decay of the C3 convertase by properdin and factor H, respectively, is key for complement activation on surfaces through the alternative pathway.

Introduction:

The complement system is part of the humoral immune system and is responsible for the recognition and clearance of foreign particles and host debris (1). Whereas the classical pathway (CP) and lectin pathway (LP) initiate complement activation upon recognition of danger patterns, the alternative pathway (AP) does not require pattern recognition for initiation and is constitutively active at a low level. After initiation through either of the three pathways, the AP augments complement activation through a feed-back loop.

Continuous low-level AP activation is caused by the spontaneous conformational rearrangement of C3 into a bioactive state (ca. 0.3% per hour) (2), referred to as C3(H_2O) or C3*. C3* associates with factor B (FB) and after cleavage by factor D (FD) forms a C3 convertase (C3*Bb) that cleaves C3 into C3a and C3b. C3 cleavage exposes a reactive thioester in C3b that rapidly reacts with available nucleophiles resulting in covalent attachment (3). Like C3*, deposited C3b associates with FB, which is subsequently cleaved by FD, generating the AP C3 convertase, C3bBb. Surface-bound C3bBb cleaves C3 resulting in further deposition of C3b and generation of C3 convertases. This amplification loop results in C3b opsonization of the targeted surface. Subsequently, a high C3b-surface density triggers a switch in substrate specificity of C3bBb from C3 to C5, yielding C5-convertase activity (4, 5), thereby initiating the terminal pathway leading to lytic pores in the cell membranes formed by membrane attack complexes (MAC) (6).

Regulation of AP activation is heavily dependent on the rate of inactivation of C3bBb by irreversible decay into C3b and Bb. The rate of inactivation is modulated by both positive and negative regulators of the complement system (7). Properdin is an oligomeric plasma protein that enhances AP activation by stabilizing the C3 convertase 5-10 fold (8). Properdin oligomerization directs positive regulation to target surfaces by binding with high avidity to C3b coated surfaces (9–12). Enhanced AP activation by properdin is crucial for defense against infection by microorganisms like *Chlamydia pneumoniae* and *Neisseria meningitides* (13–15). Besides stabilizing the C3 convertase it has been proposed that properdin positively regulates AP activation by enhancing the formation of the C3 convertase (16) and by reducing factor I (FI)-mediated inactivation of C3b by competing with FI for binding to C3b (9, 11, 12, 17). Alternatively, properdin serves to recognize surfaces, where it is recruited through binding various ligands (e.g. soluble collectin-12 or heparan sulfate), and promote AP activation on these surfaces (18–20).

Factor H (FH) is an essential negative regulator of the complement system in serum (21). Its decay-acceleration activity (DAA) dissociates C3 convertases into its constituent components thereby reducing the amount of complement activation. In addition to DAA, FH exhibits a co-factor activity (CA) (21). CA allows FI to inactivate C3b proteolytically and thereby prevent formation of new C3 convertases (22, 23). Both DAA and CA are important to prevent activation and consumption of complement components in the fluid phase and loss of DAA or CA resulting in increased susceptibility to microbial infections and potentially leading to disorders like dense-deposit disease

(21, 24, 25). FH may also be recruited to healthy host tissue by interacting with glycans on cells or matrix material, where it protects against complement activation (26, 27). Impaired recruitment of FH renders self surfaces vulnerable to complement activation, which leads to diseases such as atypical haemolytic uremic syndrome and age-related macular degeneration (28).

Properdin and FH have opposing effects on the lifetime of the AP C3 convertase; however, it is unclear whether these proteins affect each other's function. Properdin has been reported to reduce the rate of decay induced by FH (29–31), but it is unclear if this reduction is due to a direct or indirect effect of properdin on FH activity. A negative-stain EM model of properdin in complex with the C3 convertase indicates that properdin induces a rearrangement of the thioester containing domain of C3b, which could impair FH binding to C3b (17). However, it has also been reported that properdin and FH are able to bind C3b simultaneously (12, 32–34). Recently Pedersen et al. suggested a persistent conformational change in C3 convertases after properdin binding that reduces the DAA of FH (11). However, it is unclear if and how properdin binding to the C3 convertase affects the interactions of negative regulators with either C3b or Bb.

Here we developed a liposome-based assay that enables monitoring of AP activation. Using this assay we studied the effect of properdin on AP activation. Furthermore, with SPR we characterized the effect of properdin on the formation and lifetime of the C3

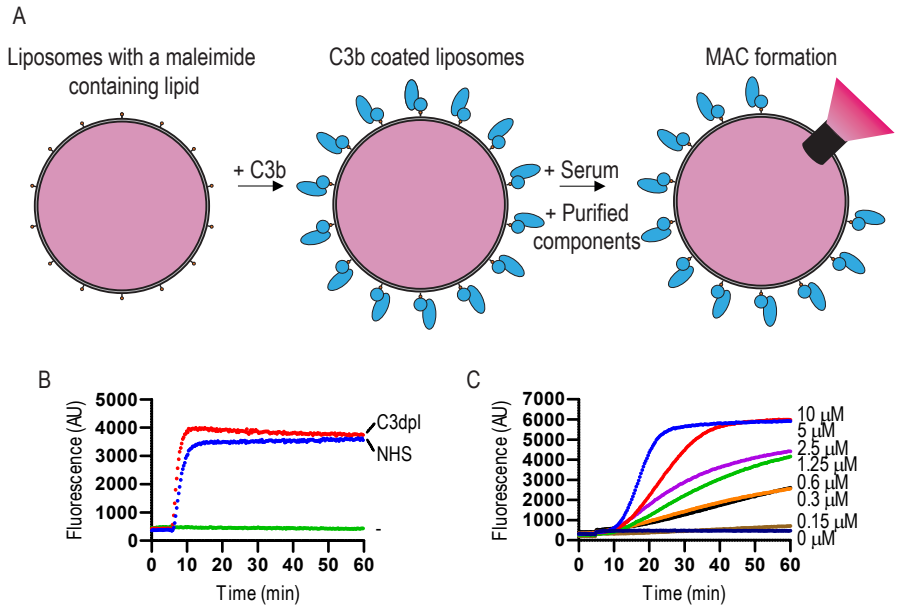

Figure 1 | Alternative pathway activation on liposomes coated with C3b

(A) Cartoon representation of a liposome based alternative pathway (AP) activity assay. Liposomes containing a lipid with a maleimide group were incubated with freshly generated C3b. The free cysteine in C3b that is generated after hydrolysis of the reactive thioester can covalently react with the maleimide-lipid. The liposomes encapsulate a self-quenching dye. AP activation can be monitored by the increase in fluorescence that occurs after the release of the dye through the MAC pore. **(B)** Normal human serum and C3-dpl serum can induce AP activation on C3b-coated liposomes. The negative control where no serum was added is indicated with -. **(C)** The level of AP activation induced by C3-dpl serum is proportional to the C3b concentration (indicated next to the curves) used for coating the liposomes.

(pro) convertase. These experiments revealed that stabilization of the C3 convertase by properdin is critical for AP activation in the presence of negative regulators with DAA. Furthermore, it showed that the enhanced formation of the C3 convertase and the reduced FI mediated proteolytic inactivation by properdin only play a minor role in AP activation.

Results:

Alternative pathway activation can be monitored on C3b-coated liposomes

Liposome-based assays have been previously used to biochemically and structurally study CP activation, however these liposomes displayed no or only limited AP activation (35, 36). To enable AP activation on liposomes we bypassed the initiation step of the AP by pre-coating liposomes with C3b. C3b was covalently attached to liposomes by coupling the free cysteine, which remains after hydrolysis of the thioester (37), to a maleimide containing lipid that was incorporated into the liposomes (**Fig. 1A schematic**). We tested the C3b-coated liposomes for AP activation by measuring fluorescence upon pore formation by the terminal pathway of complement (36). Incubation of C3b-coated liposomes with normal human serum (NHS) resulted in an increase in fluorescent signal indicating complement activation (**Fig. 1B**), whereas NHS with non-coated liposomes did not induce lysis in the timeframe of 60 minutes (**Supplemental Fig. 1**).

Next, we determined whether the density of C3b on the C3b pre-coated liposomes enabled terminal pathway activation and, thus, implicitly formation of C5 convertases. Incubation of the C3b-coated liposomes with serum devoid of C3 (C3-dpl) resulted in complement activation (**Fig. 1B**), which shows the C3b density on the pre-coated liposomes was sufficient for enabling the formation of C5 convertases. Next, we varied the density of C3b pre-coated on the liposomes. The amount of lysis induced by C3-dpl

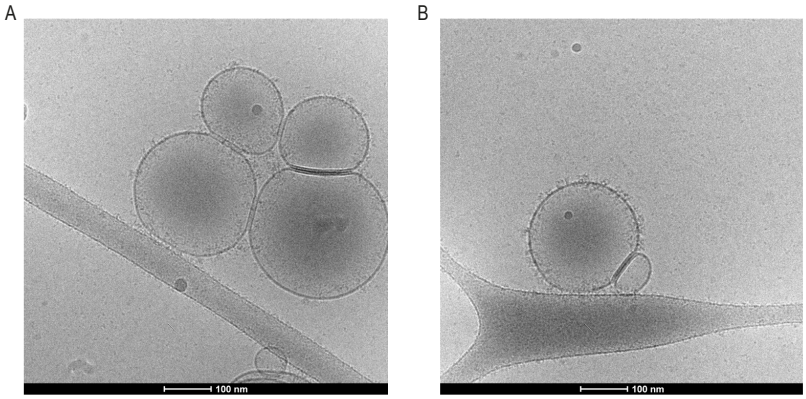

Figure 2 | Cryo-EM micrographs of C3b coated liposomes incubated with FB^{dg‡}, FD and C5

(A-B): Cryo-EM micrographs of C3b (0.3 μM) coated liposomes incubated with inactive FB^{dg‡}, FD and C5 suspended in a thin layer of vitreous ice. The liposomes are uni-lamellar and have a protein coat on their outsides.

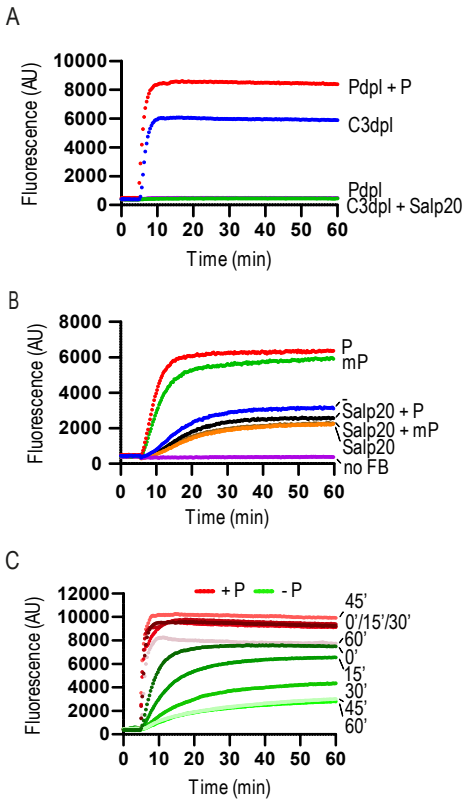

Figure 3 | Properdin is essential for inducing AP activation with serum

(A) There is no AP activation on C3b coated liposomes using P-dpl serum or when properdin inhibitor Salp20 is present. AP activity in P-dpl serum can be recovered by the addition of properdin (P). **(B)** Properdin is not essential for AP activation when using purified complement components FD, FB and C5-C9 (indicated with – next to the curve). Addition of properdin or a monomerized properdin variant (mP) enhances AP activation (indicated with P and mP) that can be counteracted by addition of Salp20. **(C)** Properdin prolongs the lifetime of the C3/C5 convertase. $C3bBb^{dgf}$ was generated on liposomes by incubating C3b-coated liposomes with FB^{dgf} and FD. $C3bBb^{dgf}$ coated liposomes were incubated with or without properdin at room temperature. Addition of terminal components C5-C9 leads to MAC formation that is proportional to the amount of remaining $C3bBb^{dgf}$. Liposomes incubated with properdin retain the ability to induce AP activation after prolonged periods of time compared to the liposomes without properdin.

serum of these liposomes was proportional to the amount of C3b used for pre-coating the liposomes, which likely corresponds to increased C5 convertase activity at higher C3b densities (4) (**Fig. 1C and Supplemental Fig. 2**).

We inspected the C3b pre-coated liposomes by imaging them by cryo-EM, which showed predominantly uni-lamellar liposomes with a diameter of roughly 200-300 nm (**Fig. 2A-B**). C3b-coated liposomes that were incubated with a FB variant that is catalytically inactive and which forms a more stable C3 convertase ($FB^{dgf‡}$) (38), FD and C5 revealed an electron dense layer protruding ca. 15 nm from the membrane (**Fig. 2A-B**), which matches well with the height of C3 convertase complexes (39). These observations suggest that C3b-coated liposomes could be suitable for structural characterization of different stages of the AP.

Properdin enhances complement activation on C3b-coated liposomes

We assessed the role of properdin in AP activation by inhibiting properdin activity with a properdin specific inhibitor, Salp20 (40), or by using properdin depleted (P-dpl) serum . The addition of Salp20 to either C3-dpl serum or NHS abolished AP activation on C3b-coated liposomes (**Fig. 3A and Supplemental Fig. 3**). Furthermore, no AP activation was observed when incubating C3b-coated liposomes with P-dpl serum. However, AP activation by P-dpl serum could be recovered by the addition of purified properdin. Next, we performed liposome leakage assays using purified complement components FD, FB and C5 through to C9. Addition of the purified components to C3b-coated liposomes resulted in AP activation. Supplementing the purified components with either properdin or a monomerized properdin variant (mP) (12) resulted in

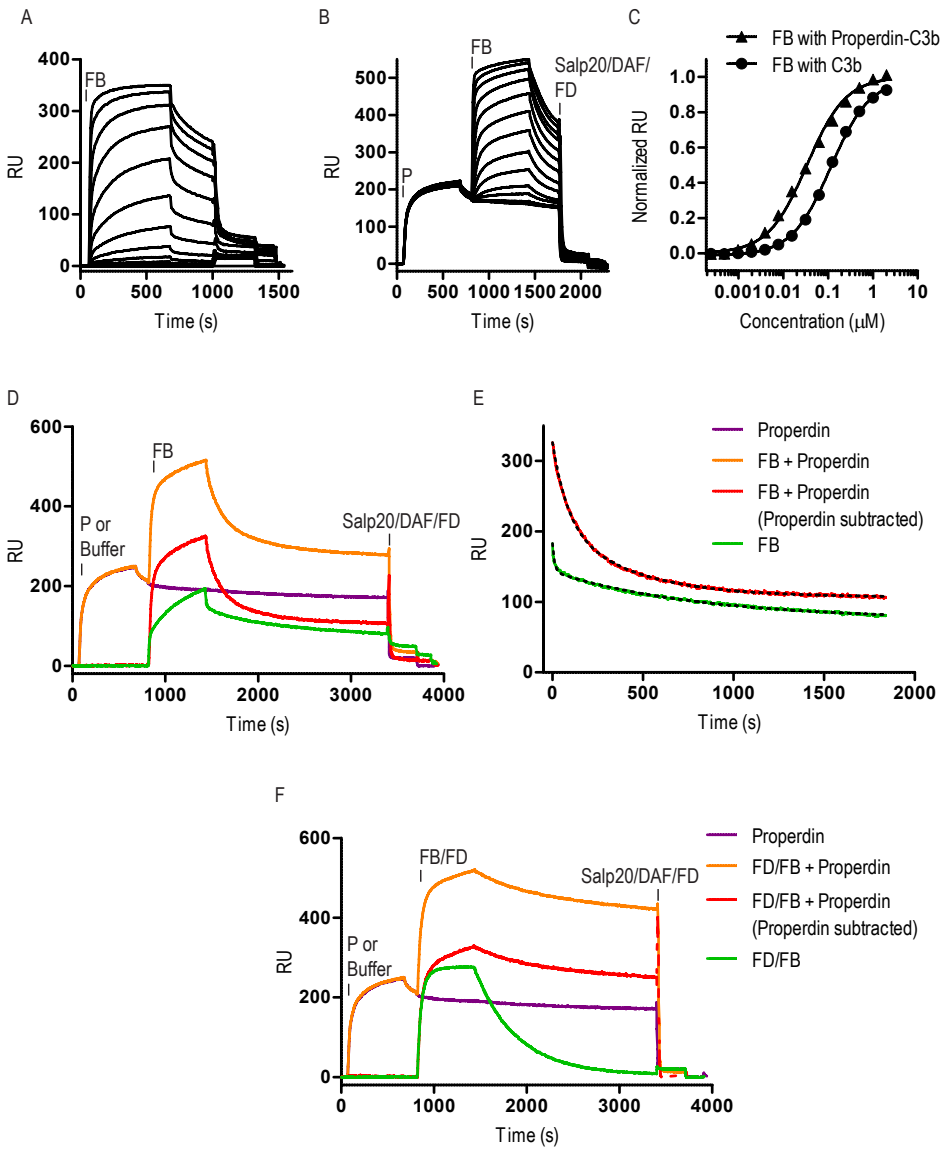

Figure 4 | Binding kinetics of FB interacting with C3b or with properdin-C3b complexes

SPR equilibrium experiment of FB (concentration range = 2.4 x 10^{-4} – 2 μM) binding to a SPR surface coated with C3b **(A)** or a SPR surface coated with properdin-C3b complexes that were generated by injecting 50 nM properdin (P) onto a C3b coated SPR surface **(B)**. **(C)** Endpoint data of A and B fitted with a one site specific binding curve. The data was normalized based on the Bmax of the binding curve. **(D-E)** Comparison of the formation and decay of the pro-convertase in the presence and absence of properdin by injecting FB (100 nM) on a SPR surface coated with C3b or with properdin-C3b complexes. The curve of properdin binding to C3b was subtracted from the interaction of FB with properdin-C3b and the data (continuous line) was fitted with a two-phase exponential decay (black dotted line). **(F)** Effect of properdin on the formation of the C3 convertase by injecting a mixture of FD and FB (both 100 nM) on a SPR surface coated with C3b or with properdin-C3b complexes. After each run, properdin, FB or Bb were dissociated from C3b by co-injecting a mixture of Salp20, DAF and FD at 5 μM, 1 μM and 0.1 μM, respectively.

Table 1: Kinetic parameters that define the interaction of FB with C3b and properdin-C3b				
Complex on SPR surface	K_D (nM)	K_{off} fast (10^{-3} s^{-1}) (fraction %)	K_{off} slow (10^{-3} s^{-1}) (fraction %)	Calculated K_{on} (10^5 $M^{-1}s^{-1}$)
C3b	108 ± 5	77 ± 4 (38 ± 3)	1.3 ± 0.04 (62 ± 3)	2.8
Properdin-C3b	32.7 ± 1.4	13 ± 1 (49 ± 1)	2.6 ± 0.1 (51 ± 1)	2.4
fold difference	3.3	6	0.5	1.17

Experiments were performed in triplicate

enhanced AP activation on the C3b pre-coated liposomes (**Fig. 3B**). Thus, properdin was critical for AP activation induced by serum but not when induced by purified complement components.

We tested the effect of properdin on the lifetime of C3 convertase complexes that were generated on C3b pre-coated liposomes by incubating them with FB^{dgf} and FD. The $C3bBb^{dgf}$ coated liposomes were incubated in the presence or absence of properdin. In the presence of properdin, the lifetime of $C3bBb^{dgf}$ was greatly increased compared to that of $C3bBb^{dgf}$ without properdin, with only minor loss of AP activity after incubation for 60 minutes (**Fig. 3C**).

Using SPR we compared the binding kinetics of FB interacting with C3b or properdin-C3b. SPR equilibrium experiments revealed that FB binds stronger to properdin-C3b compared to C3b alone with K_D's of 32.7 ± 1.4 and 108 ± 5 nM, respectively (**Fig. 4A-C**). The dissociation of FB from C3b fitted best with a two-phase exponential decay model, in which the fast and slow decay are attributed to the binding of only Ba or both Ba and Bb to C3b, respectively (39). FB decayed from C3b with a fast decay with a $t_{1/2}$ of 0.15 ± 0.01 min and a slow decay with a $t_{1/2}$ of 9.2 ± 0.3 min (**Fig. 4D-E**). In the presence of properdin, the fast decay of FB from C3b is decreased 6-fold resulting in a $t_{1/2}$ of 0.88 ± 0.1 min. Properdin slightly increased the slow decay rate, resulting in a $t_{1/2}$ of 4.4 ± 0.2 min. Using the measured K_D and K_{off} we calculated the K_{on} for FB binding to C3b and properdin-C3b (**Table 1**). Both K_{on} were very similar, which indicates that the increased affinity of FB to properdin-C3b is due to a lower K_{off}.

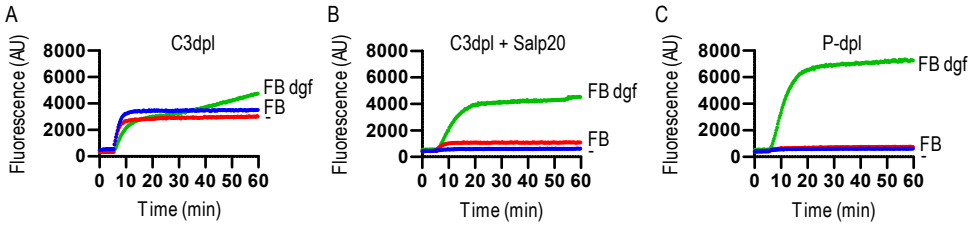

Figure 5 | Preformation of C3bBb on liposomes has minimal effect on AP activation

(A-C) Effect of pre-forming C3bBb on liposomes on properdin dependency. Pre-forming C3bBb on liposomes by incubating the C3b coated liposomes with FB and FD before adding serum C3-dpl serum had limited effect on AP activation when properdin is present **(A)**. Pre-formation of C3bBb has minimal effect on recovering AP activation when using C3-dpl serum supplemented with Salp20 **(B)** or when using P-dpl serum **(C)**. Pre-formation of $C3bBb^{dgf}$ with FD and FB^{dgf}, a FB mutant that generates a more stable complex, does recovers AP activation in absence of positive regulation by properdin **(B-C)**. The FB variant used for preforming C3bBb is indicated next to the curve. The – denotes the experiment where C3bBb was not preformed.

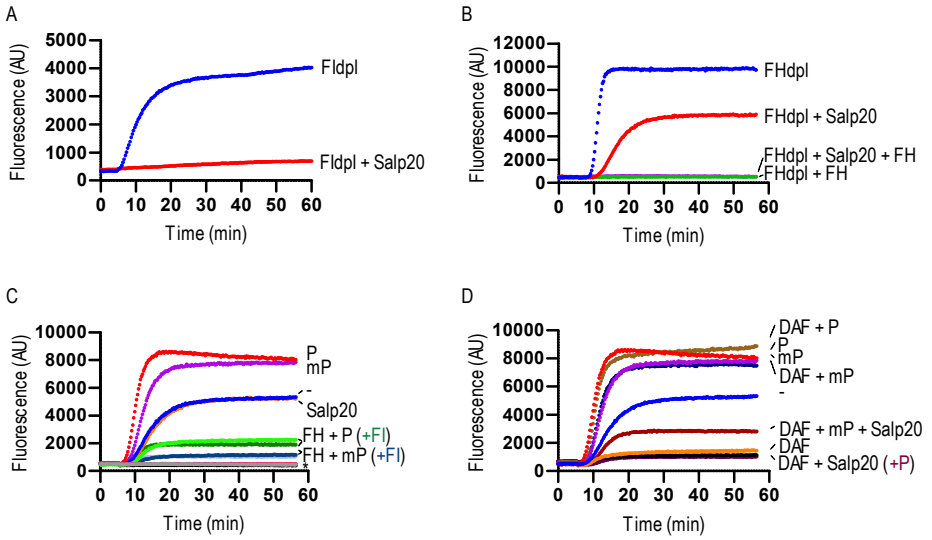

Figure 6 | Characterizing the effect of the interplay between positive and negative regulation on AP activation on C3b-coated liposomes.

(A) Inhibition of properdin activity by Salp20 prevents AP activation on C3b coated liposomes induced by FI-dpl serum **(B)** Inhibition of properdin by Salp20 only partially reduces the amount of AP activation induced by FH-dpl serum on C3b-coated liposomes. Reconstituting FH-dpl serum with FH results in complete inhibition, both in absence and presence of Salp20. **(C-D)** Properdin dependency can be induced when inducing AP activation with the purified complement components FD, FB and C5-C9 by addition of proteins with decay accelerating activity: FH **(C)** or DAF **(D)**. The addition of FI **(C)** has no effect on the amount of AP activation. In panel C and D the same curves are used for the experiment with no added properdin and for the experiments with P or mP added to the purified components. The * indicates overlapping curves for FH, FH + Salp20, FH + mP or P + Salp20, FH + FI, FH + FI + Salp20, FH + FI + mP or P + Salp20. In A and B the serum used and the proteins added to the serum are indicated next to the curve. In C and D the proteins added to the purified components FB, FD and C5 to through C9 are indicated next to the curve.

Next, we used SPR to test the effect of properdin on C3bBb formation. Simultaneous injection of FD and FB on a SPR surface coated with either C3b or properdin-C3b (**Fig. 4F**) resulted in 18 ± 1 % more C3bBb formation on properdin-C3b compared to C3b alone. This is less than the 67 ± 7 % increase in complex formation observed for FB binding to propedin-C3b compared to C3b alone (**Fig. 4D**). To mimic the effect of enhanced convertase assembly by properdin we preformed C3bBb on liposomes. Pre-formation of C3bBb only had limited effect on AP activation induced by C3-dpl serum in the absence or presence of Salp20 and no effect on AP activation induced by P-dpl serum (**Fig. 5A-C**). Altogether, the enhanced C3 convertase formation by properdin likely only plays a minor role in AP activation. Preformation of C3bBb using FB^{dgf} did partially recover AP activation in absence of positive regulation by properdin (**Fig. 5B-C**), which indicates that the increased stability of C3bBb provided by either properdin or FB^{dgf} is important for AP activation.

Stabilization of C3bBb by properdin is required to counteract the effect of C3bBb decay induced by negative regulators.

As properdin is critical for AP activation while using serum but not when using purified

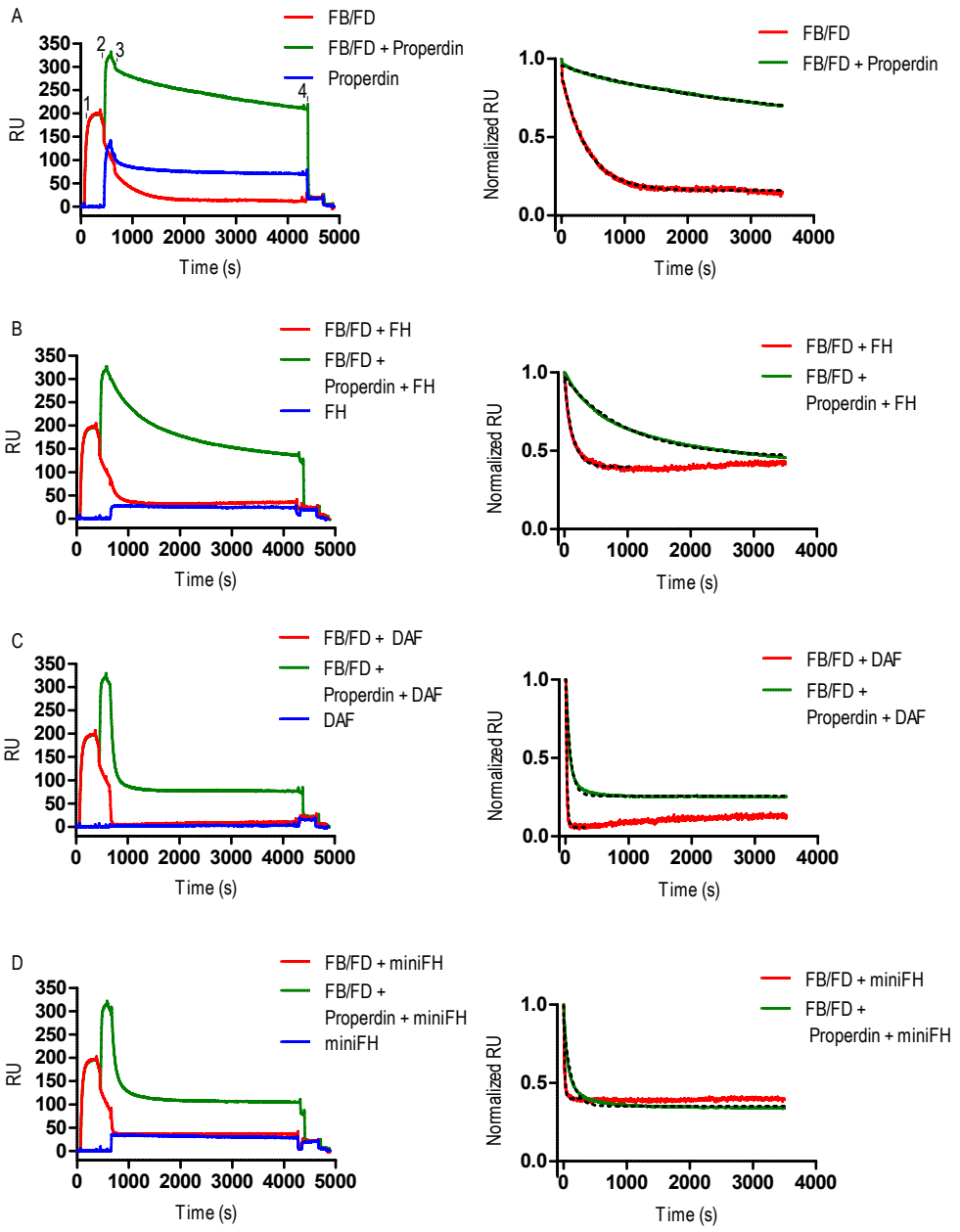

Figure 7 | The effect of C3bBb stabilization by properdin on the decay acceleration activity of FH, DAF and miniFH

(A-D) SPR sensorgrams of the generation and decay of C3bBb (left panel) and the normalized decay of C3bBb (right panel). C3bBb was generated by simultaneously injecting FD and FB at 100 nM (1). Subsequently, buffer or properdin at 50 nM was injected (2). Next, either buffer or a negative regulator at 100 nM was injected for 60 minutes (3). Afterwards, properdin and Bb were dissociated from C3b by injecting Salp20 and DAF at 5 μM and 1 μM, respectively (4). In the right panels the data was normalized on the amount of RU at the buffer or negative regulator injection (3). Effect of properdin on the intrinsic decay of C3bBb **(A)** or on the decay of C3bBb induced by FH **(B)**, DAF **(C)** and miniFH **(D)**. The data (continuous line) is fitted with a one phase exponential decay (black dotted line).

components, we investigated the relation between the positive regulator properdin and the negative regulators FH and FI. Both serum devoid of FI (FI-dpl) or FH (FH-dpl) induced AP activation on C3b-coated liposomes (**Fig. 6A-B**). Inhibition of properdin activity with Salp20 in FI-dpl serum resulted in complete inhibition of AP activation (**Fig. 6A**). In contrast, inhibition of properdin activity with Salp20 did not result in complete inhibition of AP activation in FH-dpl serum (**Fig. 6B**). Instead, properdin inhibition reduced the amount of AP activation induced by FH-dpl serum by ca. 40 %. Addition of purified FH to FH-dpl serum resulted in complete inhibition of AP activation, even without the addition of Salp20 (**Fig. 6B**). Next, we tested the effect of positive and negative regulation on AP activation on C3b-coated liposomes induced by the purified complement components, FB, FD and C5 through to C9. Supplementing the purified components with FH or decay acceleration factor (DAF), a negative regulator with only DAA, in absence of properdin resulted in no or minimal AP activation, respectively (**Fig. 6C-D**). AP activation in the presence of FH and DAF could be partially recovered by the addition of either properdin or mP. The addition of FI together with FH did not alter the amount of complement activation in the presence of properdin compared to the addition of only FH. Properdin dependency could therefore be induced by supplementing the purified components with negative regulators that have DAA.

With SPR we quantified the effect of stabilization by properdin and accelerated decay by FH and DAF on the $t_{1/2}$ of C3bBb. C3bBb intrinsically decays into C3b and Bb with a $t_{1/2}$ of 4.3 minutes (**Fig. 7A**). Stabilization of C3bBb by properdin increased the $t_{1/2}$ of C3bBb from 4.3 to 27 min, which is in agreement with previous reported $t_{1/2}$ of C3bBb and C3bBb stabilized by properdin (8, 29). In the presence of FH, miniFH or DAF the $t_{1/2}$ of C3bBb is decreased to 1.3 min, 0.18 min and 0.17 min, respectively. The addition of properdin reduced the rate of decay of C3bBb in the presence of the negative regulators, resulting in a $t_{1/2}$ of 10 min, 1.3 min and 0.7 min for FH, miniFH and DAF, respectively (**Fig. 7B-D**). The relative increase of the lifetime of C3bBb induced by properdin was similar with and without negative regulators (**Table 2**), suggesting they act independently.

Table 2: Effect of properdin and negative regulators on the $t_{1/2}$ of C3bBb

Complex	C3bBb	C3bBbP	C3bBb	C3bBbP	C3bBb	C3bBbP	C3bBb	C3bBbP
Negative regulator	-		FH		miniFH		DAF	
$t_{1/2}$ (min)	4.3 ± 0.37	27.3 ± 3.7	1.3 ± 0.13	10.3 ± 0.88	0.18 ± 0.01	1.29 ± 0.04	0.17 ± 0.03	0.74 ± 0.08
fold stabilization by properdin	6.3		7.9		7.1		4.4	

Experiments were performed in triplicate

Discussion

We generated a liposome-based complement activation assay to study the role of properdin in AP activation (**Fig. 1A**). In this assay we pre-coated liposomes with C3b, through coupling of the free cysteine in C3b that remains after hydrolysis of the reactive thioester with a maleimide containing lipid, to circumvent the slow and uncontrolled auto-activation through C3*. Using these C3b-coated liposomes, we showed that properdin is critical for AP activation induced by serum (and C3-dpl serum), but not for AP activation induced by the purified complement components FB, FD and C5 through to C9 (**Fig. 3**).

With SPR we investigated the effect of properdin on formation and stabilization of C3 (pro)- convertases. In agreement with previous data (16), properdin reduced the dissociation of FB from C3b leading to a 3 times higher affinity of FB for C3b binding in presence of properdin. However, FB at physiological concentrations (2 to 8 μM (41, 42)) nearly saturated both C3b and properdin-C3b complexes in our SPR experiments (**Fig. 4C**). Simultaneous injection of FB and FD to C3b or properdin-C3b coated SPR surfaces increased convertase formation by 18 ± 1 % (**Fig. 4F**). Assessing the effect of properdin on the stability of C3bBb revealed that properdin increased the lifetime of the C3 convertase 6 fold (**Table 2**), which is in agreement with previously reported values (8). Virtually no AP activation was observed with pre-formed C3bBb on liposomes in the absence of properdin activity (**Fig. 4A-C**). However, a major effect on increasing the lifetime of C3bBb on liposomes was observed in the presence of properdin (**Fig. 3C**). Furthermore, the preformation of C3 convertases using FB^{dgf}, which yields more stable C3 convertases, allowed for AP activation in the absence of properdin activity (**Fig. 5B-C**). Thus, our data indicated that properdin enhances AP activation through stabilization of C3bBb but that its effect on enhanced formation of C3 convertases only has minor influence on activation.

We tested the importance of reduction of FI activity by properdin in AP activation. FI-dpl serum induced AP activation on the C3b-coated liposomes, whereas addition of the properdin inhibitor Salp20 to FI-dpl serum completely inhibited activation. Thus, in absence of FI mediated inactivation of C3b properdin was still required for AP activation, which shows that reduction of FI activity by properdin is not what makes it critical for AP activation. Furthermore, the addition of FI to the purified complement components FB, FD, FH, properdin and C5 through to C9 had minimal effect on AP activation. The limited effect of FI on AP activation suggests that activation of the terminal pathway on C3b-coated liposomes occurred more efficiently than FI-mediated inactivation of C3b.

Properdin and FH have opposite effects on the lifetime of C3 convertases. We assessed the relationship between properdin and FH on AP activation using the C3b-coated liposomes. Supplementing FH-dpl serum with Salp20 reduced the amount of AP activation induced by FH-dpl serum by 40 % (**Fig. 6B**), which shows that properdin activity is not essential for AP activation in FH-dpl serum. Furthermore, the addition

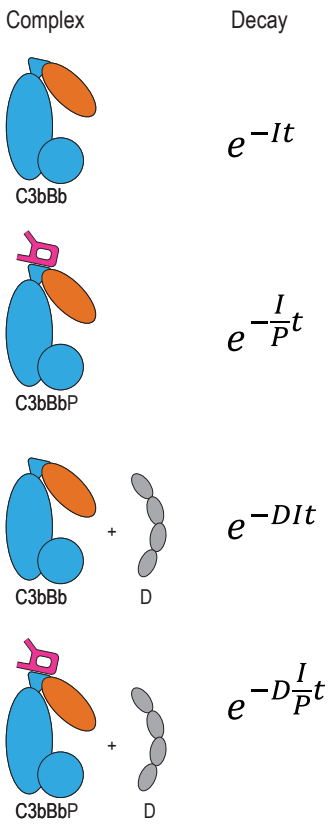

Figure 8 | Model of the effect of positive and negative regulation on the decay of C3bBb

The heterodimeric enzyme complex C3bBb intrinsically decays (I) into C3b and Bb. The effect of properdin (P) and negative regulators with decay acceleration activity (D) on the exponential decay of C3bBb is indicated in the formulas on the right. P (if P > 1) decreases the exponential decay and thus stabilizes C3bBb and D (if D > 1) increases the exponential decay and thus destabilizes C3bBb. P and D independently modulate the decay of C3bBb.

of FH or a soluble version of DAF (both regulators with DAA) to the purified complement components FB, FD and C5 through to C9 completely abolished AP activation in the absence of properdin. AP activation in the presence of FH and DAF could be partially recovered with the addition of properdin to the purified components (**Fig. 6C-D**). These results showed that stabilization of the C3 convertase by properdin is critical for AP activation to counteract the increased decay of the C3 convertase by negative regulators with DAA, which is in line with previously observed reduced DAA of FH in the presence of properdin (29–31). However, how properdin affects DAA remains unclear. Previous structural and biochemical data show that properdin and FH may bind simultaneously to C3b (12, 32–34). On the other hand, it is unclear if properdin affects the interaction of FH with C3 convertases. Recently, it was suggested that properdin induces a conformational change in C3bBb that affects the DAA of negative regulators (11, 17). Using SPR we characterized the effect of C3bBb stabilization by properdin on DAA of FH, DAF and miniFH (**Fig. 7**). The relative stabilization of C3bBb by properdin was similar both in absence and in presence of the negative regulators FH, DAF and miniFH (**Table 2**). This shows that stabilization by properdin and decay acceleration by negative regulators are two independent processes that, with their opposing effects, determine the lifetime of pivotal C3bBb complexes (**Fig. 8**).

In summary, we studied the effect of properdin on AP activation using a liposome-based assay suitable for monitoring AP activation. This revealed that the balance between positive regulation by properdin and negative regulation by FH in serum is key to AP activation. Furthermore, we show that properdin primarily exerts its positive regulatory effect by stabilization of C3bBb.

Materials and Methods

Protein production

Human wildtype FB, a FB double gain of function mutant FB^{dgf} (D279G, N285D) (38), a catalytically inactive FB double gain of function mutant (D279G, N285D, S699A) $FB^{dgf‡}$, FD, properdin, a monomerized properdin (mP) variant (STB-TSR1/TSR4-5-6), Salp20, and soluble DAF (CCP 1-4) were generated as described previously (12, 43–45). Briefly, proteins were expressed in HEK293 (FB, FD and properdin) or HEK293 GNTI- (FB^{dgf}, $FB^{dgf‡}$, Salp20, DAF and mP) suspension cells (provided by U-protein express BV). Cells were grown at 37 °C for 6 days post transfection. The suspension was centrifuged at 1000 g for 10 minutes to remove the cells and subsequently the supernatant was centrifuged at 4000 g for 10 minutes to remove any remaining cell debris. For all proteins except FD, the supernatant was incubated at 4 °C with 3 ml/L Ni-Sepharose Excel beads (GE Healthcare) for 2-3 hours. Next, the beads were collected by centrifuging at 1000 g for 10 min. The beads were washed with 10 column volume (CV) IMAC buffer (20 mM HEPES pH 7.8, 500 mM NaCl) and subsequently with 10 CV IMAC buffer supplemented with 10 mM imidazole. The proteins were eluted from the beads with IMAC buffer supplemented with 250 mM imidazole. Next, the proteins were purified by size exclusion chromatography (SEC) using a Superdex 200 10/300 (GE Healthcare) column pre-equilibrated in SEC buffer (20 mM HEPES pH 7.4 and 150 mM NaCl). FD was purified by cation exchange using a HiScreen Capto S column (GE Healthcare). First the medium was concentrated and exchanged to the CaptoS buffer (10 mM Citrate pH 6.0) using a Quickstand (GE Healthcare) fitted with a 5 kDa membrane. Next, the supernatant was centrifuged for 45 min at 8000 g and passed through a 0.2 μm filter (Whatman). Subsequently, the sample was loaded onto the CaptoS column pre-equilibrated in 10 mM Citrate pH 6.0. FD was eluted with a gradient of 0-50% of the CaptoS buffer supplemented with 1 M NaCl. FD was further purified by SEC using a Superdex 75 10/300 column pre-equilibrated in SEC buffer. C3 was purified from plasma as described by Wu et al (23) and the complement proteins C5 through to C9, FI and FH were purchased from Complement Technology. MiniFH was a kind gift from Christoph Q Schmidt. All proteins were stored at -80 °C except for properdin which was stored at 4 °C.

Serum

Normal human serum (NHS) was kindly provided by Suzan H.M. Rooijakkers. Serum depleted of complement components was purchased from Complement Technology.

Preparation of C3b coated liposomes

For the preparation of the liposomes, 1,2-dimyristoyl-*sn*-glycero-3-phosphocholine

(14:0) (DMPC), 1,2-dimyristoyl-*sn*-glycero-3-phosphoglycerol (14:0) (DMPG), cholesterol, 1,2-dipalmitoyl-*sn*-glycero-3-phosphoethanolamine-N-[6-[(2,4-dinitrophenyl) amino] hexanoyl] (16:0 DNP-cap-PE)(Avanti Polar) and 1,2-Distearoyl-sn-Glycero-3-Phosphoethanolamine-maleimide (DSPE-maleimide, Nanosoft Polymers) were mixed in the molar ratios of 44, 4.5, 49.5, 1, and 1, respectively. In total 2 μmol of lipids were dissolved in 0.5 ml of a $CHCl_3$/MeOH mixture (90:10). A thin lipid film was created by rotating the test tube at 37 °C under a continuous N_2 flow. To remove any residual solvent, the lipid film was left under vacuum for 2-18 h in the dark. Subsequently 1 ml of SRB buffer (20 mM sulforhodamine B, 20 mM HEPES pH 7.4, 150 mM NaCl, 0.5mM $MgCl_2$ and 0.5 mM $CaCl_2$) was added to the lipid film and the mixture was incubated for 1 h at 37 °C. Liposomes were created by subjecting the mixture to 5 freeze-thaw cycles consisting of freezing in liquid N_2 and thawing at 37 °C. After the generation of the liposomes, they were extruded at 37 °C through a 200 nm extrusion membrane (Avanti Polar). Excess SRB was removed by desalting the liposomes using a 5 ml HiTrap Desalting column (GE Healthcare) pre-equilibrated in the liposome buffer (20 mM HEPES pH 7.4, 150 mM NaCl, 0.5 mM $MgCl_2$ and 0.5 mM $CaCl_2$). C3b was freshly generated from C3 by incubating C3 at 37 °C with FB and FD in the molar ratios of 1,1,0.01 respectively in liposome buffer supplemented to a 2mM final $MgCl_2$ concentration. The freshly generated C3b was incubated with the liposomes at various concentrations of C3b overnight at 4°C. The excess C3b was separated from the liposomes by centrifugation at 100,000 g for 1 h. The supernatant was removed, and the pellet was resuspended in liposome buffer.

Measuring AP activation on the C3b coated liposomes

Alternative pathway activation on liposomes was evaluated by measuring leakage of fluorophore sulforhodamine B through MAC pores formed on the liposomes upon addition of sera or purified complement proteins. For this, 100 or 20 μl reactions were set up in black, flat bottomed 96 or 384 well plates (Greiner), respectively. All fluorescence measurements were carried out on a CLARIOStar Plus microplate reader (BMG LabTech) at room temperature. Data were analyzed using MARS data analysis software (BMG LabTech) and GraphPad Prism 8. An initial baseline fluorescence measurement was carried out for 5 minutes before addition of either serum or purified complement components (unless otherwise indicated). After addition, fluorescence was recorded over the following 55 mins, with fluorescence measurements taking place at 20 s intervals.

All reactions were set up to contain a final 10% v/v liposomes in assay buffer (20 mM Hepes pH 7.4, 150 mM NaCl, 2 mM EGTA and 2 mM $MgCl_2$). Where serum was employed, it was added to a final 10% v/v. Where purified complement components were used, they were added to reach the following final concentrations: FB/FB^{dgf} – 0.8 μM, FD – 0.02 μM, C5 – 0.045 μM, C6 – 0.043 μM, C7 – 0.059 μM, C8 – 0.06 μM, C9 – 0.095 μM, Salp20 – 1 μM, FH – 0.3 μM, FI – 0.03 μM, DAF – 0.3 μM, properdin – 0.03

μM, mP – 0.3 μM.

Except for the experiments with coating with various amount of C3b all experiments were performed on liposomes coated with C3b at 10 μM. Data shown within each figure panel are from the same liposome batch to prevent misinterpretation of differences which could arise from batch-to-batch variation. The data shown is representative of 2 to 3 experiments.

Cryo-electron microscopy

Liposomes coated with C3b to a final concentration of 0.3 μM were centrifuged at 100,000 rpm for 1h at 4 °C and resuspended in liposome buffer (20 mM HEPES pH 7.4, 150 mM NaCl, 0.5 mM $MgCl_2$ and 0.5 mM $CaCl_2$). The coated liposomes were incubated with $FB^{dgf‡}$ - 0.3 μM, FD - 0.01 μM and C5 - 0.3 μM for 10 minutes on ice in a reaction where 50% v/v is composed by the liposome preparation. 3.5 μl of this mixture was applied to plasma cleaned 200 mesh copper grids with lacey-carbon support (Quantifoil). Grids were blotted for 3 s and flash frozen in a liquid ethane/propane mixture using a manual grid plunger. Samples were imaged on a Talos Arctica transmission electron microscope operating at 200 keV (Thermo Fisher Scientific) and fitted with a K2 Summit direct electron detector (Gatan). Images were acquired at a pixel size of 2.17 Å, with 6 s exposure and a dose rate of 7.4 e^-/pix/s.

Surface plasmon resonance

Biotinylated C3b was generated as before (12). Briefly, C3b was produced by incubating C3 together with FB and FD in the presence of 5 mM $MgCl_2$ at 37 °C. Subsequently the freshly produced C3b was incubated with 1mM EZ-Link Maleimide-PEG2-Biotin (Thermofisher) for 3 h at RT. Subsequently, the biotinylated C3b was separated from Bb, FD and the excess Maleimide-PEG2-Biotin by SEC purification with a S200 10/300 increase column (GE Healthcare) pre-equilibrated with SEC buffer. The biotinylated C3b (25 nM) was spotted on a streptavidin coated SPR chip (P-strep) (Ssens BV, Enschede) for 1 h using a continuous flow microspotter (CFM, Wasatch). After spotting, the surface was treated with 1 mM biotin in SPR buffer (20 mM HEPES pH 7.4, 150 mM NaCl, 5 mM $MgCl_2$ and 0.005% Tween-20) to occupy all free streptavidin. SPR experiments were performed with the IBIS-MX96 at 25°C and using SPR buffer. Equilibrium binding experiments with FB were performed with a 14 step, 2-fold dilution series. In all experiments properdin-C3b was generated by injecting 50 nM properdin onto the C3b coated surface. To regenerate the surface and remove any remaining FB and properdin, a mixture of 100 nM FD, 1 μM DAF and 5 μM Salp20 was injected. In experiments for monitoring the amount of formation of C3bB or C3bBb 100 nM FB or 100 nM FB and FD, respectively, were injected on a C3b or a properdin-C3b coated surface. In the SPR experiments monitoring the half-life of C3bBb, the C3 convertase

was generated by injecting a mixture of FB and FD (both 100 nM) onto a C3b coated surface. Subsequently, either buffer or properdin (50 nM) was injected. Next, either buffer or a negative regulator (100 nM) was injected for 1 hour. The surface was regenerated by injecting 1 μM DAF and 5 μM Salp20. After each run, the surface was treated with SPR buffer supplemented with 1 M NaCl. The K_D of FB for C3b and properdin-C3b was determined by fitting the endpoint data to $Y = \frac{Bmax * x}{KD + x} + Background$. The decay of FB from C3b and properdin-C3b was calculated by fitting the data with a two-phase exponential decay model. The decay of the C3 convertase was fitted with a one-phase exponential decay model. All fits were performed with GraphPad Prism 5.

Acknowledgements

We thank the members of the Crystal and Structural Chemistry and of the Cryo-electron microscopy groups for experimental support, useful discussions and suggestions. U-protein Express BV for providing and transfecting the HEK cell cultures. Suzan Rooijakkers for providing the human serum for the liposome leakage assays and for useful discussions. Maartje Ruyken for assistance with the C3 purification. Christoph Q Schmidt for providing MiniFH.

Author Contributions

RvdB, ISM, PG designed the experiments. RvdB and JA performed the initial design and validation of the alternative pathway liposome-based assay. Both RvdB and ISM performed protein production and purification. ISM performed the liposome leakage assays. RvdB performed SPR experiments. ISM performed the EM experiments. RvdB, ISM and PG wrote the manuscript.

References

1. Merle, N. S., S. E. Church, V. Fremeaux-Bacchi, and L. T. Roumenina. 2015. Complement system part I - molecular mechanisms of activation and regulation. *Front. Immunol.* 6: 1–30.

2. Pangburn, M. K., and H. J. Muller-Eberhard. 1980. Relation of a putative thioester bond in C3 to activation of the alternative pathway and the binding of C3b to biological targets of complement. *J. Exp. Med.* 152: 1102–1114.

3. Sim, R. B., T. M. Twose, D. S. Paterson, and E. Sim. 1981. The covalent-binding reaction of complement component C3. *Biochem. J.* 193: 115–127.

4. Rawal, N., and M. K. Pangburn. 2001. Formation of High-Affinity C5 Convertases of the Alternative Pathway of Complement. *J. Immunol.* 166: 2635–2642.

5. Rawal, N., and M. K. Pangburn. 2003. Formation of high affinity C5 convertase of the classical pathway of complement. *J. Biol. Chem.* 278: 38476–38483.

6. Menny, A., M. Serna, C. M. Boyd, S. Gardner, A. P. Joseph, B. P. Morgan, M. Topf, N. J. Brooks, and D. Bubeck. 2018. CryoEM reveals how the complement membrane attack complex ruptures lipid bilayers. *Nat. Commun.* 9: 1–11.

7. Ricklin, D., G. Hajishengallis, K. Yang, and J. D. Lambris. 2010. Complement: A key system for immune surveillance

and homeostasis. *Nat. Immunol.* 11: 785–797.

8. Fearon, D. T., and K. F. Austen. 1975. Properdin: binding to C3b and stabilization of the C3b-dependent C3 convertase. *J. Exp. Med.* 142: 856–63.

9. Farries, T. C., P. J. Lachmann, and R. A. Harrison. 1988. Analysis of the interactions between properdin, the third component of complement (C3), and its physiological activation products. *Biochem. J.* 252: 47–54.

10. Pangburn, M. K. 1989. Analysis of the natural polymeric forms of human properdin and their functions in complement activation. *J. Immunol.* 142: 202–7.

11. Pedersen, D. V, L. Roumenina, R. K. Jensen, T. A. Gadeberg, C. Marinozzi, C. Picard, T. Rybkine, S. Thiel, U. B. Sørensen, C. Stover, et al. 2017. Functional and structural insight into properdin control of complement alternative pathway amplification. *EMBO J.* 36: 1084–1099.

12. van den Bos, R. M., N. M. Pearce, J. Granneman, T. H. C. Brondijk, and P. Gros. 2019. Insights Into Enhanced Complement Activation by Structures of Properdin and Its Complex With the C-Terminal Domain of C3b. *Front. Immunol.* 10.

13. Chen, J. Y., C. Cortes, and V. P. Ferreira. 2018. Properdin: A multifaceted molecule involved in inflammation and diseases. *Mol. Immunol.* 102: 58–72.

14. Fijen, C. A. P., R. van den Bogaard, M. Schipper, M. Mannens, M. Schlesinger, F. G. Nordin, J. Dankert, M. R. Daha, A. G. Sjöholm, L. Truedsson, et al. 1999. Properdin deficiency: molecular basis and disease association. *Mol. Immunol.* 36: 863–867.

15. Blatt, A. Z., S. Pathan, and V. P. Ferreira. 2016. Properdin: a tightly regulated critical inflammatory modulator. *Immunol. Rev.* 274: 172–190.

16. Hourcade, D. E. 2006. The role of properdin in the assembly of the alternative pathway C3 convertases of complement. *J. Biol. Chem.* 281: 2128–2132.

17. Alcorlo, M., A. Tortajada, S. Rodríguez de Córdoba, and O. Llorca. 2013. Structural basis for the stabilization of the complement alternative pathway C3 convertase by properdin. *Proc. Natl. Acad. Sci. U. S. A.* 110: 13504–9.

18. Zhang, J., L. Song, D. V Pedersen, A. Li, J. D. Lambris, G. R. Andersen, T. E. Mollnes, Y. J. Ma, and P. Garred. 2020. Soluble collectin-12 mediates C3-independent docking of properdin that activates the alternative pathway of complement. *Elife* 9.

19. Xu, W., S. P. Berger, L. A. Trouw, H. C. de Boer, N. Schlagwein, C. Mutsaers, M. R. Daha, and C. van Kooten. 2008. Properdin Binds to Late Apoptotic and Necrotic Cells Independently of C3b and Regulates Alternative Pathway Complement Activation. *J. Immunol.* 180: 7613–7621.

20. Lammerts, R. G. M., D. T. Talsma, W. A. Dam, M. Daha, M. Seelen, S. P. Berger, and J. Van Den Born. 2020. Properdin pattern recognition on proximal tubular cells is heparan sulfate/Syndecan-1 but not C3b dependent and can be blocked by tick protein Salp20. *Front. Immunol.* 11: 1643.

21. Parente, R., S. J. Clark, A. Inforzato, and A. J. Day. 2017. Complement factor H in host defense and immune evasion. *Cell. Mol. Life Sci.* 74: 1605–1624.

22. Xue, X., J. Wu, D. Ricklin, F. Forneris, P. Di Crescenzio, C. Q. Schmidt, J. Granneman, T. H. Sharp, J. D. Lambris, and P. Gros. 2017. Regulator-dependent mechanisms of C3b processing by factor i allow differentiation of immune responses. *Nat. Struct. Mol. Biol.* 24: 643–651.

23. Wu, J., Y. Q. Wu, D. Ricklin, B. J. C. Janssen, J. D. Lambris, and P. Gros. 2009. Structure of complement fragment C3b-factor H and implications for host protection by complement regulators. *Nat. Immunol.* 10: 728–733.

24. S. Reis, E., D. A. Falcão, and L. Isaac. 2006. Clinical aspects and molecular basis of primary deficiencies of complement component C3 and its regulatory proteins factor I and factor H. *Scand. J. Immunol.* 63: 155–168.

25. De Córdoba, S. R., and E. G. De Jorge. 2008. Translational Mini-Review Series on Complement Factor H: Genetics and disease associations of human complement factor H. *Clin. Exp. Immunol.* 151: 1–13.

26. Blaum, B. S., J. P. Hannan, A. P. Herbert, D. Kavanagh, D. Uhrín, and T. Stehle. 2014. Structural basis for sialic acid-mediated self-recognition by complement factor H. *Nat. Chem. Biol.* 11: 77–83.

27. Prosser, B. E., S. Johnson, P. Roversi, A. P. Herbert, B. S. Blaum, J. Tyrrell, T. A. Jowitt, S. J. Clark, E. Tarelli, D. Uhrín, et al. 2007. Structural basis for complement factor H-linked age-related macular degeneration. *J. Exp. Med.* 204: 2277–2283.

28. Ricklin, D., E. S. Reis, and J. D. Lambris. 2016. Complement in disease: a defence system turning offensive. *Nat. Rev. Nephrol.* 12: 383–401.

29. Fearon, D. T., and K. Frank Austen. 1977. Activation of the alternative complement pathway with rabbit erythrocytes by circumvention of the regulatory action of endogenous control proteins. *J. Exp. Med.* 146: 22–33.

30. Weiler, J. M., M. R. Daha, K. F. Austen, and D. T. Fearon. 1976. Control of the amplification convertase of complement by the plasma protein beta1H. *Proc. Natl. Acad. Sci. U. S. A.* 73: 3268–72.

31. Whaley, K., and S. Ruddy. 1976. Modulation of the alternative complement pathway by β1H globulin. *J. Exp. Med.* 144: 1147–1163.

32. Medicus, R. G., O. Götze, and H. J. Müller-Eberhard. 1976. Alternative pathway of complement: Recruitment of precursor properdin by the labile C3/C5 convertase and the potentiation of the pathway. *J. Exp. Med.* 144: 1076–1093.

33. Pedersen, D. V., T. A. F. Gadeberg, C. Thomas, Y. Wang, N. Joram, R. K. Jensen, S. M. M. Mazarakis, M. Revel, C. El Sissy, S. V. Petersen, et al. 2019. Structural Basis for Properdin Oligomerization and Convertase Stimulation in the Human Complement System. *Front. Immunol.* 10.

34. DiScipio, R. G. 1981. The binding of human complement proteins C5, factor B, β1H and properdin to complement fragment C3b on zymosan. *Biochem. J.* 199: 485–496.

35. Sharp, T. H., F. G. A. Faas, A. J. Koster, and P. Gros. 2017. Imaging complement by phase-plate cryo-electron tomography from initiation to pore formation. *J. Struct. Biol.* .

36. Sharp, T. H., A. J. Koster, and P. Gros. 2016. Heterogeneous MAC Initiator and Pore Structures in a Lipid Bilayer by Phase-Plate Cryo-electron Tomography. *Cell Rep.* 15: 1–8.

37. Law, S. K. A., and A. W. Dodds. 1996. The internal thioester and the covalent binding properties of the complement proteins C3 and C4. *Protein Sci.* 6: 263–274.

38. Hourcade, D. E., L. M. Mitchell, and T. J. Oglesby. 1999. Mutations of the type A domain of complement factor B that promote high- affinity C3b-binding. *J. Immunol.* 162: 2906–2911.

39. Rooijakkers, S. H. M., J. Wu, M. Ruyken, R. van Domselaar, K. L. Planken, A. Tzekou, D. Ricklin, J. D. Lambris, B. J. C. Janssen, J. a G. van Strijp, et al. 2009. Structural and functional implications of the alternative complement pathway C3 convertase stabilized by a staphylococcal inhibitor. *Nat. Immunol.* 10: 721–727.

40. Tyson, K. R., C. Elkins, and A. M. de Silva. 2008. A Novel Mechanism of Complement Inhibition Unmasked by a Tick Salivary Protein That Binds to Properdin. *J. Immunol.* 180: 3964–3968.

41. Zhang, Y., C. M. Nester, B. Martin, M. O. Skjoedt, N. C. Meyer, D. Shao, N. Borsa, Y. Palarasah, and R. J. H. Smith. 2014. Defining the complement biomarker profile of C3 glomerulopathy. *Clin. J. Am. Soc. Nephrol.* 9: 1876–1882.

42. Scholl, H. P. N., P. C. Issa, M. Walier, S. Janzer, B. Pollok-Kopp, F. Börncke, L. G. Fritsche, N. V. Chong, R. Fimmers, T. Wienker, et al. 2008. Systemic complement activation in age-related macular degeneration. *PLoS One* 3: e2593.

43. Forneris, F., D. Ricklin, J. Wu, A. Tzekou, R. S. Wallace, J. D. Lambris, and P. Gros. 2010. Structures of C3b in complex with factors B and D give insight into complement convertase formation. *Science (80-.).* 330: 1816–1820.

44. Forneris, F., J. Wu, X. Xue, D. Ricklin, Z. Lin, G. Sfyroera, A. Tzekou, E. Volokhina, J. C. Granneman, R. Hauhart, et al. 2016. Regulators of complement activity mediate inhibitory mechanisms through a common C3b-binding mode. *EMBO J.* 35: 1133–1149.

45. Michels, M. A. H. M., N. C. A. J. Van De Kar, R. M. Van Den Bos, T. J. A. M. Van Der Velden, S. A. W. Van Kraaij, S. A. Sarlea, V. Gracchi, M. J. S. Oosterveld, E. B. Volokhina, L. P. W. J. Van Den Heuvel, et al. 2019. Novel assays to distinguish between properdin-dependent and properdin-independent C3 nephritic factors provide insight into properdin-inhibiting therapy. *Front. Immunol.* 10.

Supplemental information

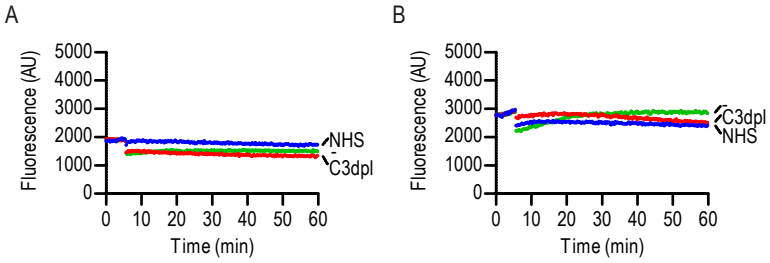

Supplemental figure 1 | No AP activation on non-coated liposomes

(A-B) Normal human serum and C3-dpl serum do not induce AP activation on non-coated liposomes without **(A)** or with **(B)** a maleimide lipid incorporated in the liposomes. The serum that was used is indicated next to the curves.

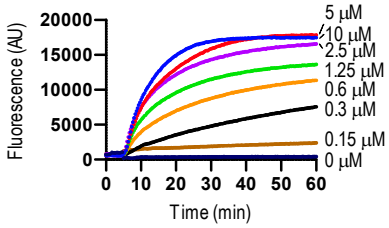

Supplemental figure 2 | AP activation by purified complement components is proportional to C3b coating on liposomes

The level of AP activation induced by the purified complement components FB, FD and C5-C9 is proportional to the C3b concentration (indicated next to the curves) used for coating the liposomes.

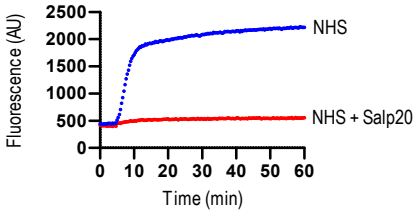

Supplemental figure 3 | Salp20 inhibits AP activation on C3b coated liposomes

Supplementing normal human serum (NHS) with Salp20 inhibits AP activation on C3b-coated liposomes. The serum that was used and the protein that was added is indicated next to the curves.

Chapter 4

Structure-based design of a properdin-specific complement inhibitor based on the C3b-CTC domain

Ramon M. van den Bos[1], Ezra Slingerland[1], Marloes A.H.M. Michels[2], Lambertus P.W.J. van den Heuvel[2] and Piet Gros[1], on behalf of the COMBAT consortium.

1 *Crystal and Structural Chemistry, Bijvoet Centre for Biomolecular Research, Department of Chemistry, Faculty of Science, Utrecht University, Utrecht, Netherlands.*

2 *Department of Pediatric Nephrology, Radboud University Medical Center, Radboud Institute for Molecular Life Sciences, Amalia Children's Hospital, Nijmegen, Netherlands.*

Abstract

Attack of healthy host cells by the complement system strongly contributes to the pathogenesis of various diseases. Properdin is the only known positive regulator of the complement system and facilitates complement activation by increasing the lifetime of the heterodimeric complex C3bBb, which is the pivotal serine protease of the complement system. Therefore, properdin is an attractive therapeutic target for reducing complement activation. Here we report a novel strategy for inhibiting properdin activity by the isolated CTC domain of C3b, which is the domain that is important for properdin binding. Biochemical characterization revealed that the CTC domain can act as a complement inhibitor, albeit with a low efficacy. Using structure-based design, we developed a CTC variant, termed CTC^{NNA}, that displays ca. 100-fold higher affinity and efficacy for binding to properdin and inhibiting complement activation, respectively, compared to the wildtype CTC domain. In conclusion, this work outlines a new strategy for inhibiting complement through properdin. Our approach of modifying the isolated properdin-binding CTC domain to competitively block the interaction of properdin with C3b is likely wider applicable in other signaling cascades and may be instrumental in the design of novel therapeutics.

Introduction:

The complement system is an important part of humoral innate immunity and is involved in the clearance of invading microbes, foreign particles and altered host cells (1, 2). Under normal conditions, healthy host cells are protected against complement activation (3). However, overactivation or mis-regulation of the complement system can lead to activation on healthy host cells. This is associated with a wide variety of diseases that include paroxysmal nocturnal hemoglobinuria (PNH), atypical hemolytic uremic syndrome (aHUS) and ischemia-reperfusion injury (IRI) (4).

Inappropriate complement activation through initiation via the alternative pathway (AP) of the complement system is responsible for a majority of the complement related diseases (5). The AP can be activated non-specifically on surfaces without the aid of pattern recognition molecules. AP activation leads to the deposition of C3b on surfaces. C3b can bind Factor B (FB), which is then cleaved by Factor D (FD), generating the AP C3 convertase, C3bBb (6). The C3 convertase cleaves C3 into C3a and C3b. The generated C3b can then covalently attach to the surface through its reactive thioester and form a new C3 convertase on the surface (7). This constitutes the amplification loop of the AP, which results in massive consumption of C3, release of the anaphylatoxin C3a to induce inflammatory responses (8), and the opsonization of the targeted surface with C3b (9). C3b on the surface can be recognized by complement receptors on immune cells and induce phagocytosis (1). Once the density of C3b on the surface is high enough the specificity of the C3 convertase switches and it starts to cleave C5 into C5a, a potent anaphylatoxin, and C5b (10, 11). The generation of C5b initiates the terminal pathway, which results in in the formation of a lytic pore.

Regulation of the complement system in solution and on healthy host cells is essential to prevent depletion of complement components and damage to healthy tissues (3). As the central component of the amplification loop the activity of the AP C3 convertase is heavily regulated; C3bBb is intrinsically unstable and dissociation of Bb from C3b is irreversible (12). This decay of C3bBb is accelerated by several soluble and membrane-bound negative regulators, such as Factor H (FH) and decay accelerating factor. Additionally, negative regulators with co-factor activity (e.g. FH and membrane cofactor protein) assist Factor I in the proteolytic inactivation of C3b, thereby preventing the formation of new C3 convertases (3, 13, 14). The only known positive regulator of the complement system is properdin. It stabilizes C3bBb and increases its half-life five to ten-fold (15). Furthermore, properdin increases the formation of the pro-convertase (C3bB) (16) and reduces the inactivation of C3b by FI (17–19). Properdin is an oligomeric plasma protein which occurs as dimers, trimers and tetramers (20). Properdin oligomerization results in an avidity effect when bound to a C3b-coated surface. This avidity is important to direct positive regulation to targeted surfaces (21, 22). Recent structural advances have shown that properdin binds to the C-terminal domain (CTC) of C3b and likely stabilizes the C3 convertase by forming a bridge between the C3b and Bb (18, 19, 21, 22).

Currently, eculizumab and ravulizumab are the only complement inhibitors that are approved for clinical use and both have significantly improved treatment of complement related diseases like PNH and aHUS (23, 24). Eculizumab and ravulizumab are monoclonal antibodies that inhibit the terminal pathway by binding to C5 and preventing its cleavage into C5a and C5b (23). However, they do not prevent activation of the amplification loop, which means that opsonization of surfaces with C3b still occurs. This can result in breakthrough events (25) and extravascular hemolysis due to phagocytosis of erythrocytes (26). As the positive regulator of the AP that acts during the amplification loop, properdin is an attractive therapeutic target to reduce AP activation. Although, in mouse models for C3 glomerulopathy, an AP-mediated kidney disease, that have no or very little FH show that properdin inhibition exacerbates disease outcome (27, 28), suggesting that care needs to be taken when using properdin inhibiting therapeutics. Mouse studies with properdin inhibiting antibodies revealed that blocking properdin is beneficial in several complement related diseases, which include, aHUS (29), IRI (30), K/BxN mediated arthritis (31) and neonatal hypoxic-ischemic brain injury (32). Inhibition of properdin limits opsonization of the surface with C3b, which is shown to prevent intravascular and extravascular hemolysis (33, 34). Furthermore, properdin inhibition is specific for the AP and leaves complement activation through the other pathways largely intact (35, 36).

Here we show that the isolated CTC domain of C3b can serve as an inhibitor of the AP. Using structure-based design we increased the efficacy of the CTC and created a potent properdin specific inhibitor that is therapeutically interesting and can potentially be useful as a tool in studying properdin-dependent complement activation.

Results:

The isolated CTC domain of C3b is a competitive binder for the interaction between properdin and C3b

Previously, we showed that properdin binds both the isolated CTC domain of C3b (ICTC) and full length C3b with comparable affinities (22). We therefore hypothesized that ICTC could act as a competitive binder for the interaction between properdin and C3b. Using surface plasmon resonance (SPR) we tested the effect of the ICTC on the stability of the properdin-C3b complex. The complex was generated by injecting properdin on a C3b coated chip (**Fig. 1A**). The subsequent injection of ICTC resulted in a concentration-dependent dissociation of properdin from C3b with an IC50 of 54 ± 2 μM e(**Fig. 1B**), indicating that ICTC indeed acts as a competitive binder for the interaction between properdin and C3b. Next, we investigated the inhibitory properties of ICTC on AP activation on rabbit erythrocytes, which lack regulators against human complement and are therefore highly susceptible to AP activation. Incubation of the erythrocytes with normal human serum (NHS) supplemented with increasing concentrations of ICTC revealed that ICTC reduced the amount of AP-mediated lysis by ca.

20% at the high concentration of 200 μM (**Fig. 1C**), defining ICTC as a moderate inhibitor of properdin-mediated AP activation**.**

Structure based optimization of the efficacy of ICTC

The low efficacy of ICTC in inhibiting AP activation limits its potential use as a therapeutic and as a tool to study properdin-mediated complement activation. We therefore set out to increase the efficacy of ICTC by structure-based design. Using the structure of monomerized properdin in complex with ICTC (PDB ID: 6S0B), we generated the following mutations in the CTC domain: D1534Q, Q1647N, A1651N, P1662N and ΔP1662, to increase the number of hydrophilic interactions and to optimize hydro-

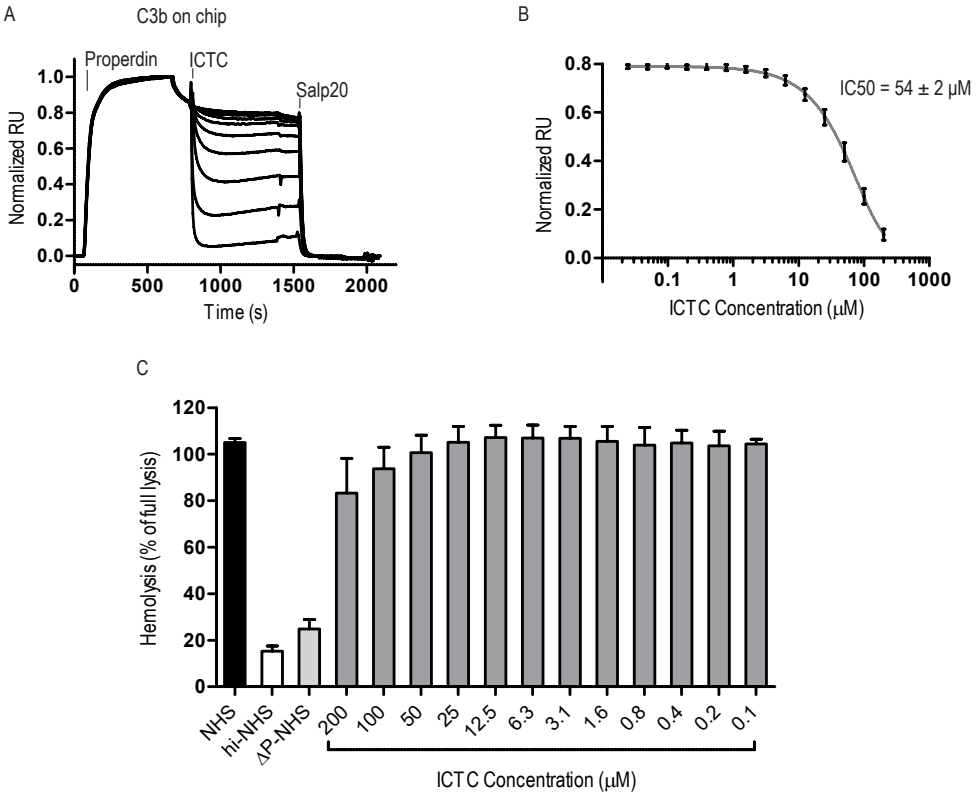

Figure 1 | Complement inhibition by the isolated C3b CTC domain (ICTC)

(A) Surface plasmon resonance (SPR) sensorgrams of the effect of the injection of ICTC (concentration range: 0.024 - 200 μM) on the dissociation of properdin-C3b. The resonance units (RU) are normalized with the maximum properdin binding. After the ICTC injection the remaining properdin bound to C3b is removed with the injection of Salp20. **(B)** Endpoint data of the fraction of properdin-C3b complex remaining after 10 min of ICTC injection fitted to a four-parameter logistic regression model. The IC50 represents the CTC domain concentration where half of the properdin-C3b complexes are dissociated. The error bars represent the standard deviation from three experiments. **(C)** Percentage of alternative pathway (AP)-mediated hemolysis after incubation of rabbit erythrocytes with 5% (v/v) normal human serum (NHS) and ICTC (concentration range: 0.1 - 200 μM). Controls for AP activation are heat-inactivated NHS (hi-NHS) and properdin-depleted NHS (ΔP-NHS). Hemolysis levels are presented as the percentage of full lysis of an equal volume of erythrocytes in water. The error bars indicate the standard deviation from two independent experiments.

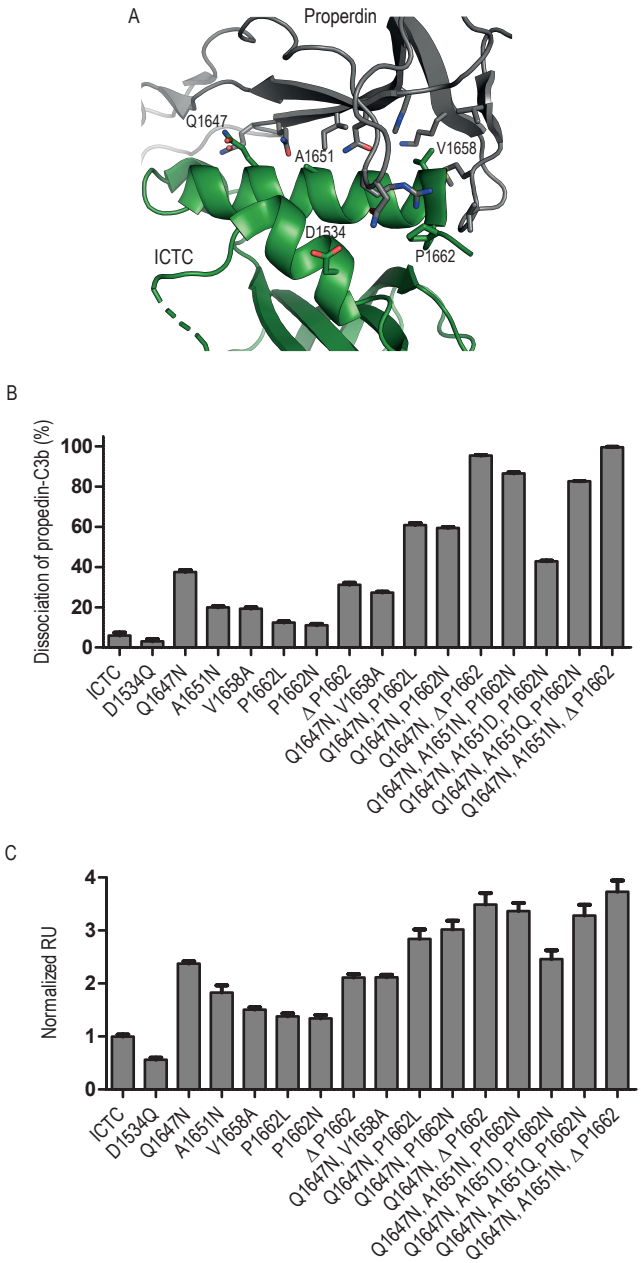

Figure 2 | Design and biochemical characterization of CTC variants

(A) Cartoon representation of monomerized properdin in complex with the isolated CTC domain of C3b (ICTC) (PDB ID 6S0B). The mutated ICTC residues and the properdin residues within 5 Å of the mutated ICTC residues are shown as sticks. The ICTC residues are annotated **(B)** The percentage of ICTC induced properdin-C3b dissociation after 10 minutes injection of the ICTC variants at 5 μM. **(C)** Steady state analysis of the amount of ICTC variants (5 μM injected) bound to a monomerized properdin-coated SPR chip. The resonance units (RU) were normalized based on the plateau of ICTC. The error bars in B and C indicate the standard deviation from three experiments.

gen-bond distances between properdin and ICTC (**Fig. 2A**). Additionally, we included two aHUS associated C3 mutants, V1658A (37) and P1662L (38), which are both in the interface of properdin and the CTC domain of C3b. All the ICTC variants eluted as a monodisperse peak in size exclusion chromatography (SEC) experiments and analysis by SDS-PAGE showed a high purity for all ICTC mutants, except A1651N (**Supplemental Fig. 1**), indicating that the introduced mutations did not strongly impact the stability of ICTC. A1651N appeared as two bands on the SDS PAGE gel with a difference in molecular weight that corresponds to a single N-linked glycan. Sequence analysis using NetNGlyc (39), a server for N-linked glycosylation prediction, indeed suggests that the introduced N1651 can be glycosylated. However, since only ca. 19 % is glycosylated we did not deem it necessary to further purify it for initial tests of the A1651N mutant.

SPR was used to analyze the efficacy of the ICTC mutants by determining the amount of properdin-C3b complex that is dissociated after injection of 5 μM of ICTC mutants. At this concentration 7 ± 1.4 % of properdin-C3b is dissociated after injection of ICTC. Comparison of the ICTC mutants with ICTC showed that all the mutants, except D1534Q, had a higher efficacy and resulted in more dissociation of the properdin-C3b complex (**Fig. 2B-C and Supplemental Fig. 2A**). The ICTC mutants P1662L and P1662N displayed a modest increase in efficacy and injection of these mutants resulted in the dissociation of 11 ± 0.5 % and 12 ± 0.5 % of the properdin-C3b complex, respectively. The mutants Q1647N, ΔP1662, A1651N and V1658A showed a larger increase in efficacy and injection of these mutants resulted in the dissociation of 37 ± 0.8 %, 31 ± 0.5 %, 20 ± 0.5 % and 19 ± 0.8 % of the properdin-C3b complex, respectively (**Fig. 2B**). SPR steady state analysis of the binding of the ICTC mutants to a properdin coated chip gave a similar pattern. D1534Q displayed less binding to properdin while the other ICTC mutants showed increased binding to properdin (**Fig. 2C and Supplemental Fig. 2A**). Thus, these results revealed that the majority of the tested mutants result in increased disruption of the properdin-C3b complex compared to ICTC, with Q1647N, ΔP1662 and A1651N as the three most potent mutants.

To further enhance the efficacy of ICTC, we next tested if combining efficacy-increasing mutations would have a cumulative effect. We created double mutants of the most potent single mutant Q1647N combined with: P1662L, P1662N, ΔP1662 or V1658A. A cumulative effect can be observed for the combination of Q1647N together with P1662L, P1662N or ΔP1662 as these double mutants results in the dissociation of 61 ± 0.8 %, 59 ± 0.4 % and 96 ± 0.1 % of the properdin-C3b complex, respectively (**Fig. 2B and Supplemental Fig. 2**). Furthermore, these double mutants display increased interaction with properdin compared to the single mutants. However, not all mutants showed a cumulative effect as the combination of Q1647N with V1658A did not result in an increase of potency (**Fig. 2B-C and Supplemental Fig. 2**). Next, we created triple mutants by combining the double mutants, Q1647N/P1662N and Q1647N/ΔP1662, with A1651N. The introduction of the third mutant increased the efficacy even further as the amount of properdin that is dissociated from C3b by injection of the CTC

variants increased from 59 ± 0.4 % to 87 ± 0.4 % for Q1647N/A1651N/P1662N and from 96 ± 0.1 % to 100 ± 0.1 % for Q1647N/A1651N/ΔP1662 (**Fig. 2B-C and Supplemental Fig. 2B**). The combination of the three strongest single mutants Q1647N, A1651N and ΔP1662 yielded the strongest ICTC variant which we termed CTC$^{NN\Delta}$.

The glycan introduced by the A1651N mutation is located in the interface between ICTC and properdin and probably interferes with the interaction between the two. This would reduce the efficacy, as the subset of purified ICTC that contains the glycan would not be capable of interacting with properdin. We therefore attempted to remove this glycan by testing the effect of mutating A1651 into either an aspartic acid or a glutamine. The A1651D mutant displayed greatly reduced efficacy compared to the A1651N mutant whilst the efficacy of A1651Q mutant is also reduced, albeit only slightly (**Fig. 2B-C and Supplemental Fig. S-2**). We nevertheless decided to continue with the mutant that displayed the highest efficacy, A1651N. Subsequently, we successfully separated the glycosylated from the non-glycosylated CTC$^{NN\Delta}$ by anion-exchange chromatography (**Supplemental Fig. 3A-B**). As expected, the non-glycosylated CTC$^{NN\Delta}$ has a ca. 15 % increased efficacy compared to CTC$^{NN\Delta}$ not purified by ion exchange (**Supplemental Fig. 3C-F**). This matches well with the percentage of glycosylated protein observed on SDS-page (ca. 19% glycosylated) and indicates that the glycosylated form is inactive. All further experiments with CTC$^{NN\Delta}$ were performed using the non-glycosylated protein.

Biochemical characterization of CTC$^{NN\Delta}$

SPR equilibrium experiments revealed that CTC$^{NN\Delta}$ binds to properdin with a K_D of 0.21 ± 0.03 μM (**Fig. 3A-B**), which is ~90x stronger compared to the previously reported K_D of 18.6 ± 1.6 μM for binding of ICTC to properdin (22). We observed a similar increase in efficacy of the CTC$^{NN\Delta}$ induced dissociation of the properdin-C3b complex. Injection of CTC$^{NN\Delta}$ results in a concentration dependent dissociation of the properdin-C3b complex with an IC50 of 0.50 ± 0.02 μM (**Fig. 3 C-D**), which is ~108 lower compared to the IC50 of ICTC (**Fig. 1A-B**). Next, we used SPR to analyze if CTC$^{NN\Delta}$ can prevent the association of the properdin-C3b complex. A mixture of CTC$^{NN\Delta}$ and 50 nM (**Fig. 3E**) or 300 nM properdin (**Fig. 3F**) was injected on a C3b coated SPR surface. CTC$^{NN\Delta}$ prevented properdin-C3b complex formation in a dose dependent manner with an IC50 of 0.38 ± 0.01 μM and 0.75 ± 0.02 μM for co-injection with 50 nM or 300 nM properdin, respectively (**Fig. 3G**), which is similar to the IC50 for the dissociation of properdin from C3b by the injection of CTC$^{NN\Delta}$. During the dissociation phase (between 660s and 780s) RU increases, which indicates that properdin binds to the C3b-coated surface (**Fig. 3E-F**). This can be explained by the size difference of the two analytes. Due to the small and globular shape of CTC$^{NN\Delta}$ the mass-transfer is much faster compared to the large non-globular properdin. Therefore, during dissociation the CTC$^{NN\Delta}$ concentration is lowered faster compared to the concentration of properdin, and this likely results in the binding of properdin to the C3b-coated chip as the CTC$^{NN\Delta}$ concentration decreases.

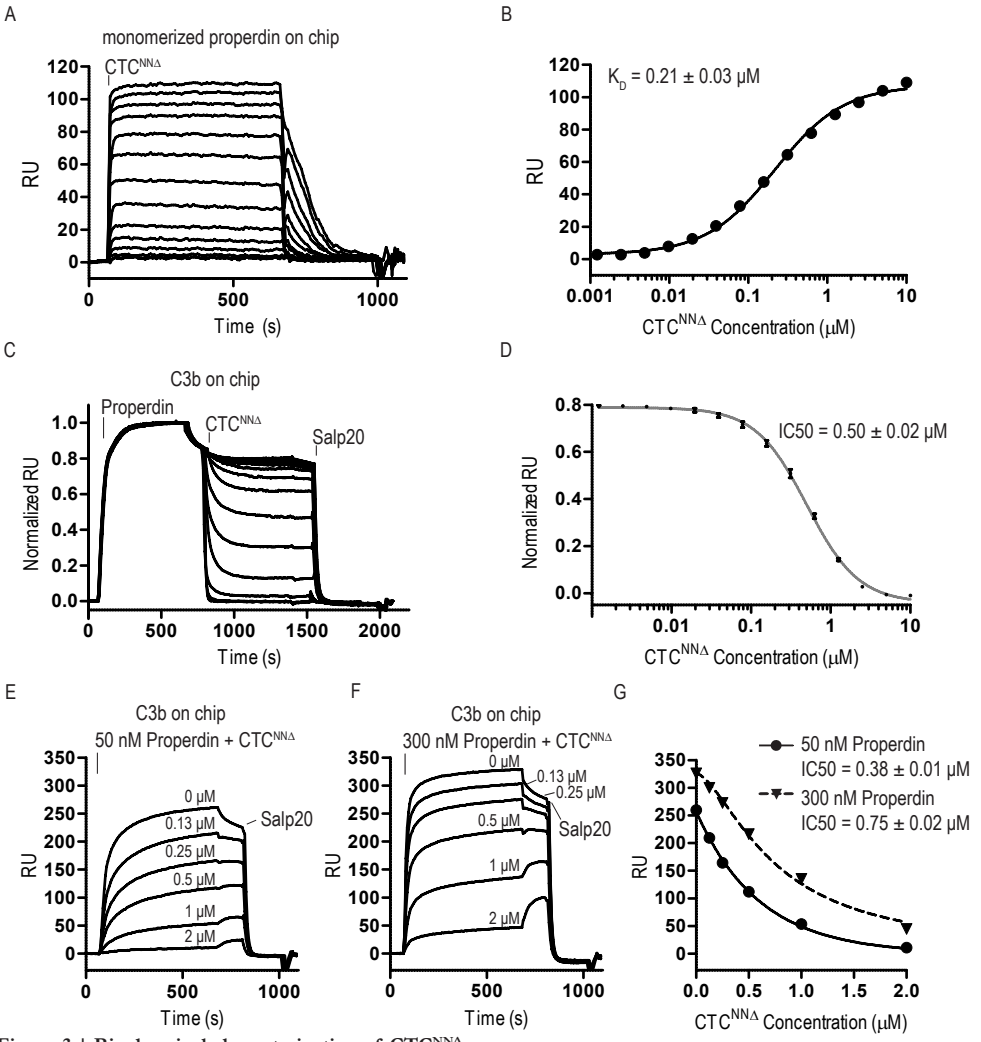

Figure 3 | Biochemical characterization of CTC$^{NN\Delta}$

(A) Surface plasmon resonance (SPR) sensorgrams of the equilibrium experiments with CTC$^{NN\Delta}$ (concentration range: 0.001 – 10 μM) binding to a monomerized properdin coated surface. **(B)** The CTC$^{NN\Delta}$ endpoint data fitted with a one site specific binding curve. K_D is the concentration of CTC$^{NN\Delta}$ which shows half-maximum binding to properdin. **(C)** SPR sensorgrams of the effect of CTC$^{NN\Delta}$ (concentration range: 0.001 – 10 μM) injection on the C3b-properdin complex. The resonance units (RU) are normalized based on the maximum properdin binding **(D)** Endpoint data of the fraction of properdin-C3b remaining after 10 min of CTC injection fitted to a four-parameter logistic regression model. The IC50 is the CTC$^{NN\Delta}$ concentration were half of properdin-C3b is dissociated. **(E, F)** SPR sensorgrams of co-injecting properdin (concentration: 50 nM (E) or 300 nM (F)) with CTC$^{NN\Delta}$ (concentration range: 0 – 2 μM) on a C3b-coated SPR surface. The CTC$^{NN\Delta}$ concentrations are indicated above the curves **(G)** Amount of properdin bound to C3b after 10 minutes co-injecting CTC$^{NN\Delta}$ with properdin (50 nM (circles) and 300 nM (triangles)). The IC50 is determined as in D. The error bars in **D** indicate the standard deviation from three experiments.

Next, we assessed the inhibiting effect of CTC$^{NN\Delta}$ on AP activation on rabbit erythrocytes. Incubation of rabbit erythrocytes with NHS in the presence of CTC$^{NN\Delta}$ at different concentrations showed a dose dependent reduction of the lysis levels of the erythrocytes with an IC50 of 6.5 ± 0.4 μM (**Fig. 4**). The effect of properdin on AP induced lysis of the rabbit erythrocytes is completely inhibited at 20 μM CTC$^{NN\Delta}$ as at

this concentration of CTC$^{NN\Delta}$ the observed percentage of lysis is similar to that after incubation with properdin depleted serum (ΔP-NHS).

Discussion

The recently solved structures of properdin show that the main interface between the C3 convertase and properdin is between TSR5 of properdin and the CTC domain of C3b (18, 19, 21, 22). We investigated if ICTC could act as a properdin specific complement inhibitor. We showed that ICTC reduces the levels of AP-mediated hemolysis of rabbit erythrocytes (**Fig. 1**), albeit with a low efficacy. In an attempt to increase the efficacy using structure-based design, we created several ICTC mutants that were screened for increased efficacy by monitoring the effect of the ICTC mutants on the dissociation of properdin-C3b. Multiple ICTC mutants showed increased efficacy for dissociating properdin-C3b and the combination of the three most effective single mutants, i.e., Q1647N, A1651N and ΔP1662 resulted in a potent ICTC variant, CTC$^{NN\Delta}$, that has a ca. 100 fold higher efficacy compared to ICTC and inhibits AP activation on rabbit erythrocytes with an IC50 of 6.5 ± 0.4 μM (**Fig. 4**). The efficacies of both ICTC and CTC$^{NN\Delta}$ are lower in the hemolysis assay compared to those measured in the SPR experiments in which the dissociation of properdin from C3b was monitored. This is likely due to the presence of C3bBb in the hemolytic assay, to which properdin binds approximately 300x stronger compared to C3b alone (17, 22).

The V1658A and P1662L polymorphisms of C3 have both been found in aHUS patients and have been classified as gain of function C3 mutants (37, 38). Sartz and collegues described that the V1658A C3b variant increases convertase formation (37). Both poly-

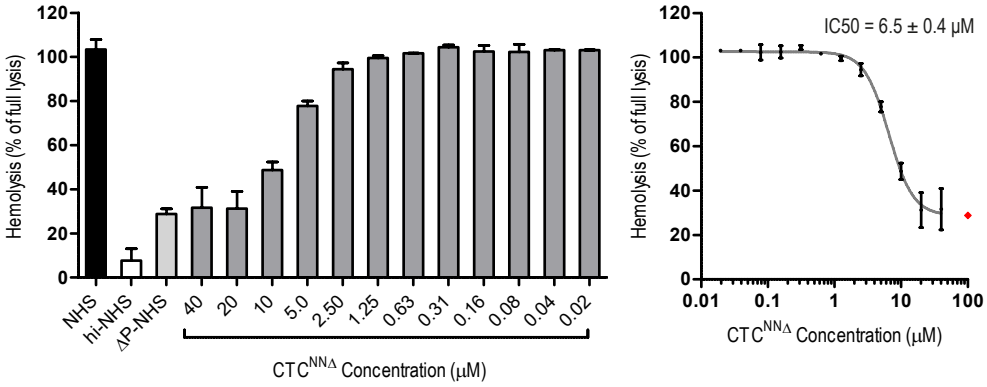

Figure 4 | Inhibition of alternative pathway activation on rabbit erythrocytes by CTC$^{NN\Delta}$

Alternative pathway (AP)-mediated hemolysis of rabbit erythrocytes after incubation with 5% normal human serum (NHS) and CTC$^{NN\Delta}$ (concentration range: 0.02 - 40 μM). Controls for AP activation are heat-inactivated NHS (hi-NHS) and properdin-depleted NHS (ΔP-NHS). On the right the data from the left panel is fitted with a four-parameter logistic regression model using the amount of hemolysis after incubation with ΔP-NHS as the plateau (indicated as red square). The IC50 is the concentration at which CTC$^{NN\Delta}$ reduces half of the lysis induced by the AP. Hemolysis levels are presented as the percentage of full lysis of an equal volume of erythrocytes in water. The error bars represent the standard deviation from two independent experiments.

morphisms are in the interface between properdin and C3b and we show that both V1658A and P1662L ICTC mutants bind stronger to properdin compared to ICTC (**Fig. 2B-C and Supplemental Fig. 2A**). The increased binding of properdin to C3b potentially results in increased positive regulation by properdin which could explain the overactivation of the complement system and the resulting aHUS in these patients.

Our results show the potential of $CTC^{NN\Delta}$ as a therapeutic and as a biochemical tool for inhibiting AP activation. For therapeutic use the efficacy of $CTC^{NN\Delta}$ would likely need to be one or two orders of magnitudes higher, which could potentially be achieved by further optimizing the sequence using directed evolution or by creating $CTC^{NN\Delta}$ dimers which could results in an avidity effect for binding to properdin oligomers. The risk for anti-drug antibodies against $CTC^{NN\Delta}$ is likely low since it is derived from C3, which is a protein with a high abundancy (40).

In summary, this work presents the discovery a novel properdin inhibitor. We demonstrate that the ICTC acts as a properdin-specific complement inhibitor, and we employed structure-based design to create an ICTC variant that displays a 100x higher potency compared to the wildtype ICTC. This strategy is likely more widely applicable and could aid the discovery of novel therapeutics.

Materials and Methods

Protein production and purification

ICTC mutants were designed by in silico mutagenesis of the residues in the interface between properdin and ICTC (PDB ID: 6S0B) using Pymol (Schrödinger). The mutations in ICTC were selected based on their ability to form additional hydrophilic interactions or hydrogen bonds with properdin. C3b CTC mutants were generated with the Q5 site directed mutagenesis kit (New England Biolabs). The ICTC construct used for mutagenesis was generated as described previously (22). The primers used for site directed mutagenesis are reported in supplemental table 1. All CTC domain constructs were transiently expressed in N-acetylglucosaminyltransferase I deficient HEK293 suspension cells (provided by U-protein Express BV). Six days post-transfection, cells were removed by centrifugation at 1000 x g for 10 min. Subsequently, the supernatant was centrifuged at 4000 x g for 10 min to remove any cell debris. The supernatant was cooled to 4°C and incubated with Ni Sepharose Excel beads (GE Healthcare) for 2-3 hours while slowly rotating. The beads were collected by centrifuging at 1000 x g for 10 min and transferred to a 20 ml Econo-Pac gravity-flow column. The beads were washed with 10 column volumes (CV) 20 mM HEPES pH 7.8, 500 mM NaCl (IMAC buffer) and 10 CV IMAC buffer supplemented with 10 mM Imidazole. Proteins were eluted with IMAC buffer supplemented with 250 mM Imidazole. The eluted protein was concentrated and purified by SEC using a Superdex 75 16/600 (GE Healthcare) column pre-equilibrated in SEC buffer (20 mM HEPES pH 7.4, 150 mM NaCl). Proteins were concentrated using an Amicon Ultracel 3K concentrator. To obtain the non-glycosyla-

ted $CTC^{NN\Delta}$ fraction an additional step was added between the IMAC and SEC; The IMAC eluate was dialyzed ON against Mono Q buffer (20 mM HEPES pH 7.8, 50 mM NaCl) with MWCO 3.5 kDa regenerated cellulose dialysis membrane (Spectrum Labs Spectra/Por 6) at 4 °C. The dialyzed sample (~2.5 mg each run) was loaded on a Mono Q 5/50 GL column (GE Healthcare) pre-equilibrated in Mono Q buffer. The sample was eluted with a gradient from 140 to 200 mM NaCl in 60 minutes at a flow rate of 0.5 ml/min. For experiments with erythrocytes the buffer of ICTC and $CTC^{NN\Delta}$ was exchanged to magnesium-ethylene glycol tetraacetic acid (Mg-EGTA; 2.03 mM veronal buffer, pH 7.4, 10 mM EGTA, 7 mM $MgCl_2$, 0.083% gelatin, 115 mM D-glucose, 60 mM NaCl) using Bio-Spin 6 desalting columns (Bio-Rad). C3, Salp20, full length properdin and a monomerized properdin variant ($P^{STB1'/456}$) were generated as described previously (22, 41, 42).

4

Surface Plasmon Resonance

C3b and monomerized properdin were biotinylated as described previously (22). Briefly, C3b was generated from C3 by incubating it with Factor B and Factor D. The cleavage of C3 into C3b and the hydrolysis of the reactive thioester results in a free cysteine in C3b. The monomerized properdin ($P^{STB1'/456}$) contains a free cysteine at the C-terminus of $P^{STB1'}$. Both proteins were biotinylated by incubating for 3 hours at room temperature with 1 mM EZ-Link Maleimide-PEG2-Bioting (Thermofisher). The biotinylated proteins (50 nM Properdin, 25 nM C3b) were spotted on a planar streptavidin-coated SPR chips (P-STREP, SensEye) for 1 hour with a continuous flow microflow spotter (CFM, Wasatch). SPR experiments were performed with the IBIS-MX96 (IBIS technology) at 25 °C. All SPR experiments were performed with the SPR running buffer (20 mM HEPES pH 7.4, 150 mM NaCl, 0.005% Tween-20). At the end of each run the SPR surface was regenerated with SPR running buffer supplemented with 1 M NaCl. Properdin-C3b was generated by injecting 50 nM properdin on a C3b coated surface. The effect of ICTC and the ICTC variants on the stability of the properdin-C3b complex was determined by injecting them on a properdin-C3b coated surface. To compare the efficacy of the ICTC variants they were injected at 5 μM. For the comparison of $CTC^{NN\Delta}$ and the mono Q purified $CTC^{NN\Delta}$ they were injected at 0.5 μM. For determining the IC50 of ICTC and $CTC^{NN\Delta}$ they were injected in a 14 step 2-fold dilution range. The data was normalized based on the maximum properdin binding. For the co-injection experiments a mixture of either 50 or 300 nM properdin and $CTC^{NN\Delta}$ (concentration range 0-2 μM) was injected on a C3b coated SPR surface. After all experiments the remaining properdin was dissociated by injecting the properdin specific complement inhibitor Salp20 (43) (1 μM) followed by a regeneration step where SPR buffer supplemented with 1 M NaCl was injected. The steady state experiments of the interaction between the CTC variants and a SPR surface coated with monomerized properdin were normalized using average of the plateau during the ICTC injection. For the SPR equilibrium experiments of $CTC^{NN\Delta}$ it was injected in a 14 step 2-fold dilution range on a monomerized properdin ($P^{STB1'/456}$) coated SPR surface. SPR data was analyzed with

SprintX (IBIS technologies) and GrapPad Prism 5. The IC50 was determined by fitting the endpoint data with $Y = \text{Ymin} + (\text{Ymax} - \text{Ymin})/(1 + \left(\frac{x}{\text{IC50}}\right)^{\text{hill}})$. The K_D was determined by fitting the endpoint data with $Y = \frac{Bmax * x}{KD + x} + Background$. The standard deviation in the IC50 and K_D is from three experiments.

Alternative pathway hemolytic assay

NHS was obtained by collecting and pooling the serum samples of ten healthy controls. Heat-inactivated NHS was created by incubating NHS at 56 °C for 30 minutes. ΔP-NHS was purchased from Complement Technology, Inc. (A339).

Alternative pathway hemolytic assays were performed with rabbit erythrocytes as described previously (44). In brief, the erythrocytes (Envigo) were washed in Mg-EGTA buffer and calibrated to obtain a working suspension of which 10 µl yields an absorbance of 0.8-1.2 at 405 nm upon 1/10 dilution in water. For each condition, 10 µl of the rabbit erythrocyte working suspension was mixed in a V-shaped 96-well plate with 20 µl of 12.5% test serum and 20 µl of Mg-EGTA or ICTC or $CTC^{NN\Delta}$ diluted in Mg-EGTA. Concentrations indicated in figure legends indicate the final concentrations in the well. After 1 hour of incubation at 37 °C and with 600 rpm, the reaction was stopped by adding 50 µl ethylenediamine-tetraacetic acid-gelatin veronal buffer (4.41 mM veronal buffer, 0.1 % gelatin, 130 mM NaCl, pH 7.4) Erythrocytes were pelleted via centrifugation and released hemoglobin in the supernatant was analyzed with a photospectrometer. The data was analyzed with GrapPad Prism 5 and the IC50 was determined as for the SPR experiments. The standard deviation is from two experiments.

Author contributions

RvdB and PG designed the project. RvdB designed the mutants. RvdB and ES cloned the constructs and carried out protein purification and biochemical assays. MM performed the hemolytic assays under the supervision of LvdH. RvdB analyzed the data. RvdB wrote the original draft. All authors reviewed and edited the manuscript.

Acknowledgements

We thank W. Hemrika (U-Protein Express BV) for HEK cell cultures; W. Oosterheert and T.H. Brondijk for proofreading of the manuscript. We thank the members of the Crystal and Structural Chemistry lab for helpful discussions.

This study was performed on behalf of the COMBAT Consortium. This is an interuniversity collaboration in the Netherlands that is formed to study basic mechanisms, assay development, and therapeutic translation of complement-mediated renal diseases. Prin-

cipal investigators are (in alphabetical order): S. Berger (Department of Internal Medicine-Nephrology, University Medical Center Groningen, Groningen, Netherlands), J. van den Born (Department of Internal Medicine-Nephrology, University Medical Center Groningen, Groningen, Netherlands), P. Gros (Department of Chemistry, Utrecht University, Utrecht, Netherlands), L. van den Heuvel (Department of Pediatric Nephrology, Radboud University Medical Center, Nijmegen, Netherlands), N. van de Kar (Department of Pediatric Nephrology, Radboud University Medical Center, Nijmegen, Netherlands), C. van Kooten (Department of Internal Medicine-Nephrology, Leiden University Medical Center, Leiden, Netherlands), M. Seelen (Department of Internal Medicine-Nephrology, University Medical Center Groningen, Groningen, Netherlands), A. de Vries (Department of Internal Medicine-Nephrology, Leiden University Medical Center, Leiden, Netherlands).

References

1. Ricklin, D., G. Hajishengallis, K. Yang, and J. D. Lambris. 2010. Complement: A key system for immune surveillance and homeostasis. *Nat. Immunol.* 11: 785–797.

2. Merle, N. S., S. E. Church, V. Fremeaux-Bacchi, and L. T. Roumenina. 2015. Complement system part I - molecular mechanisms of activation and regulation. *Front. Immunol.* 6: 1–30.

3. Schmidt, C. Q., J. D. Lambris, and D. Ricklin. 2016. Protection of host cells by complement regulators. *Immunol. Rev.* 274: 152–171.

4. Ricklin, D., E. S. Reis, and J. D. Lambris. 2016. Complement in disease: a defence system turning offensive. *Nat. Rev. Nephrol.* 12: 383–401.

5. Thurman, J. M., and V. M. Holers. 2006. The Central Role of the Alternative Complement Pathway in Human Disease. *J. Immunol.* 176: 1305–1310.

6. Rooijakkers, S. H. M., J. Wu, M. Ruyken, R. van Domselaar, K. L. Planken, A. Tzekou, D. Ricklin, J. D. Lambris, B. J. C. Janssen, J. a G. van Strijp, et al. 2009. Structural and functional implications of the alternative complement pathway C3 convertase stabilized by a staphylococcal inhibitor. *Nat. Immunol.* 10: 721–727.

7. Law, S. K. A., and A. W. Dodds. 1996. The internal thioester and the covalent binding properties of the complement proteins C3 and C4. *Protein Sci.* 6: 263–274.

8. Merle, N. S., R. Noe, L. Halbwachs-Mecarelli, V. Fremeaux-Bacchi, and L. T. Roumenina. 2015. Complement system part II: Role in immunity. *Front. Immunol.* 6: 1–26.

9. Ricklin, D., E. S. Reis, D. C. Mastellos, P. Gros, and J. D. Lambris. 2016. Complement component C3 – The "Swiss Army Knife" of innate immunity and host defense. *Immunol. Rev.* 274: 33–58.

10. Daha, M. R., D. T. Fearon, and K. F. Austen. 1976. C3 requirements for formation of alternative pathway C5 convertase. *J. Immunol.* 117: 630–634.

11. Medicus, R. G., O. Götze, and H. J. Müller-Eberhard. 1976. Alternative pathway of complement: Recruitment of precursor properdin by the labile C3/C5 convertase and the potentiation of the pathway. *J. Exp. Med.* 144: 1076–1093.

12. Pangburn, M. K., and H. J. Muller-Eberhard. 1986. The C3 convertase of the alternative pathway of human complement. Enzymic properties of the bimolecular proteinase. *Biochem. J.* 235: 723–730.

13. Forneris, F., J. Wu, X. Xue, D. Ricklin, Z. Lin, G. Sfyroera, A. Tzekou, E. Volokhina, J. C. Granneman, R. Hauhart, et al. 2016. Regulators of complement activity mediate inhibitory mechanisms through a common C3b-binding mode. *EMBO J.* 35: 1133–1149.

14. Xue, X., J. Wu, D. Ricklin, F. Forneris, P. Di Crescenzio, C. Q. Schmidt, J. Granneman, T. H. Sharp, J. D. Lambris, and P. Gros. 2017. Regulator-dependent mechanisms of C3b processing by factor i allow differentiation of immune

responses. *Nat. Struct. Mol. Biol.* 24: 643–651.

15. Fearon, D. T., and K. F. Austen. 1975. Properdin: binding to C3b and stabilization of the C3b-dependent C3 convertase. *J. Exp. Med.* 142: 856–63.

16. Hourcade, D. E. 2006. The role of properdin in the assembly of the alternative pathway C3 convertases of complement. *J. Biol. Chem.* 281: 2128–2132.

17. Farries, T. C., P. J. Lachmann, and R. A. Harrison. 1988. Analysis of the interactions between properdin, the third component of complement (C3), and its physiological activation products. *Biochem. J.* 252: 47–54.

18. Alcorlo, M., A. Tortajada, S. Rodríguez de Córdoba, and O. Llorca. 2013. Structural basis for the stabilization of the complement alternative pathway C3 convertase by properdin. *Proc. Natl. Acad. Sci. U. S. A.* 110: 13504–9.

19. Pedersen, D. V., T. A. F. Gadeberg, C. Thomas, Y. Wang, N. Joram, R. K. Jensen, S. M. M. Mazarakis, M. Revel, C. El Sissy, S. V. Petersen, et al. 2019. Structural Basis for Properdin Oligomerization and Convertase Stimulation in the Human Complement System. *Front. Immunol.* 10.

20. Pangburn, M. K. 1989. Analysis of the natural polymeric forms of human properdin and their functions in complement activation. *J. Immunol.* 142: 202–7.

21. Pedersen, D. V, L. Roumenina, R. K. Jensen, T. A. Gadeberg, C. Marinozzi, C. Picard, T. Rybkine, S. Thiel, U. B. Sørensen, C. Stover, et al. 2017. Functional and structural insight into properdin control of complement alternative pathway amplification. *EMBO J.* 36: 1084–1099.

22. van den Bos, R. M., N. M. Pearce, J. Granneman, T. H. C. Brondijk, and P. Gros. 2019. Insights Into Enhanced Complement Activation by Structures of Properdin and Its Complex With the C-Terminal Domain of C3b. *Front. Immunol.* 10.

23. Rother, R. P., S. A. Rollins, C. F. Mojcik, R. A. Brodsky, and L. Bell. 2007. Discovery and development of the complement inhibitor eculizumab for the treatment of paroxysmal nocturnal hemoglobinuria. *Nat. Biotechnol.* 25: 1256–1264.

24. Kulasekararaj, A. G., A. Hill, S. T. Rottinghaus, S. Langemeijer, R. Wells, F. A. Gonzalez-Fernandez, A. Gaya, J. W. Lee, E. O. Gutierrez, C. I. Piatek, et al. 2019. Ravulizumab (ALXN1210) vs eculizumab in C5-inhibitor–experienced adult patients with PNH: The 302 study. *Blood* 133: 540–549.

25. Harder, M. J., N. Kuhn, H. Schrezenmeier, B. Höchsmann, I. Von Zabern, C. Weinstock, T. Simmet, D. Ricklin, J. D. Lambris, A. Skerra, et al. 2017. Incomplete inhibition by eculizumab: Mechanistic evidence for residual C5 activity during strong complement activation. *Blood* 129: 970–980.

26. Lin, Z., C. Q. Schmidt, S. Koutsogiannaki, P. Ricci, A. M. Risitano, J. D. Lambris, and D. Ricklin. 2015. Complement C3dg-mediated erythrophagocytosis: Implications for paroxysmal nocturnal hemoglobinuria. *Blood* 126: 891–894.

27. Ruseva, M. M., K. A. Vernon, A. M. Lesher, W. J. Schwaeble, Y. M. Ali, M. Botto, T. Cook, W. Song, C. M. Stover, and M. C. Pickering. 2013. Loss of properdin exacerbates C3 glomerulopathy resulting from factor H deficiency. *J. Am. Soc. Nephrol.* 24: 43–52.

28. Lesher, A. M., L. Zhou, Y. Kimura, S. Sato, D. Gullipalli, A. P. Herbert, P. N. Barlow, H. U. Eberhardt, C. Skerka, P. F. Zipfel, et al. 2013. Combination of factor H mutation and properdin deficiency causes severe C3 glomerulonephritis. *J. Am. Soc. Nephrol.* 24: 53–65.

29. Ueda, Y., T. Miwa, D. Gullipalli, S. Sato, D. Ito, H. Kim, M. Palmer, and W. C. Song. 2018. Blocking Properdin Prevents Complement-Mediated Hemolytic Uremic Syndrome and Systemic Thrombophilia. *J. Am. Soc. Nephrol.* 29: 1928–1937.

30. Miwa, T., S. Sato, D. Gullipalli, M. Nangaku, and W.-C. Song. 2013. Blocking Properdin, the Alternative Pathway, and Anaphylatoxin Receptors Ameliorates Renal Ischemia-Reperfusion Injury in Decay-Accelerating Factor and CD59 Double-Knockout Mice. *J. Immunol.* 190: 3552–3559.

31. Kimura, Y., L. Zhou, T. Miwa, and W. C. Song. 2010. Genetic and therapeutic targeting of properdin in mice prevents complement-mediated tissue injury. *J. Clin. Invest.* 120: 3545–3554.

32. Sisa, C., Q. Agha-Shah, B. Sanghera, A. Carno, C. Stover, and M. Hristova. 2019. Properdin: A Novel Target for Neuroprotection in Neonatal Hypoxic-Ischemic Brain Injury. *Front. Immunol.* 10: 2610.

33. Gullipalli, D., F. Zhang, S. Sato, Y. Ueda, Y. Kimura, M. Golla, T. Miwa, J. Wang, and W.-C. Song. 2018. Antibody Inhibition of Properdin Prevents Complement-Mediated Intravascular and Extravascular Hemolysis. *J. Immunol.* 201: 1021–1029.

34. Chen, J. Y., N. S. Galwankar, H. N. Emch, S. S. Menon, C. Cortes, J. M. Thurman, S. A. Merrill, R. A. Brodsky, and V. P. Ferreira. 2020. Properdin Is a Key Player in Lysis of Red Blood Cells and Complement Activation on Endothelial Cells in Hemolytic Anemias Caused by Complement Dysregulation. *Front. Immunol.* 11: 1460.

35. Kimura, Y., T. Miwa, L. Zhou, and W. C. Song. 2008. Activator-specific requirement of properdin in the initiation and amplification of the alternative pathway complement. *Blood* 111: 732–740.

36. Pauly, D., B. M. Nagel, J. Reinders, T. Killian, M. Wulf, S. Ackermann, B. Ehrenstein, P. F. Zipfel, C. Skerka, and B. H. F. Weber. 2014. A novel antibody against human properdin inhibits the alternative complement system and specifically detects properdin from blood samples. *PLoS One* 9.

37. Sartz, L., A. I. Olin, A.-C. Kristoffersson, A. Ståhl, M. E. Johansson, K. Westman, V. Fremeaux-Bacchi, K. Nilsson-Ekdahl, and D. Karpman. 2012. A Novel C3 Mutation Causing Increased Formation of the C3 Convertase in Familial Atypical Hemolytic Uremic Syndrome. *J. Immunol.* 188: 2030–2037.

38. Ažukaitis, K., C. Loirat, M. Malina, I. Adomaitiene, and A. Jankauskiene. 2014. Macrovascular involvement in a child with atypical hemolytic uremic syndrome. *Pediatr. Nephrol.* 29: 1273–1277.

39. Gupta, R., E. Jung, and S. Brunak. 2004. NetNGlyc: Prediction of N-glycosylation sites in human proteins. *Prep.* 2004.

40. Sauna, Z. E., D. Lagassé, J. Pedras-Vasconcelos, B. Golding, and A. S. Rosenberg. 2018. Evaluating and Mitigating the Immunogenicity of Therapeutic Proteins. *Trends Biotechnol.* 36: 1068–1084.

41. Michels, M. A. H. M., N. C. A. J. Van De Kar, R. M. Van Den Bos, T. J. A. M. Van Der Velden, S. A. W. Van Kraaij, S. A. Sarlea, V. Gracchi, M. J. S. Oosterveld, E. B. Volokhina, L. P. W. J. Van Den Heuvel, et al. 2019. Novel assays to distinguish between properdin-dependent and properdin-independent C3 nephritic factors provide insight into properdin-inhibiting therapy. *Front. Immunol.* 10.

42. Wu, J., Y. Q. Wu, D. Ricklin, B. J. C. Janssen, J. D. Lambris, and P. Gros. 2009. Structure of complement fragment C3b-factor H and implications for host protection by complement regulators. *Nat. Immunol.* 10: 728–733.

43. Tyson, K. R., C. Elkins, and A. M. de Silva. 2008. A Novel Mechanism of Complement Inhibition Unmasked by a Tick Salivary Protein That Binds to Properdin. *J. Immunol.* 180: 3964–3968.

44. van den Heuvel, L. P., N. C. A. J. van de Kar, C. Duineveld, A. Sarlea, T. J. A. M. van der Velden, W. T. B. Liebrand, S. van Kraaij, C. Schjalm, R. Bouwmeester, J. F. M. Wetzels, et al. 2020. The complement component C5 is not responsible for the alternative pathway activity in rabbit erythrocyte hemolytic assays during eculizumab treatment. *Cell. Mol. Immunol.* 17: 653–655.

Supplemental information

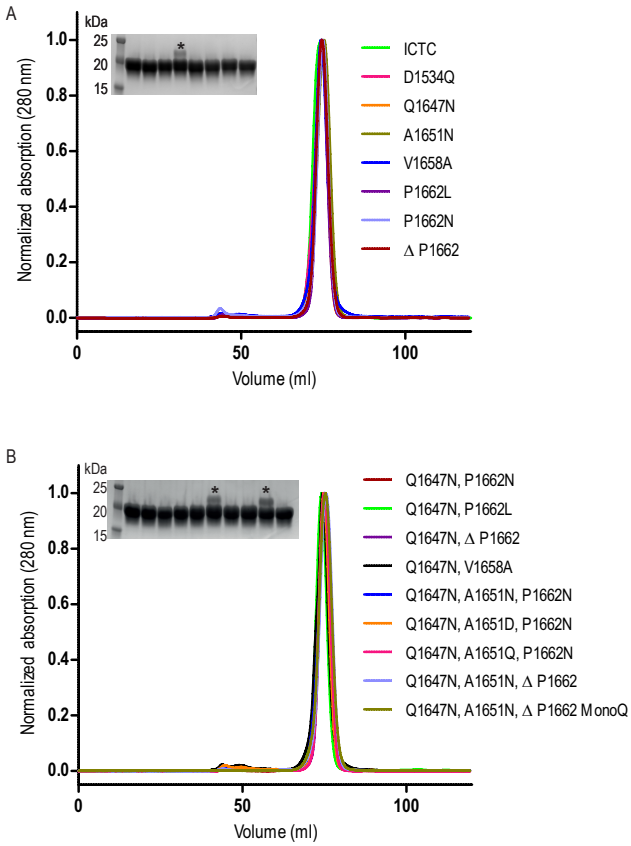

Supplemental figure 1 | Purification of the ICTC variants

(A & B) Size exclusion chromatography (SEC) elution profile of the isolated CTC domain of C3b (ICTC) single mutants (A) and the double and triple mutants (B), results are normalized based on the maximum absorption. **Inset:** SDS-PAGE analysis of the ICTC variants. The order on the gel from left to right is the same as the top to bottom order of the legend for the SEC but in B the first sample is ICTC. The glycosylated fraction of the A1651N mutant is indicated with *.

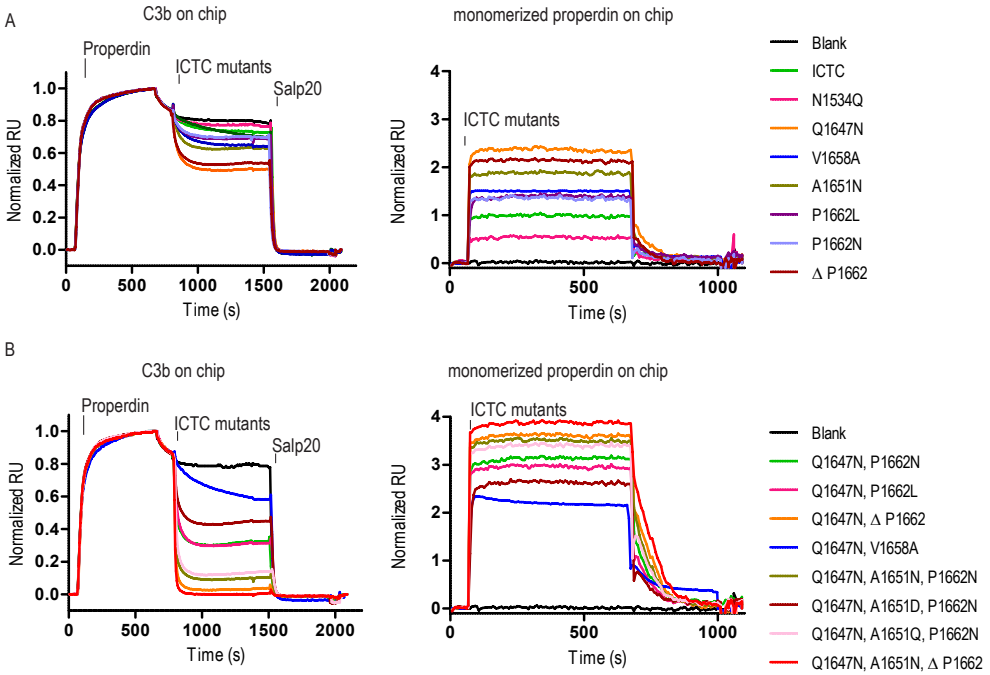

Supplemental figure 2 | Surface plasmon resonance (SPR) sensorgrams of ICTC variants

(A & B) The figures on the left are the SPR sensorgrams of the effect of the isolated CTC domain of C3b (ICTC) (5 μM) single **(A),** double and triple mutants **(B)** on properdin-C3b complex. The response units are normalized to the maximum properdin binding. The right part are the SPR sensorgrams of the ICTC (5 μM) single **(A),** double and triple mutants **(B)** binding to monomerized properdin coated on a SPR surface. The signal is normalized based on the plateau of the wildtype ICTC.

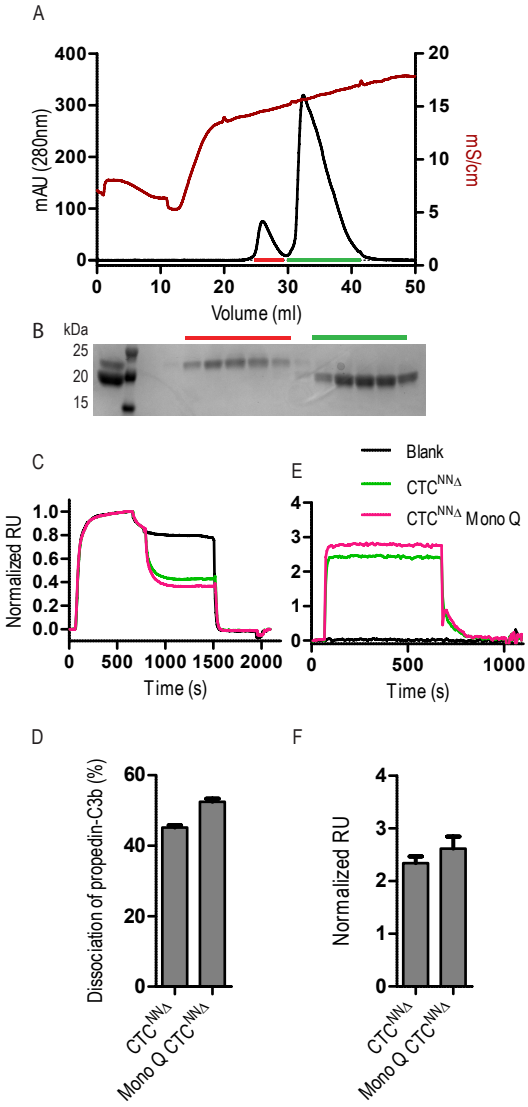

Supplemental figure 3 | Separation of glycosylated and non-glycosylated CTC$^{NN\Delta}$

(A) Separation of the glycosylated fraction (first peak, red bar) of Q1647N, A1651N, ΔP1662 (CTC$^{NN\Delta}$) from the non-glycosylated fraction (second peak, green bar) by ion exchange chromatography. **(B)** SDS-PAGE analysis of the fractions from the ion exchange in (A). **(C&D)** SPR sensorgrams (C) and the percentage of properdin-C3b dissociated after injecting CTC$^{NN\Delta}$ (0.5 μM) before (CTC$^{NN\Delta}$) and after purification (Mono Q CTC$^{NN\Delta}$) by ion exchange. The resonance units (RU) are normalized based on the maximum properdin binding. **(E&F)** SPR sensorgrams (E) and steady state analysis (F) of the amount of CTC$^{NN\Delta}$ (0.5 μM), before and after purification by ion exchange, bound to monomerized properdin. The RU are normalized to 5 μM ICTC. The error bars in **D** and **F** indicate the standard deviation from three experiments.

Supplemental table 1: Primers used for mutagenesis			
Mutation	Forward primer	Reverse primer	Input construct
P1662N	CTTTGGGTGCaacAACTGAGCGG	ACAACCATGCTCTCGGTG	ICTC
P1662L	CTTTGGGTGCctcAACTGAGCGG	ACAACCATGCTCTCGGTG	CTC P1662N
ΔP1662	TGGGTGCAACtgaTGAGCGGCCG	AAGACAACCATGCTCTCG	CTC P1662N
Q1647N	GAAACAATGCaacGACCTCGGCG	TGGTTCTCTTCGTCTTGG	ICTC
A1651N	GGACCTCGGCaacTTCACCGAGA	TGGCATTGTTTCTGGTTC	ICTC
N1534Q	AGAACGGCTGcaaAAGGCCTGTG	TCCAGGGTGACCTTGTCAT	ICTC
V1658A	GAGCATGGTTgctTTTGGGTGCCCCAACTG	TCGGTGAAGGCGCCGAGG	ICTC
Q1647N, A1651N, P1662N	CGACCTCGGCaacTTCACCGAGA	TTGCATTGTTTCTGGTTCTC	CTC Q1647N P1662N
Q1647N, A1651D, P1662N	CGACCTCGGCgatTTCACCGAGA	TTGCATTGTTTCTGGTTCTC TTC	CTC Q1647N P1662N
Q1647N, A1651Q, P1662N	CGACCTCGGCcagTTCACCGAGAG	TTGCATTGTTTCTGGTTC	CTC Q1647N P1662N

Chapter 5

Summarizing discussion

Ramon M. van den Bos

Crystal and Structural Chemistry, Bijvoet Centre for Biomolecular Research, Department of Chemistry, Utrecht University, Utrecht, The Netherlands.

The complement system is an important part of our innate immunity. Complement is involved in the clearance of microorganisms, foreign particles and altered host cells. Initiation of complement activation can occur through three pathways. The classical pathway (CP) and lectin pathway (LP) require pattern recognition molecules for initiation, while the alternative pathway (AP) has a continuously low-level activity and does not depend specific pattern recognition for activation (1). Regulation of AP activation is vital to direct activation to appropriate surfaces and to protect healthy host cells. In this thesis we focused on properdin, which is the only known positive, activation stimulating, regulator of the complement system. Properdin positively stimulates activation by increasing the lifetime of the AP C3 convertase (C3bBb) that is pivotal to the AP (2). Furthermore, properdin reduces the proteolytic inactivation of C3b by factor I (FI) (3). Positive regulation by properdin is crucial for complement-mediated host protection against infection by various microorganism, such as Chlamydia pneumoniae, Neisseria meningitides and gonorrhoeae (4). In addition, properdin plays an important role in multiple diseases that are caused by unwanted AP activation, including paroxysmal nocturnal hemoglobinuria (PNH) and atypical hemolytic uremic syndrome (aHUS) (5–7). In this thesis we presented novel insights into the molecular mechanism of positive regulation by properdin and in this chapter I will discuss the main findings.

Structural insight into positive regulation of complement activation by properdin

Over the last two decades, structural characterization of the complement system has provided great insights into the molecular mechanism of complement activation. Despite the importance of properdin in AP activation, it remained one of the last proteins in the complement cascade to be structurally characterized. Negative-stain EM experiments revealed that properdin occurs as multiple oligomeric species that consist of multiple rings connected by thin flexible linkers (8, 9). The heterogeneity and flexibility of properdin make it a difficult protein for structural characterization. In addition, properdin has the propensity to form unnatural, large aggregates upon freeze thaw cycles, prolonged storage and upon purification using harsh conditions (4, 10). Recent advances in overcoming these hurdles, by our lab and by others, enabled the structural characterization of properdin.

Based on previous data it was postulated that properdin oligomerizes by the interaction between the N-terminal part of one protomer with the C-terminal part of another protomer (8, 9). A properdin protomer is composed of a N-terminal domain and six thrombospondin type-I repeat (TSR) domains (11). The fold of the N-terminal domain was unknown and was often referred to as TSR0 since, like other TSR domains, it harbors three conserved disulfides (12), even though it lacks the conserved WxxWxxW and Q/RxRxR sequence motifs that make up the core of the TSR domain (13). Negative-stain EM images showed that the ring-like parts of properdin likely mediate stabilization of the AP C3 convertase (C3bBb) as each ring within a properdin oligomer binds to a separate C3bBb (9). In addition, biochemical data indicated that TSR3 of properdin is not necessary for the generation of properdin oligomers and for stabilization of C3bBb, which suggested that TSR3 resides within the flexible linkers (11). In our experiments, we set out to produce a homogeneous properdin sample with reduced flexibility, which proved to be crucial for the structural characterization of properdin. In chapter 2, we generated two monomerized properdin variants, $P^{N1/456}$ and $P^{N12/456}$, by co-expressing N-terminal constructs consisting of N-TSR1 or N-TSR1-2, respectively, together with a C-terminal construct consisting of TSR4-5-6. Both monomerized properdin variants purified as monodisperse samples and were capable of stabilizing C3bBb, which makes them suitable candidates for structural characterization.

Using x-ray crystallography, we solved the structure of both monomerized properdin variants. These structures revealed that the N-terminal domain is not a TSR domain. Instead, it adopts a short transforming-growth factor β binding protein-like (STB) fold. Additionally, these structures revealed the architecture of a C3bBb-binding ring, which is in agreement with the properdin shape that was observed by negative-stain EM (8, 9). Properdin oligomerization is facilitated through interactions between the STB and TSR1 of one properdin protomer with, respectively TSR4 and TSR6 from another properdin protomer. Thus, the C3bBb binding ring consist of the STB domain, TSR1 and TSR4-5-6 and they are connected by linkers consisting of TSR2, TSR3 and two thirds of TSR4. The structures also suggested an important role for the C-type man-

nosylation on tryptophan residues in the TSR domains. The mannosyl moiety likely contributes to the stability of the TSR domain by forming several hydrogen bonds in the TSR-domain core fold. This was recently biochemically confirmed by Shcherbakova and colleagues for UNC-5, where they showed that the presence of C-type mannosylation on the tryptophan residues increased the melting temperature of a TSR domain from UNC-5 from 50 °C to 60 °C (14).

Besides the structure of properdin alone, we also solved the crystal structure of the monomerized properdin variant $P^{N1/456}$ in complex with the isolated CTC domain of C3b. This revealed that TSR5 of properdin interacts with the last two α-helixes of the CTC domain. In addition, two loops that originate from both TSR5 and TSR6 embrace the C-terminal part of the last α-helix of the CTC domain like stirrups. These molecular stirrups are likely important for function as it was biochemically shown that a proteolytic cleavage between res. 333–334 in the TSR5 stirrup impairs the interaction between properdin and C3b and thus prevent stabilization of the C3 convertase (11). Furthermore, a disease-related mutation, Y414D, in the anchor point of the TSR6 stirrup resulted in the production of inactive properdin (15).

Previously, Pedersen and colleagues published 6-Å resolution map of properdin in complex with the SCIN stabilized C3 convertase (PDB ID: 5M6W). This map displays density for properdin on top of the C3b CTC domain, however due to the low resolution the authors were not able to generate a molecular model of properdin (16). Our high-resolution structure of properdin in complex with the CTC domain enabled us to fit a properdin model in the SCIN-stabilized C3bBb map. The resulting model of the complex revealed that properdin has only a limited interface with Bb and that the molecular stirrups from TSR5 and TSR6 reside in close proximity to the Von Willebrand factor type-A (VWA) domain in Bb, where they are likely important for interaction with Bb in the C3 convertase. However, at this low resolution no details of the interacting amino acids can be observed. Using SPR, we confirmed that properdin binds to C3b, C3bB and C3bBb with increasing affinities (3), which indicates that properdin indeed interacts with B/Bb region of the (pro) convertase. Furthermore, mutagenesis studies by Pedersen and colleagues revealed that residues K323-L324-K325 in the VWA domain of FB are important for the enhanced interaction of properdin with C3bB compared to C3b alone (17). These results indicate that properdin stabilizes C3bBb by interacting with both C3b and Bb and functioning as a bridge between them, although the exact properdin residues that mediate the interaction with Bb remain unknown. A high-resolution structure of properdin in complex with the C3 (pro) convertase would provide insights into which residues are important for stabilization. Unfortunately, we were unable to solve such a structure by crystallography after extensive trials. As an alternative to crystallography, single particle cryo-EM could be used to solve a structure of properdin in complex with the C3 convertase. However, obtaining such a structure might be challenging due flexible regions in the complex. Both properdin and Bb interact with the C3b CTC domain and it has been shown that this domain can adopt several orientations (18–20). Furthermore, the cryo-EM structures of C5 and cobra venom

factor (CVF), a homologue and orthologue of C3b, respectively, displayed poorly resolved CTC domains (21, 22). The C3 proconvertase would possibly be a more attractive complex as in this complex the Ba part of FB is still bound to C3b, which likely limits the movement of FB and the CTC domain. In the proconvertase FB can be in a closed and open conformation however this can be locked in the open conformation by generating the complex with Ni^{2+} instead of Mg^{2+} or by adding inactive FD (18, 23–25). Alternatively, the interaction between properdin and Bb could be characterized by biochemical approaches, such as mutating amino-acid residues in the properdin stirrups and in the VWA domain of FB.

Properdin oligomerization is important for directing positive regulation by properdin to surfaces (3). A properdin oligomer can bind simultaneously to multiple C3b or C3bBb on a surface, which results in a high avidity interaction between properdin and the coated surface (3, 16, 26). This avidity effect directs positive regulation by properdin to surfaces that are already coated with some C3b or C3bBb. In the structure of properdin in complex with the SCIN stabilized C3 convertase properdin sits like a mohawk on top of the C3 convertase. From this structure it is unclear how properdin would simultaneously bind multiple sites on a surface. Interestingly, a comparison between the properdin structures that we solved in chapter 2 revealed structural heterogeneity. TSR4 displays a bending like motion between the structures, with an angle of 60° between the two extremes of the TSR4 conformations. Furthermore, TSR2 is observed in two different orientations that have a change in angle of 58° between them with respect to TSR1. Using these different observed conformations, we were able to generate models of dimeric, trimeric and tetrameric properdin bound to a C3bBb coated surface. All in all, the heterogeneous oligomerization and flexible nature of properdin is likely important for enabling high avidity binding to irregular coated surfaces (8).

Recruitment of properdin to a surface promotes AP activation

The AP does not require pattern recognition molecules for initiation. However, it has been shown that properdin bound to surfaces can recruit C3b and C3 convertase complexes (27). Furthermore, the interaction of properdin with certain microorganisms and cells (e.g. *Chlamydia pneumonia* and necrotic cells) promotes AP activation (28–31). Properdin can be recruited to cells by interaction with soluble collectin-12 (32). In addition, properdin can bind directly to surfaces by interaction with a wide variety of negatively charged ligands (e.g. heparan sulfate and DNA (31, 33)), although it is unknown where these ligands bind. The electrostatic surface potential of properdin does not reveal a clear ligand binding site. The most positively charged region of properdin is within its interface with the CTC domain. A previous study reported that a heparan binding site lies within this region as it was shown that TSR5 is important for heparan-sulfate binding (11) and that heparan-sulfate can compete with properdin binding to C3b (34). These data suggest that properdin oligomers could attach to negatively charged moieties on surfaces and subsequently promote AP activation through their

remaining C3bBb-binding rings. A structure of properdin in complex with small molecule sulfated heparan derivatives could give insights in how properdin interacts with heparan sulfate.

The balance between positive and negative regulation is important for complement activation

In chapter 3 we assessed the role of properdin in AP activation on C3b-coated liposomes. Properdin was critical for AP activation induced by serum and the inhibition of properdin activity with the tick protein Salp20 resulted the complete inhibition of AP activation. Further experiments revealed that properdin was only essential in the presence of a negative regulator that has decay acceleration activity (DAA) (e.g. factor H). Properdin and factor H (FH) have opposing effects on the life time of C3bBb and it was already shown that properdin reduces the amount of decay induced by FH (35–37), although some of these experiments were performed with non-physiological properdin aggregates (36, 37). Recently it was suggested that the reduced decay by FH in the presence of properdin could be due to a conformational change in the C3 convertase induced by properdin (9, 16). However, in chapter 3 we showed that the relative increase in the lifetime of C3bBb by properdin was similar in absence and in presence of negative regulators with DAA. This indicates that properdin and negative regulators with DAA have no direct effect on each other. Based on the liposome leakage assays it seems that the effect of properdin on reducing the FI mediated proteolytic inactivation of C3b (9, 38) plays only a minor role in AP activation. However, it is possible that preventing inactivation of C3b is more important for AP activation just after initiation when there is only a limited amount of C3b on the surface.

In addition to stabilizing the C3 convertase it has been suggested that properdin can positively regulate AP activation by promoting formation of the C3 convertase (27). With SPR we showed that FB binds three times stronger to the properdin-C3b complex compared to C3b alone and that the presence of properdin results in 68 % more complex formation at 100 nM FB. However, when co-injecting FB and FD, both at 100 nM, there was only 18 % more complex formation in the presence of properdin. Furthermore, preformation of the C3 convertase on liposomes had minimal effect on AP activation suggesting that enhanced formation of the C3 convertase in the presence of properdin only plays a minor role in AP activation.

The balance between positive and negative regulation by properdin and FH, respectively, is crucial for AP activation on C3b-coated liposomes. This balance is likely also maintained in physiologically relevant situations and might explain why properdin plays such a crucial role in the defense against *Neisseria meningitides* and *Neisseria gonorrhoeae*, as these bacteria recruit FH to their surface for protection against complement activation (39). Furthermore, it has been shown that properdin is required for CP activation on a *Neisseria gonorrhea* strain that binds C4 binding protein, a negative regulator that acts on

the CP and LP C3 convertase (40).

Therapeutic intervention of unwanted complement activation

Unwanted attack of host cells by the complement system is the basis for various diseases (e.g. PNH and aHUS). The AP plays an important role in complement related diseases (41), which is likely due to its ability to activate without requiring pattern recognition molecules. In addition, the amplification loop of the AP is responsible for up to 80% of the total C3b and C3a generation after complement initiation through the AP, CP and LP (42, 43). Currently, eculizumab and its successor ravulizumab, which is a pH-dependent antigen binding variant of eculizumab, are the only complement inhibitors that are approved for therapeutic use. They both bind to C5 and block its cleavage, which inhibits the terminal pathway (TP) and prevents the formation of the lytic membrane attack complex (44). The introduction of eculizumab revolutionized the treatment of diseases like PNH and aHUS. Despite its importance, there are limitations in the use of eculizumab. Inhibition at the level of the TP leaves the amplification loop of the AP intact. Thus, the affected surface can be opsonized with C3b, which can result in complement activation breakthrough events and phagocytosis of opsonized cells (45, 46). As a result, a large portion of the PNH patients that are treated with eculizumab remain blood transfusion-dependent (47). Therapeutic intervention at the level of AP activation would reduce the amount of deposited C3b and it is therefore an attractive alternative to inhibition of the TP. C3, FB, FD and properdin are potential targets for AP inhibition. C3 is critical for all pathways whilst FB, FD and properdin are exclusive to AP activation and inhibition of these proteins would not completely inhibit CP and LP activation (42, 43).

A potential source for novel complement inhibitors is the saliva of arthropods that feed on blood (e.g. ticks and mosquitoes). These animals produce various complement inhibitors to protect against complement activation by the ingested blood (48). Currently a tick derived protein, coversin, which prevents the cleavage of C5 is being tested in clinical trials and shows promising results in the treatment of a PNH patient that is nonresponsive to treatment by eculizumab (49). Furthermore, there are also inhibitors found against components of the AP. Lufaxin, a protein found in salivary of sand flies, binds to FB and prevents its cleavage by FD and thus inhibits C3 convertase formation (50). Salp20 is a tick protein that binds to properdin and prevents it interaction with C3b and the C3 convertase (51). We have shown that Salp20 can be produced in mammalian cells and that Salp20 is a useful tool for studying the effect of properdin inhibition (34, 52). A potential downside of using proteins from arthropods as complement inhibitors in a therapeutic setting is that they are likely highly immunogenic, which could lead to the production of antidrug antibodies that reduce the efficacy of the drug or could have a harmful effect on the recipient (e.g. allergic reaction) (53).

FD and FB are interesting targets for small molecule complement inhibitors. Both are

trypsin like serine proteases and their function could be targeted by protease inhibitors. The challenge in finding protease inhibitors against FD and FB is that they need to be highly specific. Recently, structure-based drug design studies were performed to design protease inhibitors that are highly specific for FD and FB (54–56). The great benefit of small molecule inhibitors is that they can be administered orally and do not require subcutaneous or intravascular injections for administration.

Besides FD and FB, properdin also represents a potential target for the development of novel AP inhibitors; the inhibition of properdin has been shown to greatly reduce AP activation and was beneficial in mouse models for diseases like PNH and aHUS (6, 7, 57–59). Recently a comparative study that tested the efficacy of antibody mediated inhibition of properdin, FB, C3 and C5 in ex vivo experiments, showed that the properdin inhibitors have the highest efficacy in inhibiting AP activation (60). The high efficacy of the properdin inhibitors was likely due to relative low serum properdin concentration (0.1-0.5 μM) compared to serum concentration of FB (2-8 μM) and C3 (~6 μM) and to a lesser extend C5 (~0.4 μM) (61). Thus, properdin is an attractive therapeutic target for combatting complement related diseases. Therefore, in chapter 4, we explored the therapeutic capability of the isolated C3b CTC domain (ICTC). We show that ICTC can reduce AP activation, albeit with a low efficacy. With structure-based drug design we increased the efficacy of the ICTC 100-fold and created a properdin specific inhibitor. The enhanced ICTC can be used as a tool for monitoring the effect of properdin on complement activation and is potentially interesting as a therapeutic. However, for therapeutic use the efficacy would need be to further improved by one or two orders of magnitude. This could potentially be achieved with directed evolution or by creating ICTC multimers which would introduce avidity for the properdin oligomers.

Acknowledgements

Thanks to Harma Brondijk and Wout Oosterheert for critically proofreading this chapter.

References

1. Ricklin, D., G. Hajishengallis, K. Yang, and J. D. Lambris. 2010. Complement: A key system for immune surveillance and homeostasis. *Nat. Immunol.* 11: 785–797.

2. Fearon, D. T., and K. F. Austen. 1975. Properdin: binding to C3b and stabilization of the C3b-dependent C3 convertase. *J. Exp. Med.* 142: 856–63.

3. Farries, T. C., P. J. Lachmann, and R. A. Harrison. 1988. Analysis of the interactions between properdin, the third component of complement (C3), and its physiological activation products. *Biochem. J.* 252: 47–54.

4. Blatt, A. Z., S. Pathan, and V. P. Ferreira. 2016. Properdin: a tightly regulated critical inflammatory modulator. *Immunol. Rev.* 274: 172–190.

5. Chen, J. Y., C. Cortes, and V. P. Ferreira. 2018. Properdin: A multifaceted molecule involved in inflammation and diseases. *Mol. Immunol.* 102: 58–72.

6. Ueda, Y., T. Miwa, D. Gullipalli, S. Sato, D. Ito, H. Kim, M. Palmer, and W. C. Song. 2018. Blocking Properdin Prevents Complement-Mediated Hemolytic Uremic Syndrome and Systemic Thrombophilia. *J. Am. Soc. Nephrol.* 29: 1928–1937.

7. Gullipalli, D., F. Zhang, S. Sato, Y. Ueda, Y. Kimura, M. Golla, T. Miwa, J. Wang, and W.-C. Song. 2018. Antibody Inhibition of Properdin Prevents Complement-Mediated Intravascular and Extravascular Hemolysis. *J. Immunol.* 201: 1021–1029.

8. Smith CA, Pangburn MK, Vogel CW, Müller-Eberhard HJ. 1984. Molecular architecture of human properdin, a positive regulator of the alternative pathway of complement. *J. Biol. Chem.* 259: 4582–4588.

9. Alcorlo, M., A. Tortajada, S. Rodríguez de Córdoba, and O. Llorca. 2013. Structural basis for the stabilization of the complement alternative pathway C3 convertase by properdin. *Proc. Natl. Acad. Sci. U. S. A.* 110: 13504–9.

10. Pangburn, M. K. 1989. Analysis of the natural polymeric forms of human properdin and their functions in complement activation. *J. Immunol.* 142: 202–7.

11. Higgins, J. M., H. Wiedemann, R. Timpl, and K. B. Reid. 1995. Characterization of mutant forms of recombinant human properdin lacking single thrombospondin type I repeats. Identification of modules important for function. *J. Immunol.* 155: 5777–85.

12. Sun, Z., K. B. M. M. Reid, and S. J. Perkins. 2004. The dimeric and trimeric solution structures of the multidomain complement protein properdin by X-ray scattering, analytical ultracentrifugation and constrained modelling. *J. Mol. Biol.* 343: 1327–1343.

13. Tan, K., M. Duquette, J. H. Liu, Y. Dong, R. Zhang, A. Joachimiak, J. Lawler, and J. H. Wang. 2002. Crystal structure of the TSP-1 type 1 repeats: A novel layered fold and its biological implication. *J. Cell Biol.* 159: 373–382.

14. Shcherbakova, A., M. Preller, M. H. Taft, J. Pujols, S. Ventura, B. Tiemann, F. F. R. Buettner, and H. Bakker. 2019. C-mannosylation supports folding and enhances stability of thrombospondin repeats. *Elife* 8.

15. Fredrikson, G. N., J. Westberg, E. J. Kuijper, C. C. Tijssen, A. G. Sjöholm, M. Uhlén, and L. Truedsson. 1996. Molecular characterization of properdin deficiency type III: dysfunction produced by a single point mutation in exon 9 of the structural gene causing a tyrosine to aspartic acid interchange. *J. Immunol.* 157: 3666–71.

16. Pedersen, D. V, L. Roumenina, R. K. Jensen, T. A. Gadeberg, C. Marinozzi, C. Picard, T. Rybkine, S. Thiel, U. B. Sørensen, C. Stover, et al. 2017. Functional and structural insight into properdin control of complement alternative pathway amplification. *EMBO J.* 36: 1084–1099.

17. Pedersen, D. V., T. A. F. Gadeberg, C. Thomas, Y. Wang, N. Joram, R. K. Jensen, S. M. M. Mazarakis, M. Revel, C. El Sissy, S. V. Petersen, et al. 2019. Structural Basis for Properdin Oligomerization and Convertase Stimulation in the Human Complement System. *Front. Immunol.* 10.

18. Forneris, F., D. Ricklin, J. Wu, A. Tzekou, R. S. Wallace, J. D. Lambris, and P. Gros. 2010. Structures of C3b in complex with factors B and D give insight into complement convertase formation. *Science (80-.).* 330: 1816–1820.

19. Forneris, F., J. Wu, X. Xue, D. Ricklin, Z. Lin, G. Sfyroera, A. Tzekou, E. Volokhina, J. C. Granneman, R. Hauhart, et al. 2016. Regulators of complement activity mediate inhibitory mechanisms through a common C3b-binding mode. *EMBO J.* 35: 1133–1149.

20. Rooijakkers, S. H. M., J. Wu, M. Ruyken, R. van Domselaar, K. L. Planken, A. Tzekou, D. Ricklin, J. D. Lambris, B. J. C. Janssen, J. a G. van Strijp, et al. 2009. Structural and functional implications of the alternative complement pathway C3 convertase stabilized by a staphylococcal inhibitor. *Nat. Immunol.* 10: 721–727.

21. Reichhardt, M. P., S. Johnson, T. Tang, T. Morgan, N. Tebeka, N. Popitsch, J. C. Deme, M. M. Jore, and S. M. Lea. 2020. An inhibitor of complement C5 provides structural insights into activation. *Proc. Natl. Acad. Sci. U. S. A.* 117: 362–370.

22. Jendza, K., M. Kato, M. Salcius, H. Srinivas, A. De Erkenez, A. Nguyen, D. McLaughlin, C. Be, C. Wiesmann, J. Murphy, et al. 2019. A small-molecule inhibitor of C5 complement protein. *Nat. Chem. Biol.* 15: 666–668.

23. Janssen, B. J. C., L. Gomes, R. I. Koning, D. I. Svergun, A. J. Koster, D. C. Fritzinger, C. W. Vogel, and P. Gros. 2009. Insights into complement convertase formation based on the structure of the factor B-cobra venom factor complex. *EMBO J.* 28: 2469–2478.

24. Torreira, E., A. Tortajada, T. Montes, S. R. De Córdoba, and O. Llorca. 2009. 3D structure of the C3bB complex provides insights into the activation and regulation of the complement alternative pathway convertase. *Proc. Natl. Acad. Sci. U. S. A.* 106: 882–887.

25. Torreira, E., A. Tortajada, T. Montes, S. Rodríguez de Córdoba, and O. Llorca. 2009. Coexistence of Closed and Open Conformations of Complement Factor B in the Alternative Pathway C3bB(Mg 2+) Proconvertase . *J. Immunol.* 183: 7347–7351.

26. van den Bos, R. M., N. M. Pearce, J. Granneman, T. H. C. Brondijk, and P. Gros. 2019. Insights Into Enhanced Complement Activation by Structures of Properdin and Its Complex With the C-Terminal Domain of C3b. *Front. Immunol.* 10.

27. Hourcade, D. E. 2006. The role of properdin in the assembly of the alternative pathway C3 convertases of complement. *J. Biol. Chem.* 281: 2128–2132.

28. Vuagnat, B. B., J. P. Mach, and J. M. Le Doussal. 2000. Activation of the alternative pathway of human complement by autologous cells expressing transmembrane recombinant properdin. *Mol. Immunol.* 37: 467–478.

29. Pedersen, D. V., T. Rösner, A. G. Hansen, K. R. Andersen, S. Thiel, G. R. Andersen, T. Valerius, and N. S. Laursen. 2020. Recruitment of properdin by bi-specific nanobodies activates the alternative pathway of complement. *Mol. Immunol.* 124: 200–210.

30. Cortes, C., V. P. Ferreira, and M. K. Pangburn. 2011. Native properdin binds to Chlamydia pneumoniae and promotes complement activation. *Infect. Immun.* 79: 724–731.

31. Xu, W., S. P. Berger, L. A. Trouw, H. C. de Boer, N. Schlagwein, C. Mutsaers, M. R. Daha, and C. van Kooten. 2008. Properdin Binds to Late Apoptotic and Necrotic Cells Independently of C3b and Regulates Alternative Pathway Complement Activation. *J. Immunol.* 180: 7613–7621.

32. Zhang, J., L. Song, D. V Pedersen, A. Li, J. D. Lambris, G. R. Andersen, T. E. Mollnes, Y. J. Ma, and P. Garred. 2020. Soluble collectin-12 mediates C3-independent docking of properdin that activates the alternative pathway of complement. *Elife* 9.

33. Zaferani, A., R. R. Vivès, P. Van Der Pol, J. J. Hakvoort, G. J. Navis, H. Van Goor, M. R. Daha, H. Lortat-Jacob, M. A. Seelen, and J. Van Den Born. 2011. Identification of tubular heparan sulfate as a docking platform for the alternative complement component properdin in proteinuric renal disease. *J. Biol. Chem.* 286: 5359–5367.

34. Lammerts, R. G. M., D. T. Talsma, W. A. Dam, M. Daha, M. Seelen, S. P. Berger, and J. Van Den Born. 2020. Properdin pattern recognition on proximal tubular cells is heparan sulfate/Syndecan-1 but not C3b dependent and can be blocked by tick protein Salp20. *Front. Immunol.* 11: 1643.

35. Fearon, D. T., and K. Frank Austen. 1977. Activation of the alternative complement pathway with rabbit erythrocytes by circumvention of the regulatory action of endogenous control proteins. *J. Exp. Med.* 146: 22–33.

36. Weiler, J. M., M. R. Daha, K. F. Austen, and D. T. Fearon. 1976. Control of the amplification convertase of complement by the plasma protein beta1H. *Proc. Natl. Acad. Sci. U. S. A.* 73: 3268–72.

37. Whaley, K., and S. Ruddy. 1976. Modulation of the alternative complement pathway by β1H globulin. *J. Exp. Med.* 144: 1147–1163.

38. Farries, T. C., P. J. Lachmann, and R. A. Harrison. 1988. Analysis of the interaction between properdin and Factor B, components of the alternative-pathway C3 convertase of complement. *Biochem. J.* 253: 667–675.

39. Agarwal, S., V. P. Ferreira, C. Cortes, M. K. Pangburn, P. A. Rice, and S. Ram. 2010. An Evaluation of the Role of Properdin in Alternative Pathway Activation on Neisseria meningitidis and Neisseria gonorrhoeae . *J. Immunol.* 185: 507–516.

40. Gulati, S., S. Agarwal, S. Vasudhev, P. A. Rice, and S. Ram. 2012. Properdin Is Critical for Antibody-Dependent Bactericidal Activity against Neisseria gonorrhoeae That Recruit C4b-Binding Protein . *J. Immunol.* 188: 3416–3425.

41. Thurman, J. M., and V. M. Holers. 2006. The Central Role of the Alternative Complement Pathway in Human Disease. *J. Immunol.* 176: 1305–1310.

42. Harboe, M., G. Ulvund, L. Vien, M. Fung, and T. E. Mollnes. 2004. The quantitative role of alternative pathway

amplification in classical pathway induced terminal complement activation. *Clin. Exp. Immunol.* 138: 439–446.

43. Harboe, M., P. Garred, E. Karlstrøm, J. K. Lindstad, G. L. Stahl, and T. E. Mollnes. 2009. The down-stream effects of mannan-induced lectin complement pathway activation depend quantitatively on alternative pathway amplification. *Mol. Immunol.* 47: 373–380.

44. Kulasekararaj, A. G., A. Hill, S. T. Rottinghaus, S. Langemeijer, R. Wells, F. A. Gonzalez-Fernandez, A. Gaya, J. W. Lee, E. O. Gutierrez, C. I. Piatek, et al. 2019. Ravulizumab (ALXN1210) vs eculizumab in C5-inhibitor–experienced adult patients with PNH: The 302 study. *Blood* 133: 540–549.

45. De Latour, R. P., V. Fremeaux-Bacchi, R. Porcher, A. Xhaard, J. Rosain, D. C. Castaneda, P. Vieira-Martins, S. Roncelin, P. Rodriguez-Otero, A. Plessier, et al. 2015. Assessing complement blockade in patients with paroxysmal nocturnal hemoglobinuria receiving eculizumab. *Blood* 125: 775–783.

46. Harder, M. J., N. Kuhn, H. Schrezenmeier, B. Höchsmann, I. Von Zabern, C. Weinstock, T. Simmet, D. Ricklin, J. D. Lambris, A. Skerra, et al. 2017. Incomplete inhibition by eculizumab: Mechanistic evidence for residual C5 activity during strong complement activation. *Blood* 129: 970–980.

47. Harris, C. L., R. B. Pouw, D. Kavanagh, R. Sun, and D. Ricklin. 2018. Developments in anti-complement therapy; from disease to clinical trial. *Mol. Immunol.* 102: 89–119.

48. Barros, V. C., J. G. Assumpção, A. M. Cadete, V. C. Santos, R. R. Cavalcante, R. N. Araújo, M. H. Pereira, and N. F. Gontijo. 2009. The role of salivary and intestinal complement system inhibitors in the midgut protection of Triatomines and mosquitoes. *PLoS One* 4.

49. Schols, S., M. A. Nunn, I. Mackie, W. Weston-Davies, J. ichi Nishimura, Y. Kanakura, N. Blijlevens, P. Muus, and S. Langemeijer. 2020. Successful treatment of a PNH patient non-responsive to eculizumab with the novel complement C5 inhibitor coversin (nomacopan). *Br. J. Haematol.* 188: 334–337.

50. Mendes-Sousa, A. F., V. F. do Vale, N. C. S. Silva, A. B. Guimaraes-Costa, M. H. Pereira, M. R. V. Sant'Anna, F. Oliveira, S. Kamhawi, J. M. C. Ribeiro, J. F. Andersen, et al. 2017. The Sand Fly Salivary Protein Lufaxin Inhibits the Early Steps of the Alternative Pathway of Complement by Direct Binding to the Proconvertase C3b-B. *Front. Immunol.* 8: 1065.

51. Tyson, K. R., C. Elkins, and A. M. de Silva. 2008. A Novel Mechanism of Complement Inhibition Unmasked by a Tick Salivary Protein That Binds to Properdin. *J. Immunol.* 180: 3964–3968.

52. Michels, M. A. H. M., N. C. A. J. Van De Kar, R. M. Van Den Bos, T. J. A. M. Van Der Velden, S. A. W. Van Kraaij, S. A. Sarlea, V. Gracchi, M. J. S. Oosterveld, E. B. Volokhina, L. P. W. J. Van Den Heuvel, et al. 2019. Novel assays to distinguish between properdin-dependent and properdin-independent C3 nephritic factors provide insight into properdin-inhibiting therapy. *Front. Immunol.* 10.

53. Sauna, Z. E., D. Lagassé, J. Pedras-Vasconcelos, B. Golding, and A. S. Rosenberg. 2018. Evaluating and Mitigating the Immunogenicity of Therapeutic Proteins. *Trends Biotechnol.* 36: 1068–1084.

54. Wiles, J. A., M. D. Galvan, S. D. Podos, M. Geffner, and M. Huang. 2019. Discovery and Development of the Oral Complement Factor D Inhibitor Danicopan (ACH-4471). *Curr. Med. Chem.* 27: 4165–4180.

55. Maibaum, J., S. M. Liao, A. Vulpetti, N. Ostermann, S. Randl, S. Rüdisser, E. Lorthiois, P. Erbel, B. Kinzel, F. A. Kolb, et al. 2016. Small-molecule factor D inhibitors targeting the alternative complement pathway. *Nat. Chem. Biol.* 12: 1105–1110.

56. Mainolfi, N., T. Ehara, R. G. Karki, K. Anderson, A. Mac Sweeney, S. M. Liao, U. A. Argikar, K. Jendza, C. Zhang, J. Powers, et al. 2020. Discovery of 4-((2 S,4 S)-4-Ethoxy-1-((5-methoxy-7-methyl-1 H-indol-4-yl)methyl)piperidin-2-yl) benzoic Acid (LNP023), a Factor B Inhibitor Specifically Designed to Be Applicable to Treating a Diverse Array of Complement Mediated Diseases. *J. Med. Chem.* 63: 5697–5722.

57. Lesher, A. M., B. Nilsson, and W. C. Song. 2013. Properdin in complement activation and tissue injury. *Mol. Immunol.* 56: 191–198.

58. Kimura, Y., L. Zhou, T. Miwa, and W. C. Song. 2010. Genetic and therapeutic targeting of properdin in mice prevents complement-mediated tissue injury. *J. Clin. Invest.* 120: 3545–3554.

59. Song, G., and T. A. Springer. 2014. Structures of the Toxoplasma gliding motility adhesin. *Proc. Natl. Acad. Sci. U. S. A.* 111: 4862–7.

60. Chen, J. Y., N. S. Galwankar, H. N. Emch, S. S. Menon, C. Cortes, J. M. Thurman, S. A. Merrill, R. A. Brodsky, and V. P. Ferreira. 2020. Properdin Is a Key Player in Lysis of Red Blood Cells and Complement Activation on Endothelial Cells in Hemolytic Anemias Caused by Complement Dysregulation. *Front. Immunol.* 11: 1460.

61. Barnum, S. R., and S. N. Theresa. 2018. *The Complement FactsBook*,. Oxford, United Kingdom : Academic Press.

Appendix

Nederlandse samenvatting

Eiwitten zijn belangrijke bouwblokken van het leven en ze spelen een rol in vrijwel alle biologische processen. Eiwitten zijn ketens van 20 verschillende aminozuren die in een driedimensionale structuur vouwen. Deze structuur is bepalend voor de functie en verschilt per eiwit. Het oplossen van eiwitstructuren is zeer waardevol om inzicht te krijgen in het moleculaire mechanisme van eiwitten. Inzicht in de structuur van eiwitten kan daarnaast bijdragen aan het begrijpen van de oorzaak van een ziekte en kan de basis vormen voor het ontdekken van nieuwe medicijnen.

Hoofdstuk 1 geeft een inleiding in het complementsysteem. Dit systeem is een onderdeel van het aangeboren immuunsysteem en bestaat uit verschillende eiwitten die via een kettingreactie activeren. Complement is belangrijk in de verdediging tegen invasieve micro-organismen en in het opruimen van lichaamsvreemde objecten en gewijzigde gastheercellen. Het complementsysteem kan onmiddellijk reageren tegen gevaren omdat het, in tegenstelling tot het verworven immuunsysteem, niet getraind hoeft te worden voor activatie. Het complementsysteem kan worden geactiveerd door middel van herkenning van zogenaamde "gevaarsignalen". Daarnaast is er ook continue langzame aspecifieke activatie waarmee het complementsysteem doorlopend surveilleert of er gevaren zijn binnengedrongen. Activatie van het complementsysteem kan resulteren in het direct doden van micro-organismen, het labelen van micro-organismen en vreemde lichaamsobjecten voor opruiming door cellen van het immuunsysteem en in het opwekken van een ontstekingsreactie.

Het complementsysteem kan geactiveerd worden via drie routes. Het doel van dit proefschrift is om meer inzicht te krijgen in de regulatie van één van deze routes; de alternatieve route van het complementsysteem. Deze alternatieve route activeert zonder de hulp van herkenningsmoleculen. Dit gebeurt doordat het eiwit C3 spontaan van conformatie kan veranderen in een actieve staat, C3*, die ook wel C3(H_2O) wordt genoemd. C3* kan een interactie aan gaan met factor B die vervolgens geknipt kan worden door de serine protease factor D. Hierdoor ontstaat een C3 convertase, C3*Bb, wat een enzymatisch complex is. Dit enzym knipt vervolgens C3 in C3a en C3b, waarna de C3b covalent aan een oppervlakte kan binden door middel van zijn reactieve thio-ester groep. Vervolgens kan C3b interactie aangaan met factor B op een soortgelijke manier als C3* waardoor er een C3 convertase, C3bBb, op het oppervlak gevormd kan worden. Deze positieve amplificatieloop resulteert in de coating van oppervlaktes met C3b wat vervolgens kan leiden tot de formatie van een lytische porie in het membraan van cellen of het opruimen van het C3b gecoate deeltje door cellen van het immuunsysteem. Doordat de alternatieve route aspecifiek op oppervlakten kan activeren is het belangrijk dat deze activatie gereguleerd wordt, zodat gezonde gastheercellen beschermd zijn tegen activatie en dat de activatie wordt versterkt op cellen of objecten die wel aangevallen moeten worden.

Hoofdstuk 2 gaat in op de driedimensionale structuur van het eiwit properdine. Dit eiwit is de positieve regulator van de alternatieve route en is belangrijk voor het verster-

ken van complementactivatie. Dit is belangrijk voor efficiënte complementactivatie op micro-organismes zoals *Neisseria meningitis* en *Chlamydia pneumoniae*. Properdine stabiliseert de C3 convertase en zorgt er zo voor dat het enzym langer actief is en dus meer C3 kan knippen. Properdine is een eiwit dat voorkomt als dimeren, trimeren en tetrameren. Met elektronenmicroscopie was in eerdere publicaties waargenomen dat de properdine oligomeren bestaan uit meerdere C3 convertase stabiliserende ringen die verbonden zijn met dunne linkers. De properdine oligomeren zijn zeer flexibel en hebben de neiging om te aggregeren. Hierdoor was het tot voor kort lastig om de structuur van properdine te bepalen, omdat hiervoor een homogeen eiwit sample met minimale flexibiliteit nodig is. Door gebruik te maken van de beschikbare biochemische kennis konden we een soort properdine monomeren maken (mP) die bestaan uit één C3 convertase bindende ring. Vervolgens hebben wij aangetoond dat mP in staat was om de C3 convertase te stabiliseren. Verder hebben wij met surface plasmon resonance (SPR) laten zien dat door aviditeit de properdine oligomeren sterker binden aan een C3b gecoat oppervlakte vergeleken met de losse properdine ringen. Deze aviditeit is waarschijnlijk belangrijk om positieve regulatie door properdine te dirigeren naar oppervlaktes die al gedeeltelijk met C3b zijn gecoat. Het aviditeitseffect is niet aanwezig in oplossing. Verder zijn in serum de concentraties van C3*, C3b en C3 convertases heel laag. Door het gebrek aan aviditeit en de lage concentraties gaat properdine in serum waarschijnlijk geen interactie aan met deze eiwitten waardoor er geen onnodige positieve regulatie is wat zou resulteren in het opraken van complement eiwitten. Met röntgenstralingdiffractie hebben wij de structuur opgelost van de properdine ring; los en in complex met het geïsoleerde C-terminale C345c (CTC) domein van C3b. Deze structuren lieten zien welke interacties tussen properdine moleculen verantwoordelijk zijn voor de oligomerisatie. Verder konden we zien dat de mannosegroepen op de tryptofaanresiduen in de thrombospondin-like I repeat domeinen van properdine belangrijk zijn voor stabiliteit van deze domeinen. Dankzij de structuur van properdine in complex met het CTC-domein van C3b konden we de structuur oplossen van een voorheen gepubliceerde elektronen dichtheidsmap van properdine in complex met de C3 convertase. Deze structuur liet zien dat de interactie van properdine met de C3 convertase vooral gemedieerd wordt door C3b en dat er maar een beperkte interface is tussen properdine en Bb. Deze structuren in combinatie met de SPR-data suggereren dat properdine de C3 convertase stabiliseert door een brug tussen C3b en Bb te vormen.

In **hoofdstuk 3** kijken we naar de relatie tussen positieve en negatieve regulatie van het complementsysteem. Properdine is de enige positieve regulator van het complementsysteem, maar er zijn meerdere negatieve regulatoren die complementactivatie remmen. Negatieve regulatie is belangrijk om te voorkomen dat de complement componenten opraken en om gastheercellen te beschermen tegen complementactivatie. Factor H (FH) is de belangrijkste negatieve regulator in serum en remt complementactivatie door de levensduur van de C3 convertase te verkorten. Daarnaast fungeert FH als cofactor voor de factor I (FI) gemedieerde inactivatie van C3b. Voor het bestuderen van de regulatie van de alternatieve route maakten we gebruik van liposomen die pre-gecoat waren met C3b. We hebben het effect van properdine op activatie van de alternatieve

route getest door gebruik te maken van een properdine specifieke remmer, Salp20, die van origine in teken voorkomt. Het remmen van properdine door toevoeging van Salp20 aan serum zorgt voor complete remming van activatie door de alternatieve route. Dit laat zien dat properdine essentieel is voor activatie van de alternatieve route door serum. Vervolgens hebben we gekeken naar complementactivatie op de C3b gecoate liposomen geïnduceerd door de gezuiverde complementcomponenten; factor B, factor D en C5 tot en met C9. Met de gezuiverde componenten is properdine niet essentieel voor complementactivatie. De toevoeging van properdine zorgt wel voor meer complementactivatie. Doordat properdine essentieel is in serum maar niet met gezuiverde componenten hebben we gekeken naar de relatie tussen properdine en de negatieve regulatoren die in serum voorkomen, factor I en factor H. Door gebruik te maken van serum zonder factor I of factor H konden we het effect van deze regulatoren op properdine bestuderen. De toevoeging van Salp20 resulteerde in complete remming van complementactivatie in serum zonder factor I, maar zorgde alleen voor een reductie in activatie door serum zonder factor H. Verder zorgde de toevoeging van factor H aan de gezuiverde componenten voor complete remming van activatie in afwezigheid van properdine. Dit laat dus zien dat de balans tussen stabilisatie en destabilisatie van de C3 convertase door respectievelijk properdine en factor H belangrijk is voor de activatie van de alternatieve route. Met SPR hebben we laten zien dat properdine en factor H hun effect op de levensduur van de C3 convertase onafhankelijk van elkaar uitoefenen.

Ongewenste activatie of te veel activatie van de alternatieve route van het complementsysteem veroorzaakt of draagt bij aan verschillende ernstige ziektes zoals atypisch hemolytisch uremisch syndroom en paroxismale nachtelijke hemoglobinurie. Het vinden van nieuwe complementremmers om deze ziektes te behandelen is belangrijk en als positieve regulator van de alternatieve route is properdine een attractief doelwit voor het remmen van complementactivatie. In **hoofdstuk 4** verkennen we het therapeutische potentieel van het CTC-domein van C3b. We laten zien dat het CTC-domein complementactivatie door de alternatieve route kan remmen door competitie aan te gaan met C3b in de interactie met properdine. De efficiëntie waarmee het CTC-domein de alternatieve route remt is alleen erg laag. Aan de hand van de structuur van properdine in complex met het CTC-domein hebben we een aantal mutaties in de aminozuursequentie van het CTC-domein ontworpen met als doel deze efficiëntie te verhogen. Deze mutaties resulteerden in een CTC-domeinvariant, $CTC^{NN\Delta}$, met een honderd keer zo hoge efficiëntie vergeleken met het wildtype CTC-domein. $CTC^{NN\Delta}$ was in staat om complementactivatie door de alternatieve route op konijnenerytrocyten volledig te blokkeren bij een concentratie van 20 μM. Met het ontwerp van $CTC^{NN\Delta}$ hebben we laten zien dat een domein dat belangrijk is voor interactie kan worden gebruikt als remmer en dat het mogelijk is om de efficiëntie te verhogen door middel van 'op structuur gebaseerd ontwerp'.

In **hoofdstuk 5** worden de nieuwe inzichten in het moleculaire mechanisme achter positieve regulatie van properdine besproken en wordt er gediscussieerd over vervolgstappen in het onderzoek naar de alternatieve route van het complementsysteem.

A

Acknowledgements

During my PhD I worked together with many fun and interesting people. The atmosphere in the lab was always great which was an important factor for how much I enjoyed my PhD. Unfortunately, due to the current COVID-19 crisis I can't show my appreciation for all of you with a nice party.

Piet, ik wil je graag bedanken voor alle interessante wetenschappelijke discussies over het complementsysteem en voor al je hulp tijdens mijn PhD. Ik kan me één van mijn eerste gesprekken met jou nog herinneren. Je tekende een curve van mijn waarschijnlijke gemoedstoestand tijdens het traject, waarbij ik blij zou beginnen, waarna ik door een dal zou gaan, en dat ik dan hopelijk op het einde weer uit het dal zou zijn gekropen. Zelf dacht ik dat die curve onzin was en dat ik in mijn eerste, blije, gemoedstoestand zou blijven. Natuurlijk kreeg jij gelijk en ging ik door een dal. Gelukkig ben ik daar, met onder andere jouw hulp, weer uitgeklommen. Wetenschappelijk heb ik veel van je geleerd maar behalve dat heb je me ook nog andere wijze levenslessen geleerd, zoals dat het oké is om bij blijdschap op de tafel te staan, dat je als oude man ook nog uitbundig mag dansen en dat je, als je met je armen in je nek gaat zitten, een lang T-shirt moet dragen.

Eric, bedankt voor het zorgen dat het lab up en running bleef en voor alle fijne gesprekken en bemoedigende woorden. **Bert**, jij was de persoon waarbij ik voor al mijn SPR vragen terecht kon, succes met alle beursaanvragen. **Loes**, bedankt voor alle gezellige tennis avonden. **Martin**, ik heb genoten van alle koffiepauzes en de fietstochtjes naar het prachtige Zeist. **Joke**, je ben een schat. Sorry dat ik enigszins rommelig was. Bedankt voor alle interesse die je altijd toont en voor al je hulp in het lab. **Harma**, bedankt voor al je hulp en tips bij het schrijven en voor je interesse naar mijn gezin. **Arie**, bedankt voor het eindeloos uitvullen van de kristallisatiescreens en voor alle leuke gesprekken op het lab. **Toine**, bedankt voor je hulp met alle linux gerelateerde vraagstukken. Alle mensen van Cryo-EM, bedankt voor de interessante wetenschappelijke gesprekken.

Ik zou graag de hele K&S familie willen bedanken voor de geweldige sfeer in het lab. Allereerst wil ik mijn voormalig kantoorgenoten bedanken. **Matti** en **Remco**, bedankt dat jullie mij kennis hebben laten maken met het fantastische nummer Dom Lomp & Famous. **Viviana**, je ben een schat en ik bewonder je doorzettingsvermogen om Nederlands te leren. Je bent al heel goed in het formuleren van correcte zinnen, je hoeft eigenlijk alleen nog maar te werken aan de snelheid. **Deniz**, thanks for tolerating my stupid and sometimes inappropriate jokes. **Gonzalo**, you are a real meme lord, thanks for making me laugh. Diva **Dounia**, we were desk buddies during the most stressful period of my PhD. Thanks for putting up with me during this period and for creepily staring at me while you were lost in scientific thoughts. Ook alle studenten die ooit in N808 hebben gezeten, bedankt voor de gezelligheid.

Xiaoguang Xue, you were my mentor and taught me how to purify complement proteins from blood. Thanks for always being interested in my work and for being a great person. I look forward to experiencing your cooking skills again. **Matthieu,** I still have

nightmares about the day that you decided to kill your croissant by drowning it in a cappuccino. Besides this murder I loved our trips to the ESRF and to the CCP4 study weekend. **Lucas**, you are the best in producing the most random conversation topics. **Camilla**, I have definitely forgiven the fact that you 'hit' me once ;). You are a fun person and very eager to make the world a better and more sustainable place, I hope you succeed. **Nick**, thank you for helping me with all the structures and for listening to 'porn' with me at 2 in the morning at the synchrotron. I much appreciated all the candy you (and all other occupants of N804) provided. If sarcasm were a scientific field, you would eighter win the Nobel prize or be the main topic of all the studies. I hope you and your nice wife **Lindsay** quickly find the security you both desire. **Itziar**, thank you for your contributions to chapter 3 of this thesis. I really enjoyed working together with you on the project. I hope that your next research at Utrecht University will really go viral. **Mercedes**, I enjoyed our SPR talks about misbehaving proteins and how it is a bitch to regenerate the surface. **Laura**, ik kan je Nederlandse nuchterheid zeer waarderen en ik heb van onze trip naar Kopenhagen genoten. Fijn dat je nu wat dichter bij huis werkt, hopelijk kan je dan nog meer van je kinderen genieten. **Nicoletta**, I wish you good luck with unraveling the difference between A and B. **Wouter**, ik heb met veel plezier samen kristallen met jou geschoten. Ik wil je graag bedanken voor de keren dat je de Chinese kippenpootjes met mij hebt gedeeld. **Manu**, with your Italian looks and German work ethic you are the best of both worlds. Your perfectionism is admirable although sometimes it is okay to use quicker but less sophisticated methods. **Nadia**, you bend over backwards to teach me SPR. Working together with you was a real pleasure and I always knew I made a stupid joke if you were the only one laughing :). **Jonas**, you are my favorite potato farmer, and it was super fun partying with you. **Dimphna**, je was een superleuke collega en ik wens je veel plezier met je jonge gezinnetje. **Lena**, thanks for always being super cheerful. **Robert**, you are a fun guy, although I'm always afraid that you will get hurt when I look at you. **Jitse**, je bent een lekkere droogkloot. Bedankt voor de curry, ik ga je zeker missen als je naar het David de Wiedgebouw verhuisd. **Tim**, ik vond het altijd gezellig om bier met je te drinken, helaas had jij op vrijdag altijd andere borrel verplichtingen. **Karla**, you are the most energetic person I know. From dawn to dusk you run and scream around in the lab. Although you can be a bit much to deal with (especially in the morning before the first coffee) your positive energy gave a real boost to the lab, thanks for that. **Revina**, toen ik bij K&S begon was jij degene waar ik het meest bang voor was. Jij wilde alles zo netjes mogelijk houden in het lab en daar kon je een sloddervos als ik niet bij gebruiken. Gelukkig ben ik over mijn angst heen gegroeid en heb ik je leren kennen als de lieve succesvolle topvrouw die je bent. Ik hoop dat we samen met onze gezinnetjes nog vaak zullen afspreken. **Wout**, ik ben dolblij dat ik net een maandje na jou ben begonnen en dat ik daardoor dus bijna 5 jaar samen met jou heb gewerkt. Ik heb genoten van alle conferenties waarbij ik eindelijk weer samen met jou mocht slapen. Tijdens deze magische jaren heb ik dingen van je gehoord, geroken en gezien die ik allemaal liever weer zou vergeten. Nu jij in het verre buitenland zit moet ik iemand anders vinden om mee te squashen/fitnessen/hardlopen/you f*cked me mee te kijken/mountainbiken/bier te drinken/kapsalon mee te eten/voetbal mee te kijken/etc. Je was (en bent nog steeds) altijd een welkome gast in huize van den Bos en als jij

langskwam dan hadden Mees en alle dieren even geen aandacht meer voor mij. Dankjewel dat je mij soms liet winnen met Fifa.

Ik zou ook graag de studenten die ik heb mogen begeleiden bedanken. **Jelmer**, **Jeroen** en **Ezra**, ik vond het heel leuk om jullie te begeleiden en het was ook zeker nuttig voor mijn onderzoek. **Noortje**, je was een supergezellige collega, bedankt voor al het geregel. Moeder gans **Bianca**, je zorgde altijd goed voor je kuikentjes. Ik hoop dat je beter begrijpt waar je huidige collega's mee bezig zijn :). **Liza**, bedankt voor je hulp tijdens de laatste loodjes.

Maartje, bedankt voor je hulp tijdens de vele C3b zuiveringen, sorry voor het spannende moment in je bureaustoel ;). **Suzan**, ik wil jou en alle mensen van je lab bedanken voor de interessante wetenschappelijke discussies. Ik zou graag ook graag iedereen die betrokken was bij het COMBAT consortium willen bedanken voor de interessante en nuttige bijeenkomsten. **Cees**, jij was de drijvende kracht achter het consortium en had altijd grote interesse in alle projecten. Verder heb ik een leuke tijd gehad met mijn mede COMBAT PhD kandidaten **Rosa**, **Marloes** en **Mieke**. Ik wil graag iedereen bij UPE bedanken voor de gastvrijheid in jullie lab en **Wieger** die talloze transfecties voor mij heeft gedaan. Ik was altijd blij als ik een mail van Wieger terugkreeg met maar twee letters (OK). Ik wil ook graag **Marc**, **Alex** en **Chris** van IBIS-SPR bedanken voor al jullie hulp met de MX96.

Dittie, **Chantal** en **Patrick** ik heb het erg getroffen met mijn schoonfamilie en ik vind het altijd fijn om gezellig met jullie samen te zijn. Ik vind het ook super om te zien hoe gek jullie zijn met onze kinderen. Terwijl ik tijdens mijn PhD figuurlijk over pieken en door dalen heen ging vond ik het heerlijk om met mijn broers **Dominic** en **Ference** letterlijk over pieken en door dalen heen te lopen/fietsen. Bedankt dat jullie voor de nodige ontspanning hebben gezorgd. **Amanda** thanks for taking amazing care of me when I visit your 'hotel'. You are a great cook and sister-in-law. **Marieke** je bent een schat, sorry dat ik je af en toe plaag ;). Ik wil ook graag mijn lieve ouders, **Hans** en **Agnes**, bedanken voor hun onvoorwaardelijke steun voor alles wat ik doe. Doordat jullie mij de tijd en ruimte hebben gegeven om dingen op mijn eigen tempo te ontdekken ben ik hier gekomen. Papa, bedankt dat ik altijd op je kan rekenen. Ik vind het bewonderingswaardig hoe je met alle ellende van de laatste paar maanden toch nog zoveel kracht en positiviteit kan uitstralen. Lieve mama, je was één van de belangrijkste personen in mijn leven en ik heb heel veel mooie herinneringen met je. Helaas komen daar geen nieuwe meer bij en jouw afwezigheid is nog elke dag een groot gemis. Ik weet dat je heel trots op me zou zijn voor het afronden van mijn proefschrift en voor het behalen van mijn doctoraat, zoals ik ook heel trots ben op wat jij allemaal hebt bereikt in je leven. Mam, bedankt voor alles.

Als laatste wil ik mijn lieve gezin bedanken. **Nicole**, je bent nu al meer dan de helft van mijn leven mijn steun en toeverlaat. Bedankt dat je me door mijn PhD hebt heen geholpen. Je wist mij altijd op te vrolijken en hebt voor de nodige afleiding gezorgd. Wie ook heel goed zijn in mij afleiden zijn mijn twee lieve zoons **Mees** en **Jip**. Veel mensen

verklaarden me voor gek om tijdens mijn PhD aan kinderen te beginnen, maar ik ben heel blij dat ik niet naar hen heb geluisterd. Er is niets leukers dan thuiskomen in een huis met twee blije kinderen. **Muis**, **Lummel** en **Guus:** miauw, miauw, woef. Ik ben dolgelukkig met mijn leuke gezinnetje.

List of publications

van den Bos RM, Pearce NM, Granneman J, Brondijk THC, Gros P. Insights Into Enhanced Complement Activation by Structures of Properdin and Its Complex With the C-Terminal Domain of C3b. *Front Immunol* (2019) **10**: doi:10.3389/fimmu.2019.02097

Michels MAHM, van de Kar NCAJ, **van den Bos RM**, van der Velden TJAM, van Kraaij SAW, Sarlea SA, Gracchi V, Oosterveld MJS, Volokhina EB, van den Heuvel LPWJ. Novel Assays to Distinguish Between Properdin-Dependent and Properdin-Independent C3 Nephritic Factors Provide Insight Into Properdin-Inhibiting Therapy. *Front Immunol* (2019) **10**: doi:10.3389/fimmu.2019.01350

About the author

Ramon Marijs van den Bos was born in Elburg, the Netherlands on the 9th of March 1990. In September 2010 he began his scientific career at the Rijksuniversiteit Groningen where he studied molecular life sciences. After obtaining his Bachelor of Science he switched to the Utrecht University and started the master Molecular and Cellular life sciences. After obtaining his MSc degree he commenced his PhD studies in January 2016 in at Utrecht University in the Crystal and Structural Chemistry group under the supervision of Prof. dr. Piet Gros. The main results of these studies are presented in this thesis. In November 2020 he joined the lab of dr. Eefjan Breukink in the Membrane Biochemistry and Biophysics group at the Utrecht University as a post-doctoral researcher.

A

dary"